Spatiotemporal organization of a living nematic by confinement and surface anchoring

Igor Aronson
Pennsylvania State University

Penn State University

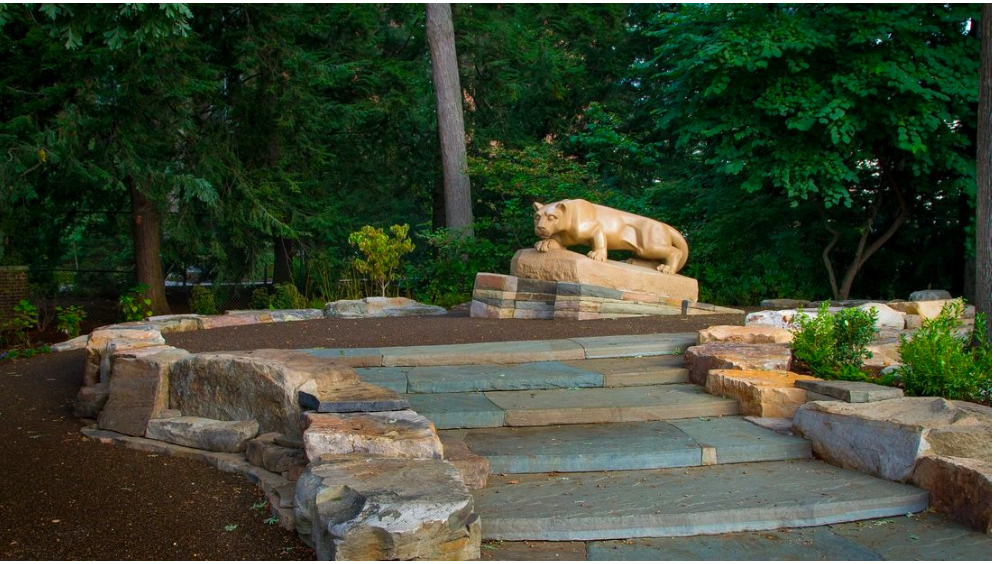

- State College: equally close to New York, Washington DC, Phladelphia, and Pittsburg (3 hours by car)
- twenty-four campuses (main campus 45,000 students)
- 17,000 faculty and staff
- >100,000 students
- second largest football stadium in the US (112,000 seats)
- operating budget >7 billion dollars

Active Matter

- Active Matter - a wide class of systems actively consuming energy from environment, such as assemblages of active self-propelled particles. The particles have a propensity to convert energy stored in the medium to motion
- Examples: suspensions of swimming bacteria and synthetic microswimmers, cytoskeletal actin-myosin networks, driven colloids
- Active materials exhibit properties not available at equilibrium: self-healing, adaptation, shape change

Suspension of microswimmers: one of the simplest realizations of active matter

Bacillus subtilis

-about 5 μm long, 0.7 μm diameter
- swim up to 20 μm/s
- low tumbling rate
- aerobic (need oxygen to swim)

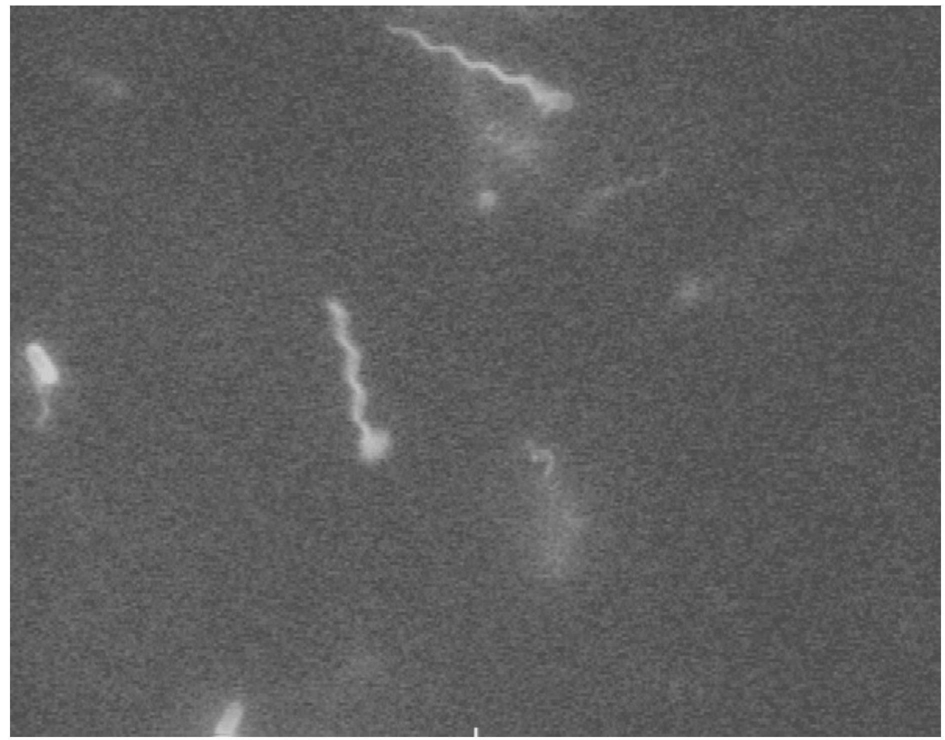

Ryu, Turner, Berg, Harvard Univ

R Goldstein,Cambridge, UK
M Graham, U Wisc
E Clement, ESPCI, France
H-P Zhang, Shanghai JT Univ
M Shelley, Courant
D Saintillan, UIUC/UCSD
Holger Stark, TU Berlin
Hartmut Lōven, U Dusseldorf
T Ishikawa, Tohuku U
A Beer, Ber Sheva , Israel

A living nematic

Zhou, Sokolov, Lavrentovich, IA PNAS 2014

Liquid crystals

Orientational and positional order

Orientational order

No order

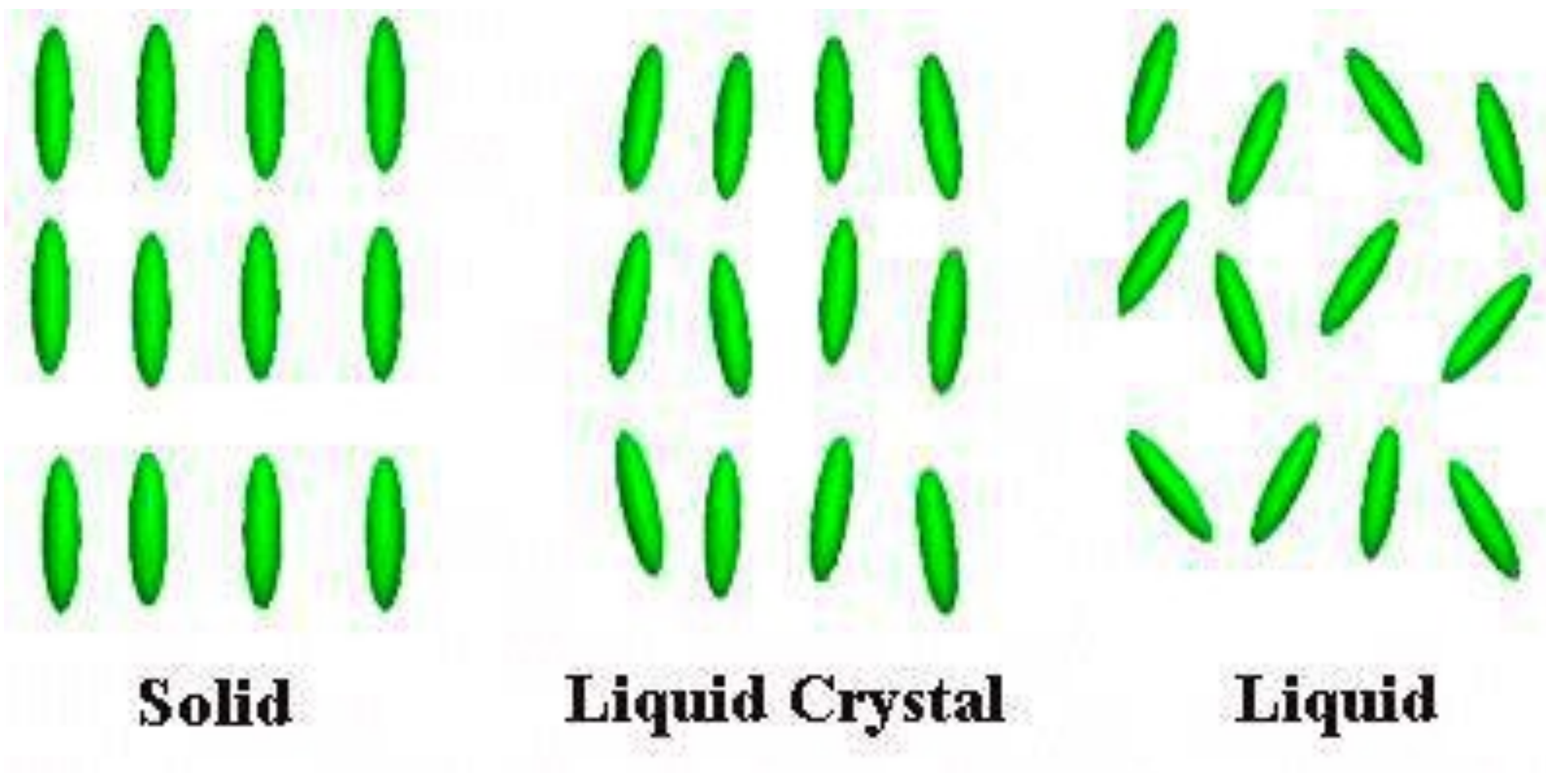

liquid crystal phases

orientational order: nematic

layering: smectic

chiral order: cholesteric

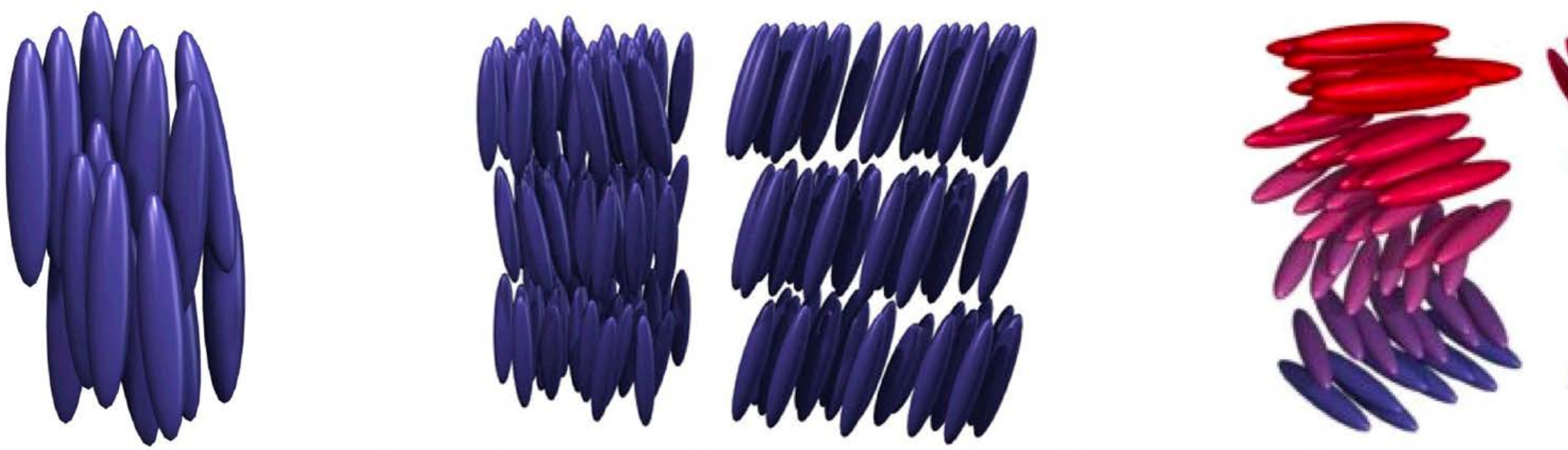

(a) (b) (c)

n *nematic director: (apolar) vector along molecular axis*

liquid crystal deformations

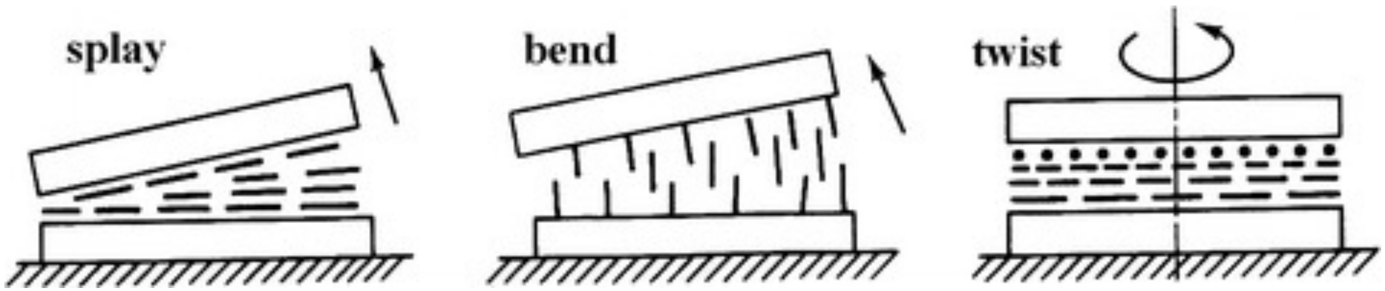

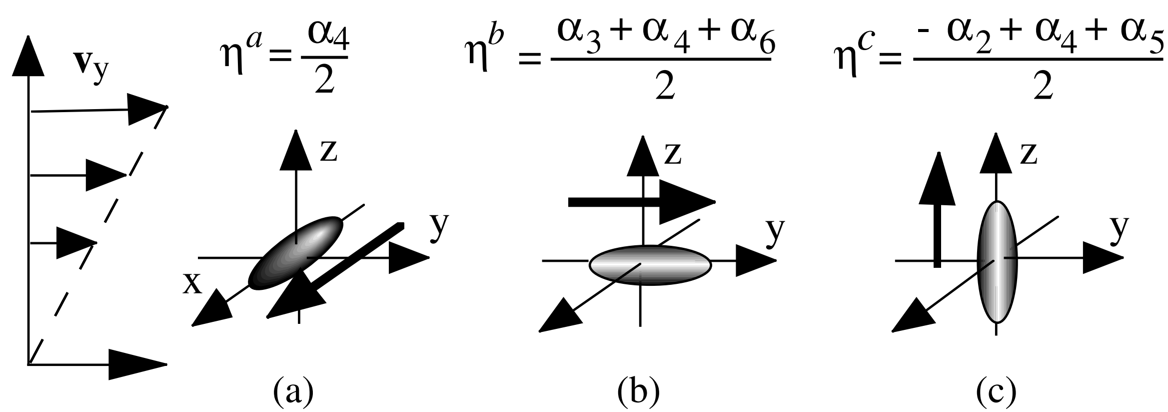

nematic liquid crystals (DSCG)

3 elastic constants $K_{1,2,3}$ (splay, bend >> twist)

3 viscosities: $\eta_{a,c} \sim 10^4 \eta_b$

LC: DSCG

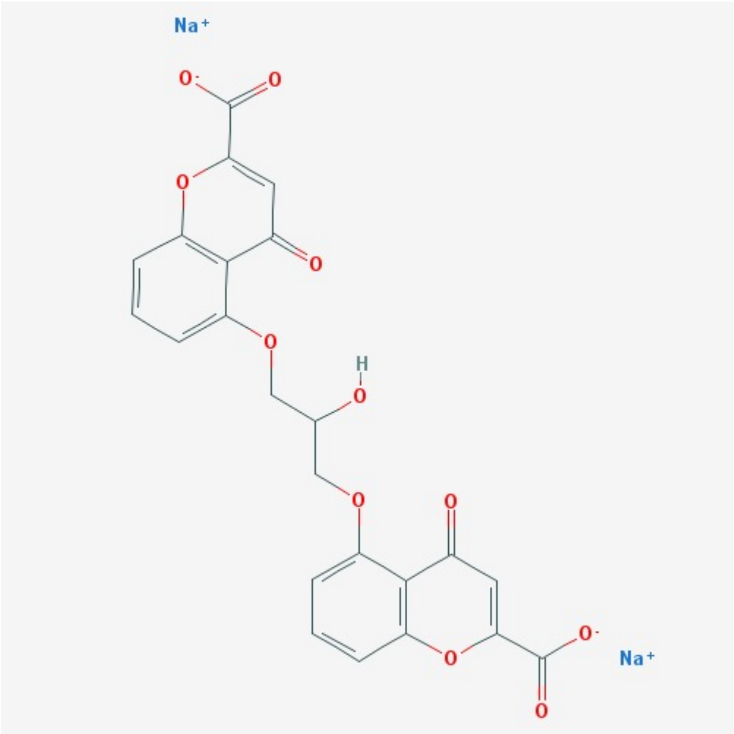

DSCG, a.k.a. cromolyn, anti-asthma drug
disc-like molecules from linear aggregates

Phase Diagram

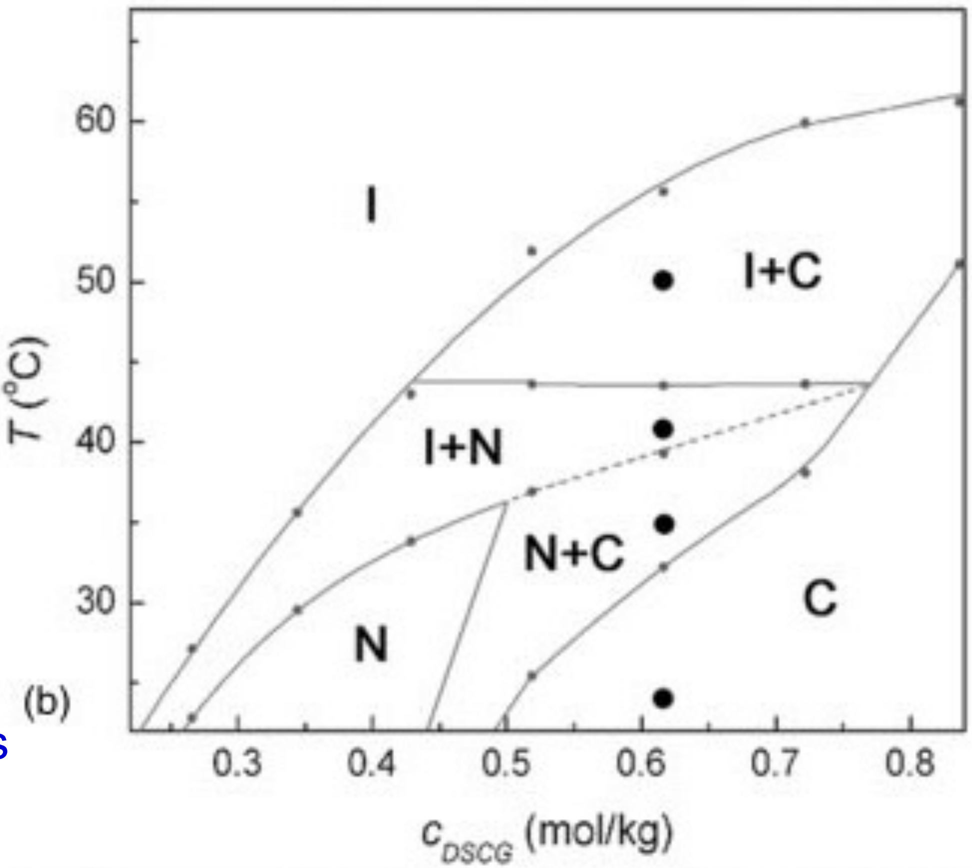

- I – isotropic
- N – nematic
- C – columnar

Mucus – biological liquid crystal

- protective, exchange, and transport medium in the digestive, respiratory and reproduction systems
- Protects against infectious agents such as fungi, bacteria, and viruses
- Better understanding of bacteria-mucus interaction is crucial for the study and development of better treatment of many diseases
- Long molecules form liquid crystalline phase of mucus

N Figueroa Morales, et al, Sci Rep, 2019

Mark I Experimental Cell

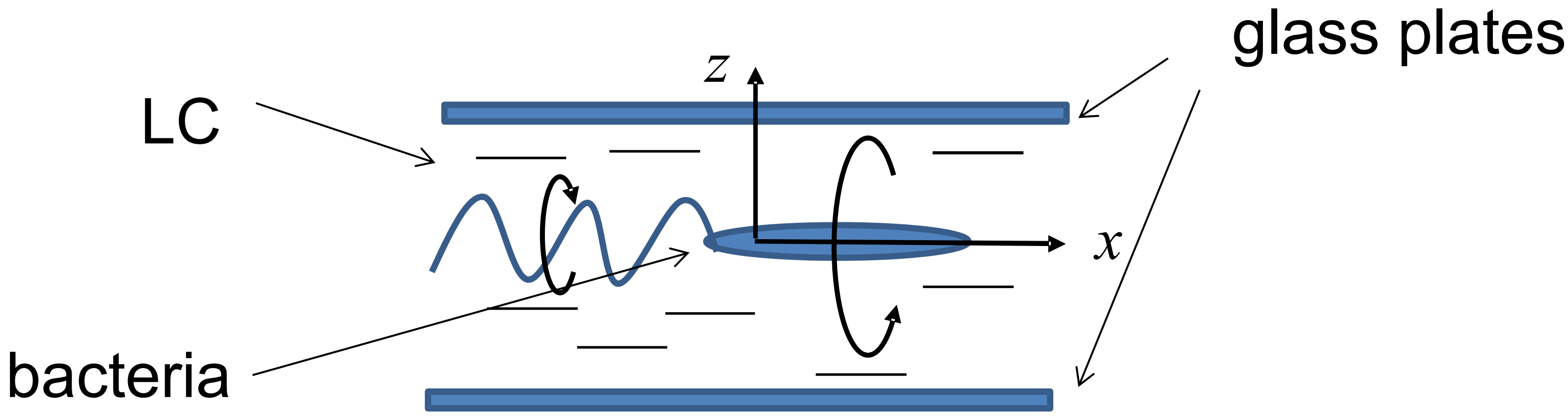

- nematic LC
- planar director surface anchoring (x-direction)
- plates coated with polyimide
- rubbed with a velvet cloth
- thickness : 5 – 500 microns
- concentration of bacteria: 0.2 – 3%
- temperature 25-35 C

Bacteria follow director of a LC (low concnetration)

director (non-polar vector) – average molecular orientation

flat glass cell

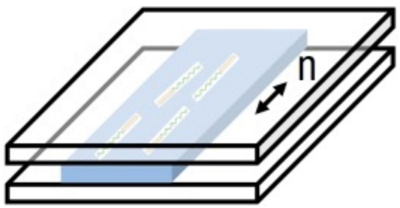

Thickness
h = 5-10 μm

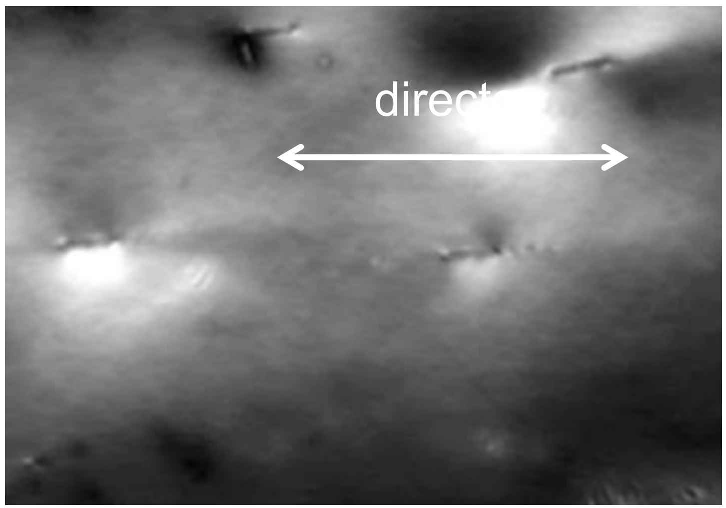

Zhou, Sokolov, Lavrentovich, IA, PNAS 2014

Zoom on individual bacterium

direct optical visualization
of the 24 nm flagella!

- flagella rotation – 10 Hz
- body counter-rotation – 2 HZ

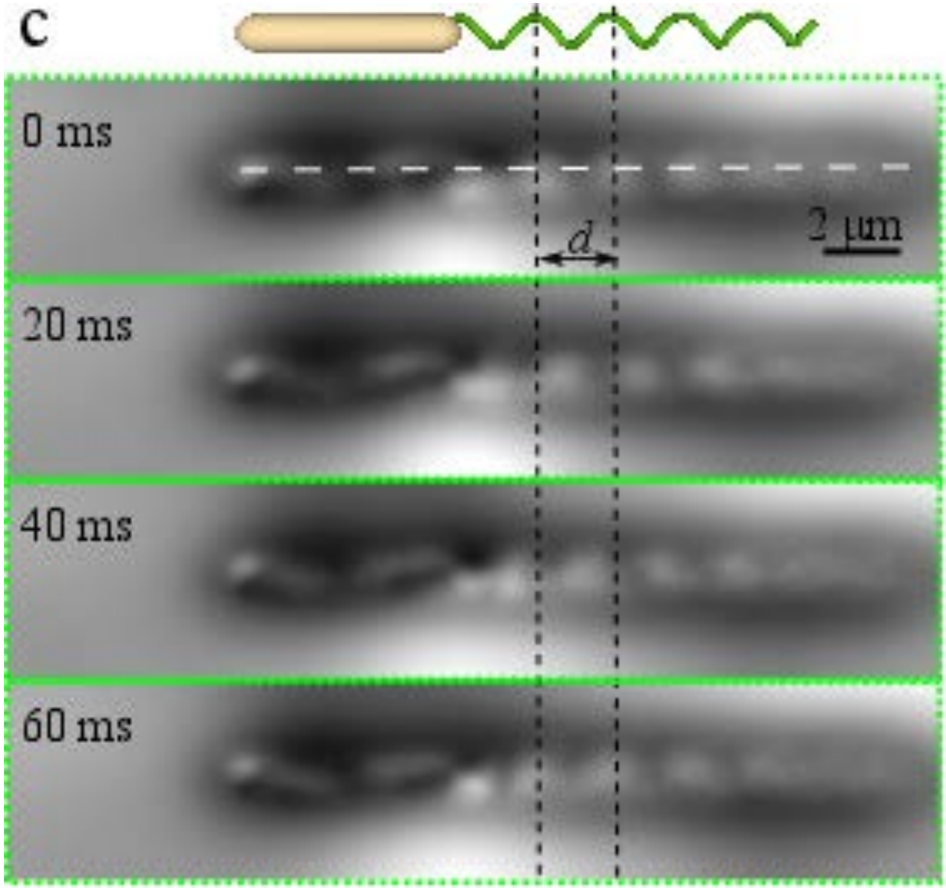

Tracer-bacterium interaction: targeted cargo transport and delivery

Evidence for the long-range interaction

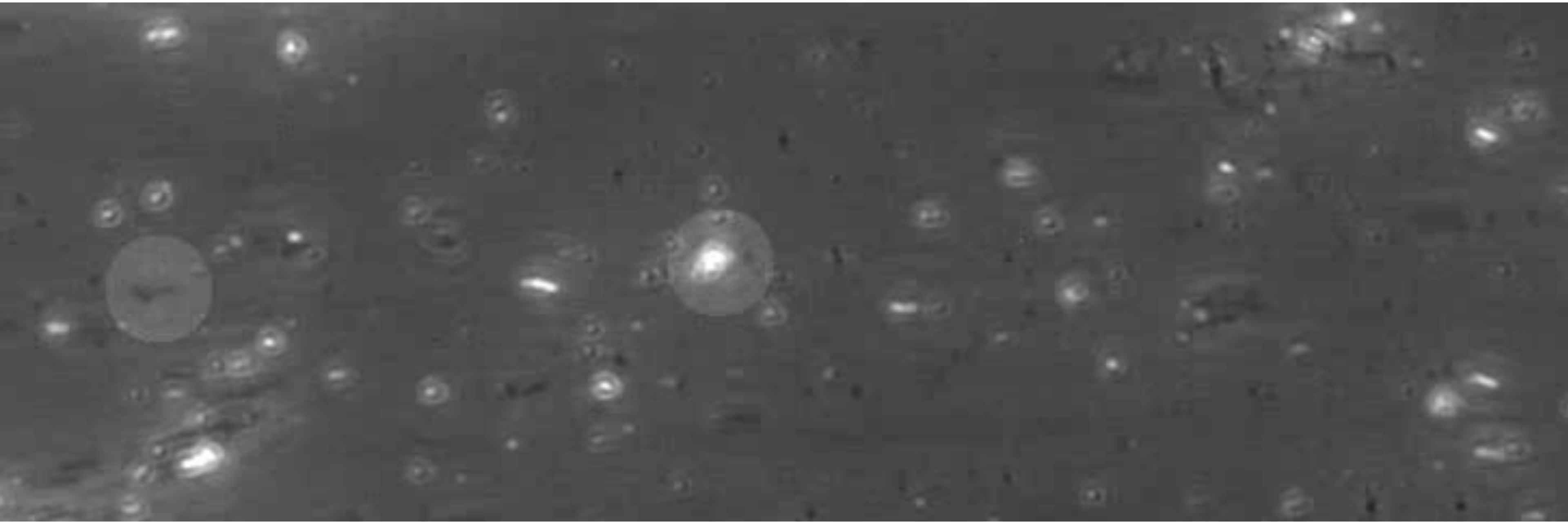

Sokolov, Zhou, Lavrentovich, IA PRE 2015

Direct flow visualization

flow ➔ butterfly pattern

Crossed-polarized image

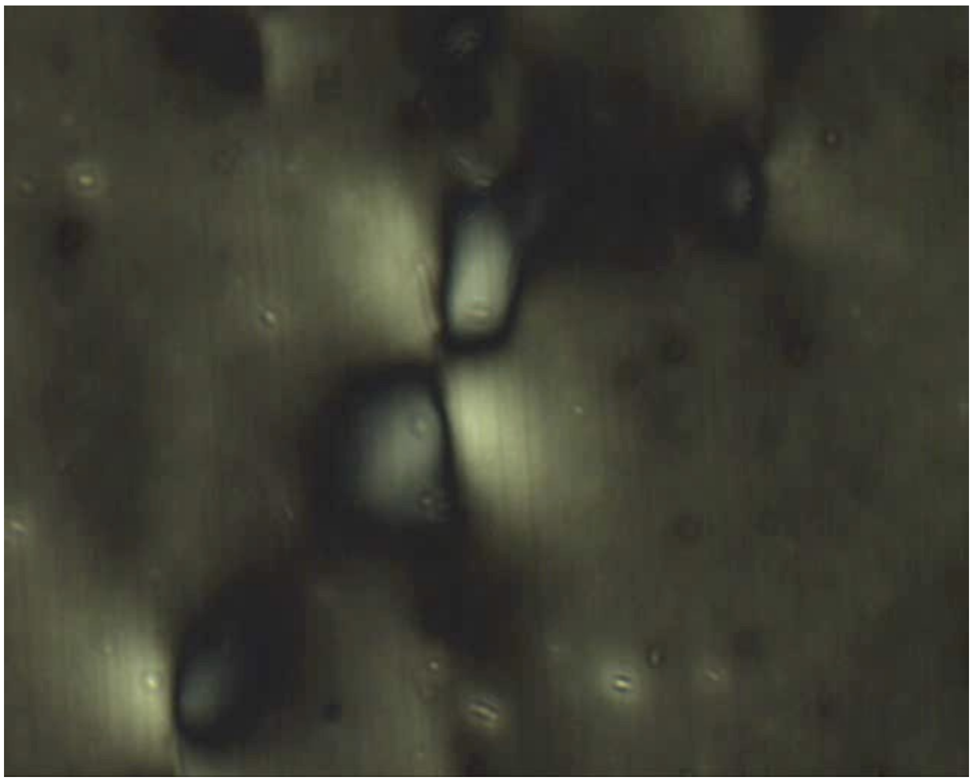

Polscope image

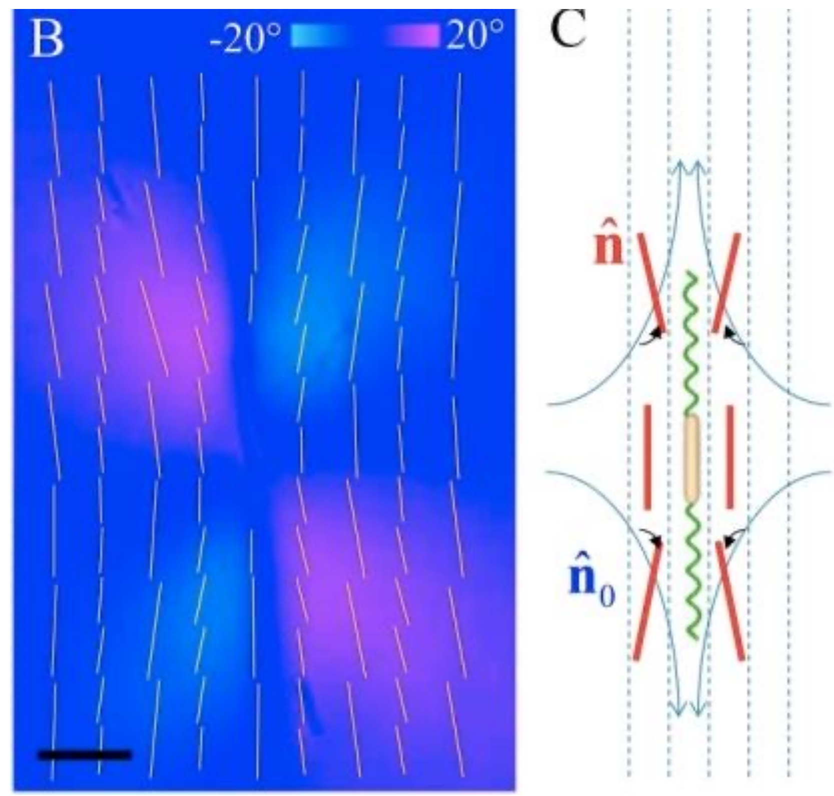

polscope directly visualizes optical retardance

Reconstructed flow field

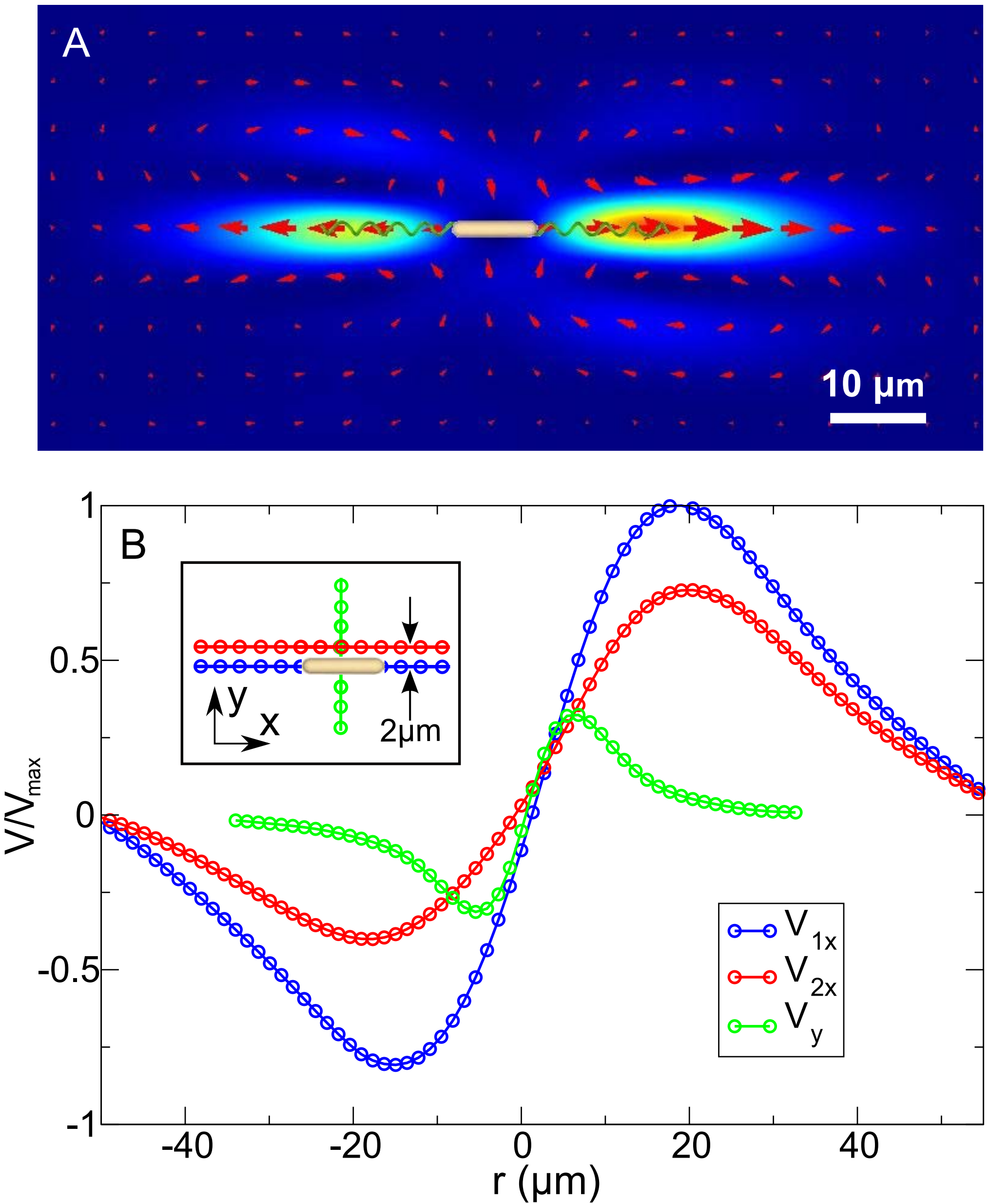

Flow field is reconstructed from the Leslie-Ericksen equation

Average flow field created by a single freely swimming bacterium far from surfaces (A–D) and close to a wall (E–H).

Induced flow comparable to the swimming speed at a distance approx 0.5 microns

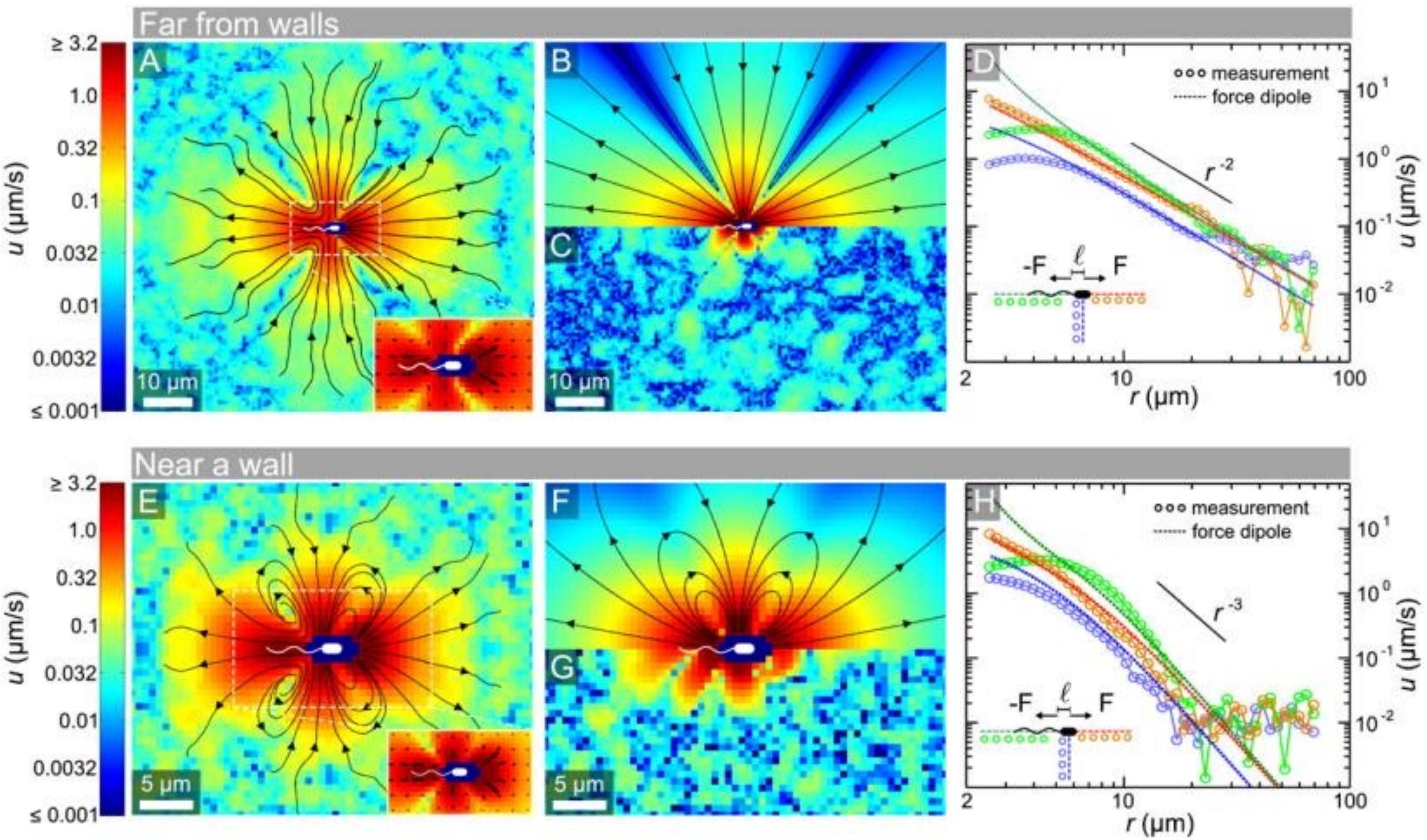

Drescher K et al. PNAS 2011;108:10940-10945

PNAS

Guidance of bacteria in a biphasic domain

higher temperature – nematic/isotropic phases co-exist

bacteria follow the boundaries of normal tactoids

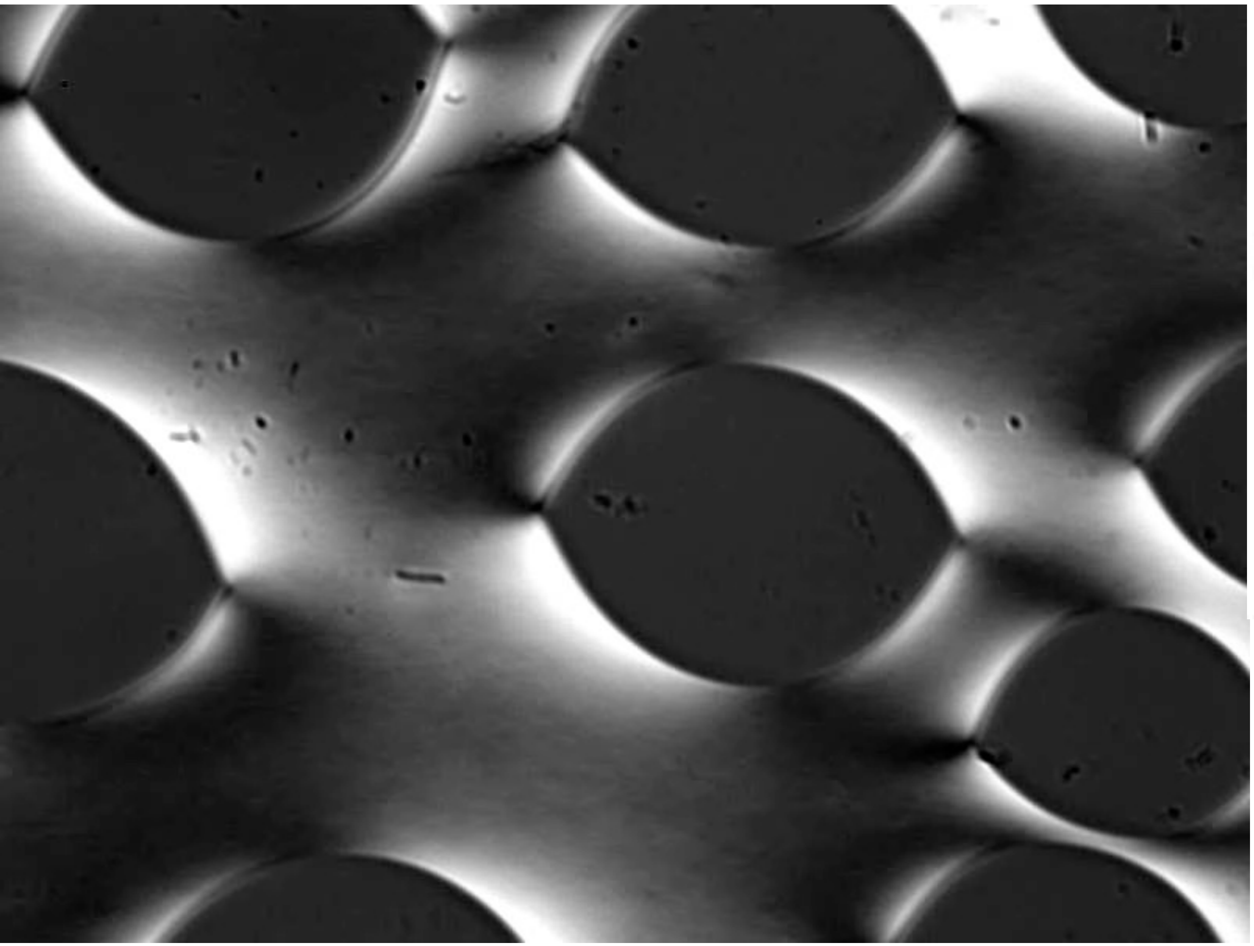

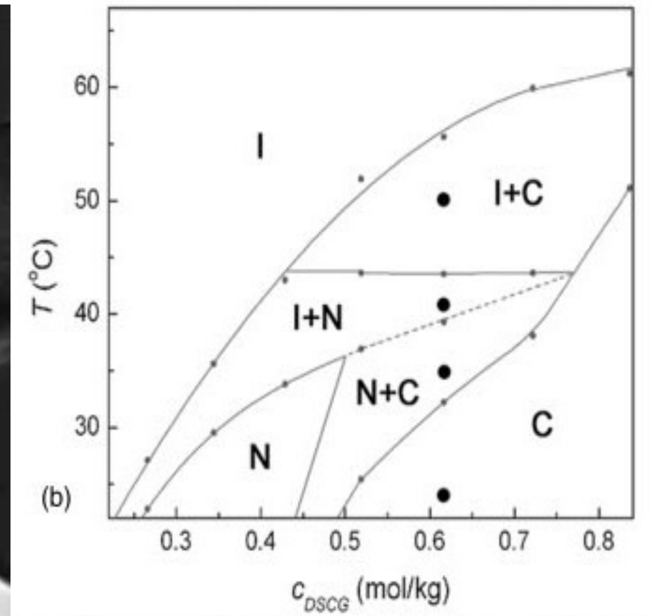

Living LC in the biphasic domain

higher temperature – nematic/isotropic phases co-exist

bacteria melt LC and nucleate tactoids – cloud chamber

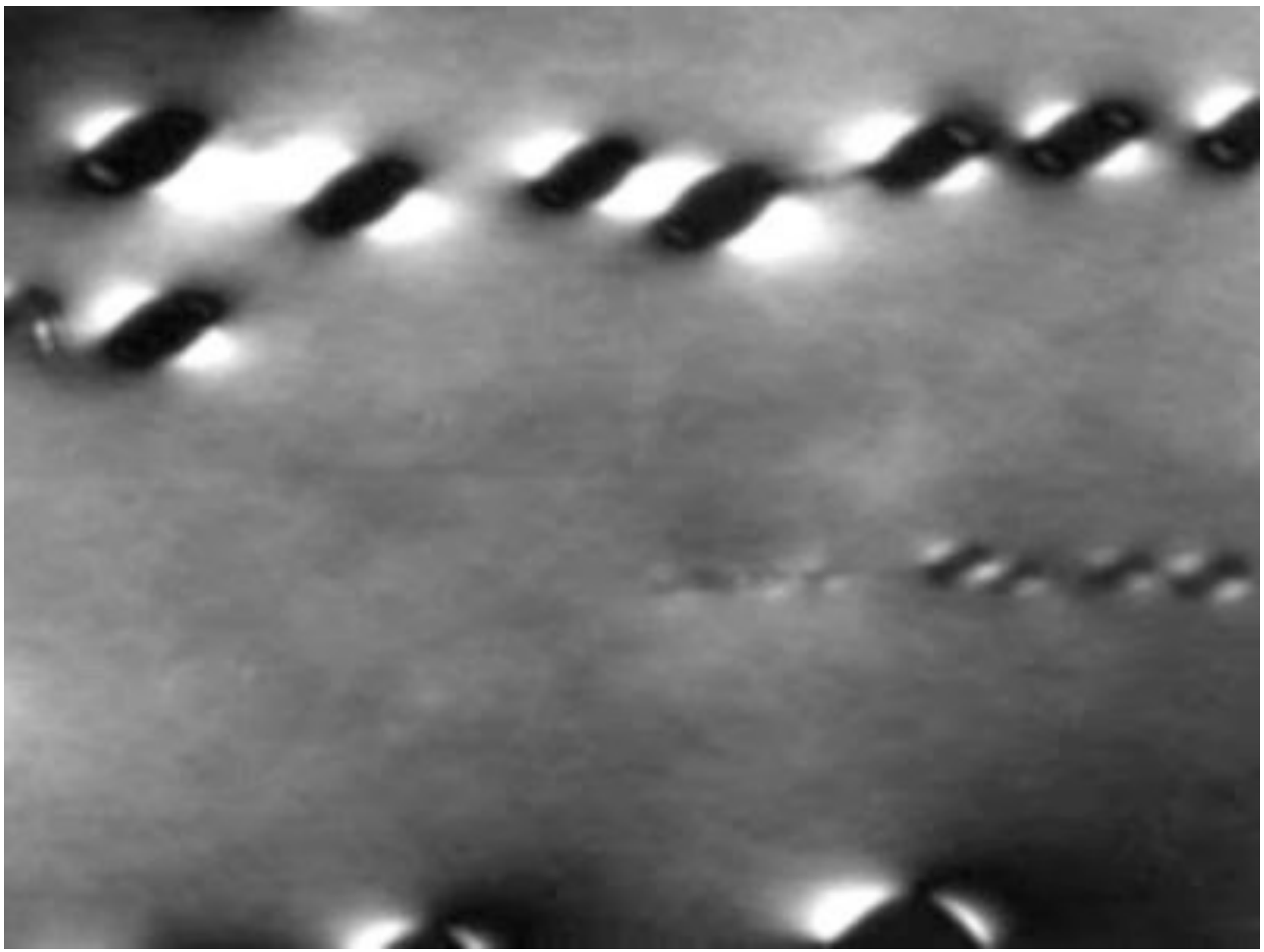

Higher Concentrations: Collective Effects

no oxygen: equilibrium state of uniform director

with oxygen: director undulations and stripes

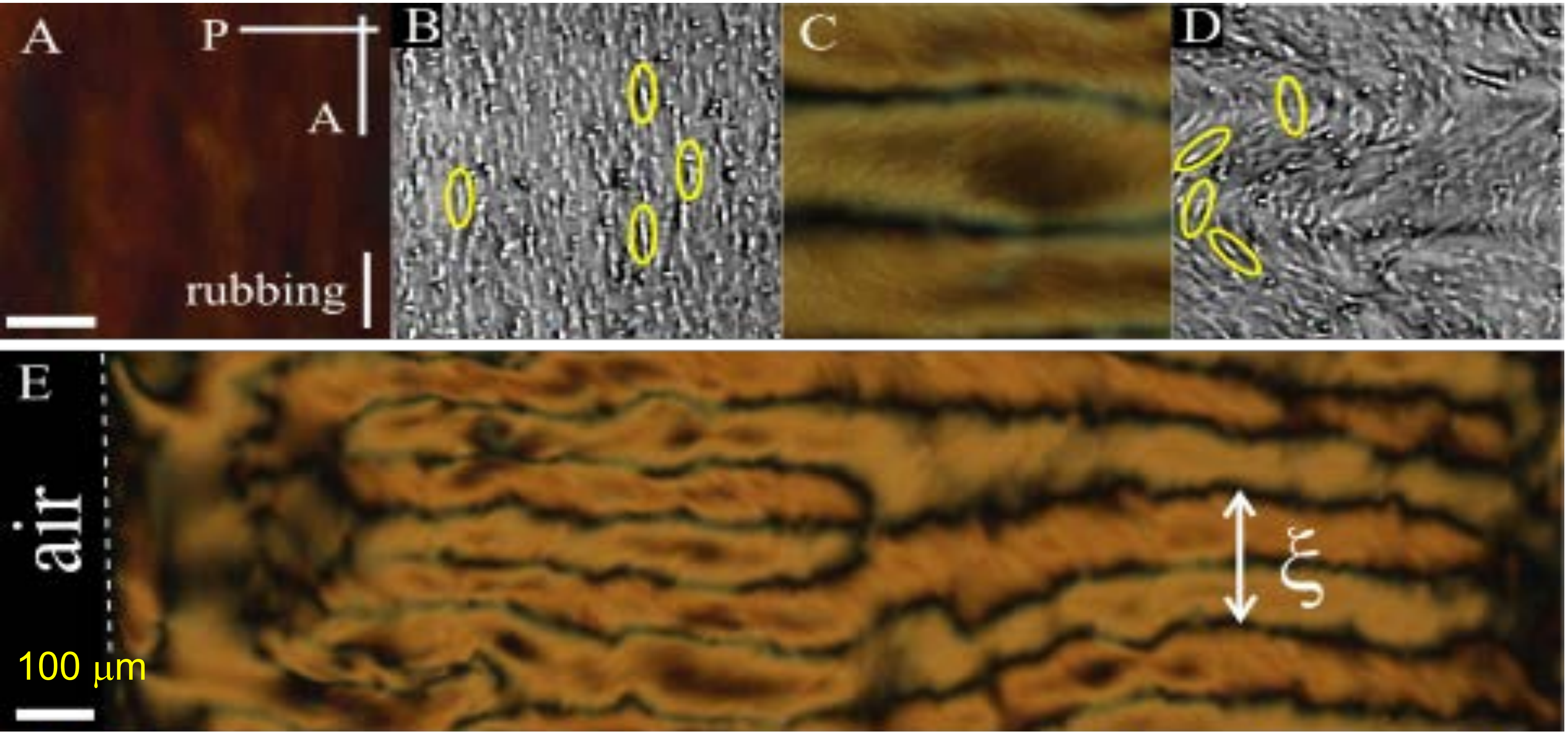

Collective Effects: Formation of Stripe Pattern

scale depends on concentration, amount of oxygen
extreme sensitivity-> possible biosensor applications

Bacterial Turbulence in LC

Bacteria in LC

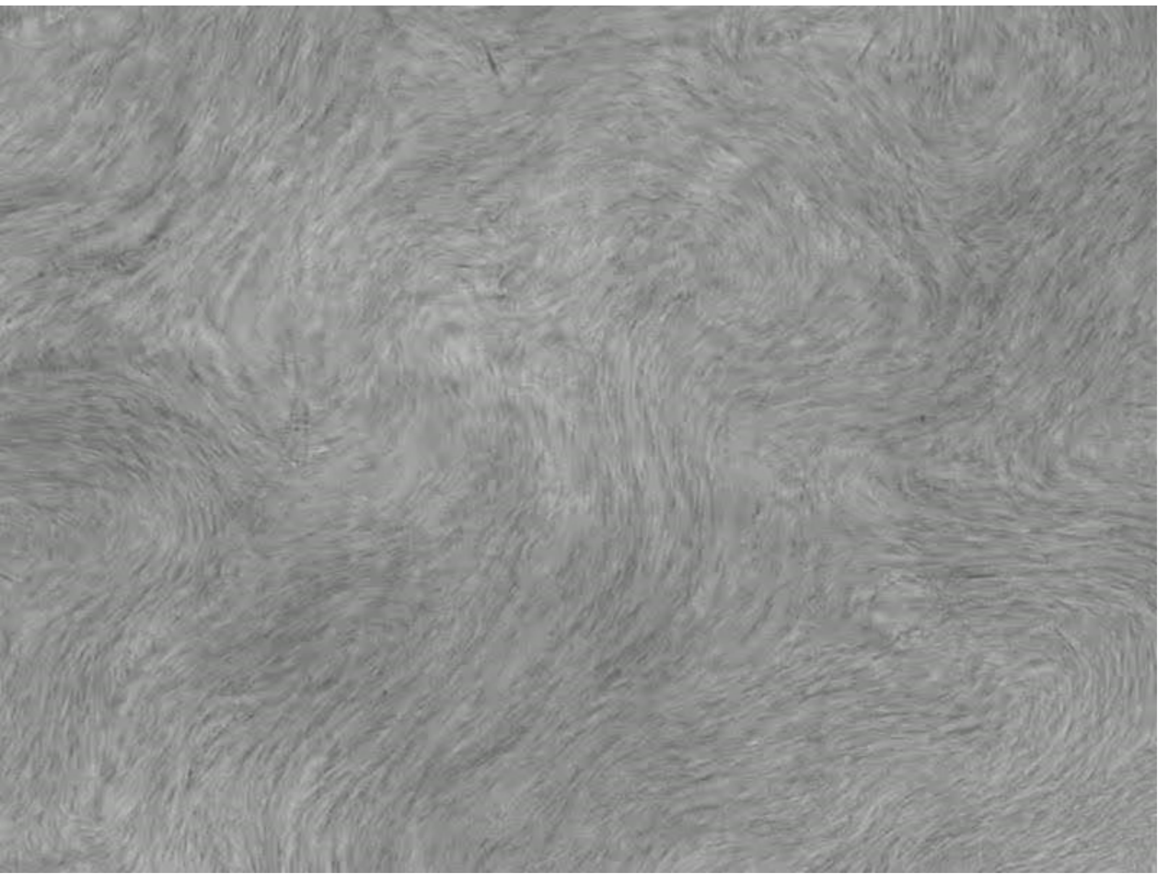

MT+ MM, Dogic group, Nature 2013

Active 2D nematic
Low curvature interface
60X mag
15μm bar

Emergence of the coherence length (period of the stripe pattern)

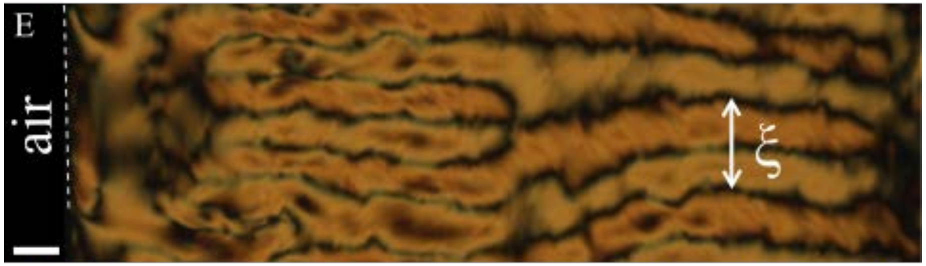

coherence length vs concentration

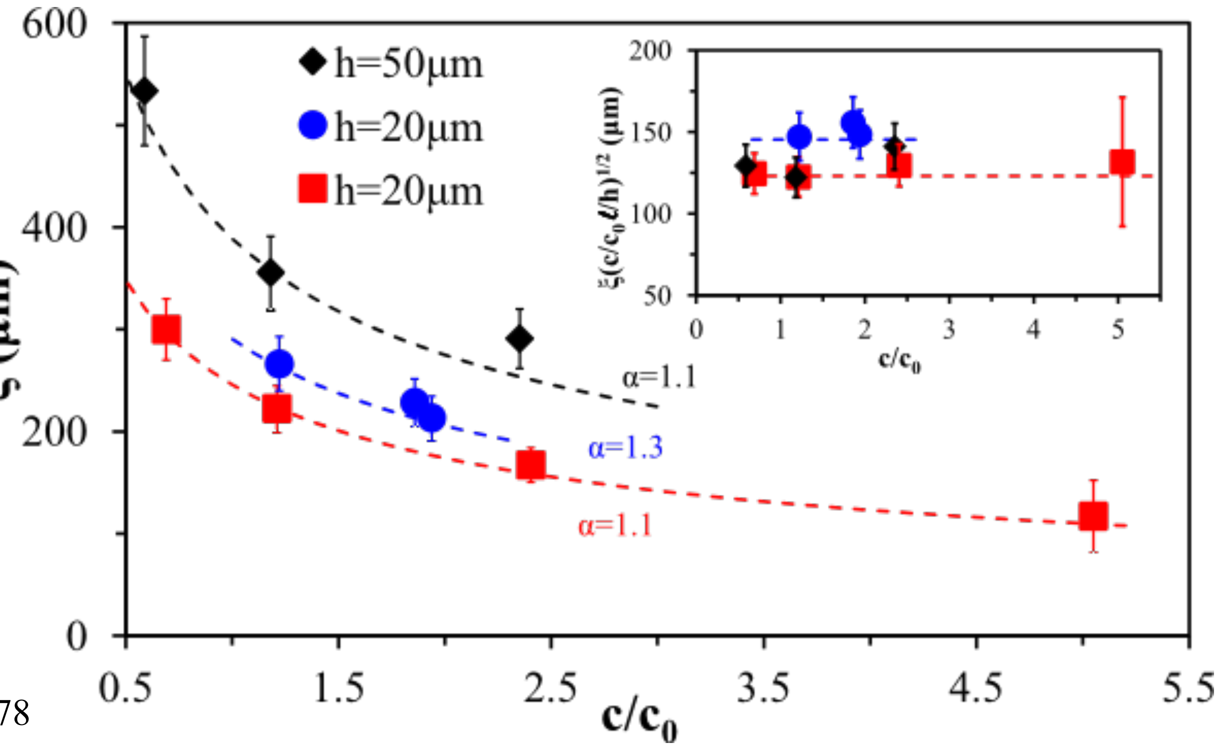

theoretical prediction

$$\xi = \sqrt{\frac{Kh}{\alpha l c U_0}}$$

Estimation of the coherence length

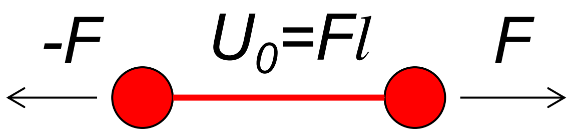

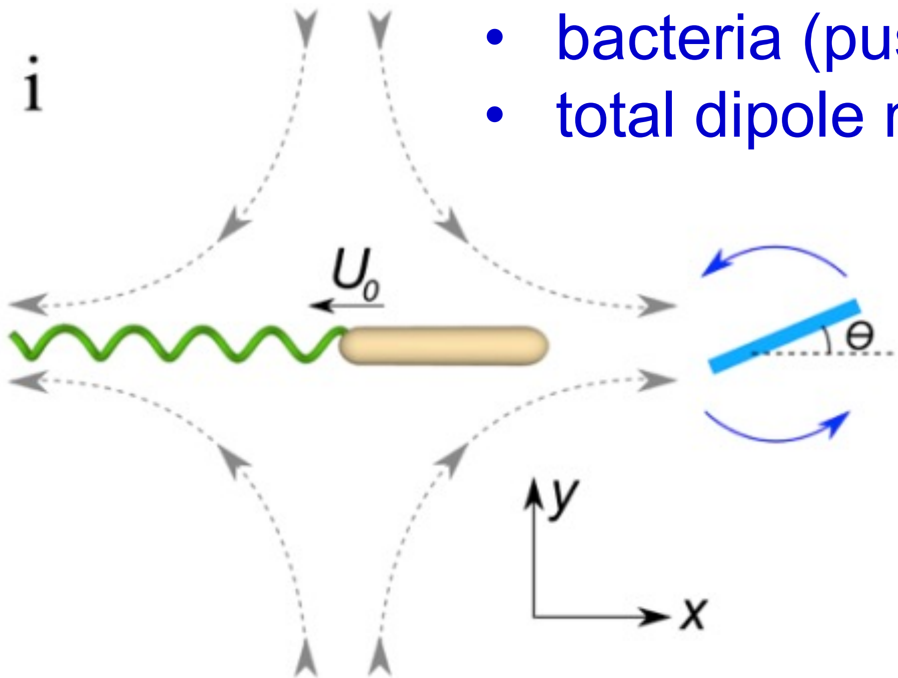

- bacteria (pushers) create force dipole U_0
- total dipole moment of the suspension cU_0

Balance of viscous and elastic (LC) torques

$$\left.\begin{aligned}\Gamma_{shear} &\sim \alpha c U_0 \theta \\ \Gamma_{elastic} &\sim K \frac{\partial^2 \theta}{\partial x^2}\end{aligned}\right\} \Rightarrow \xi = \sqrt{\frac{K}{\alpha c U_0}}$$

Correction due to the finite cell thickness (mass conservation)

$$\xi = \sqrt{\frac{Kh}{\alpha_0 l c U_0}}; \quad \alpha \to \alpha_0 l / h$$

Comparison with the Experiment

$$\xi = \sqrt{\frac{Kh}{\alpha l c U_0}}$$

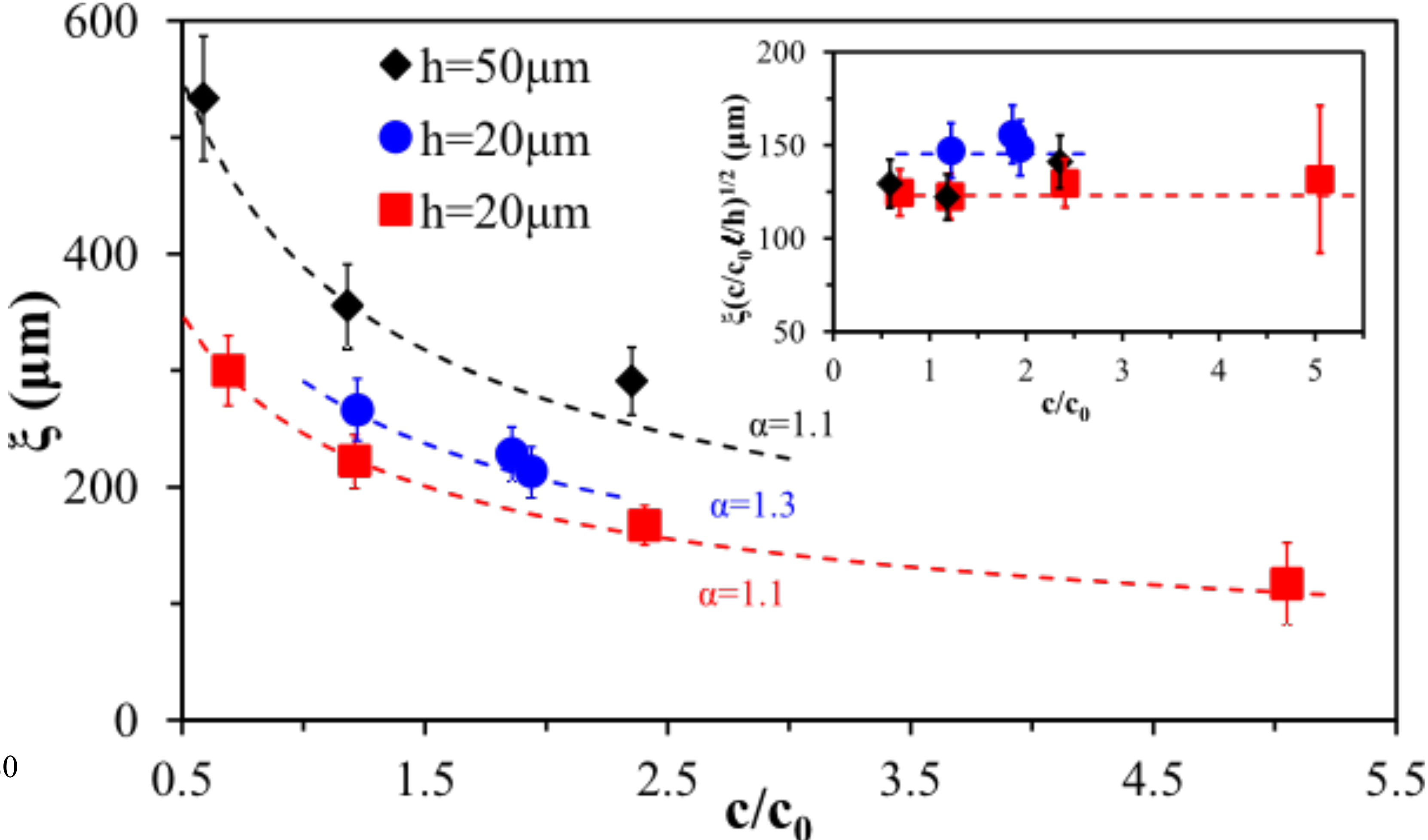

Computational model

- Edwards-Beris model for liquid crystals (tensorial order par)
- thin layer approximation (2D description)
- almost no interaction between the bacteria
- bacteria impose stress on the fluid
- bacteria swim along the LC director

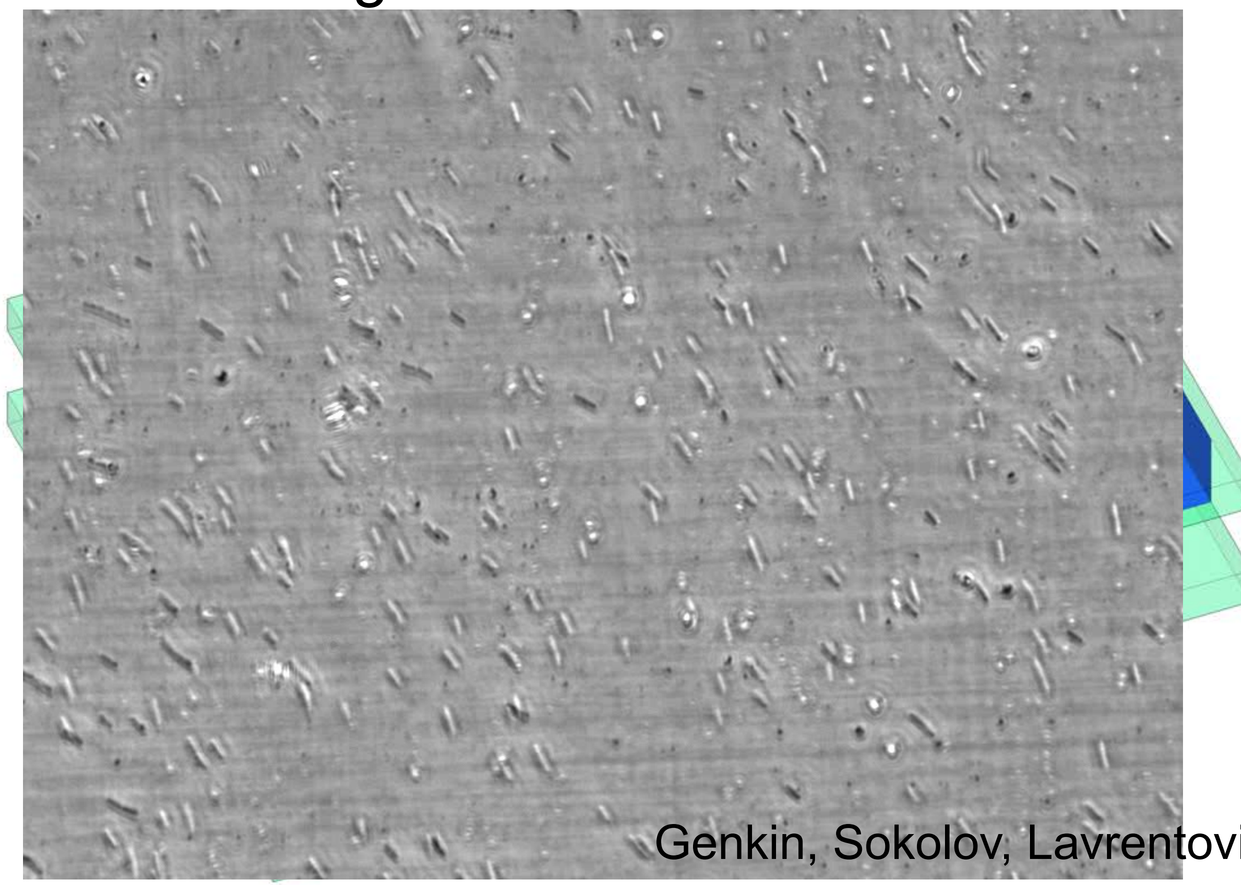

Genkin, Sokolov, Lavrentovich, IA PRX 2017

Block-diagram of the model: 3 coupled PDE modules

Ginzburg-Landau-de Gennes Eq for Tensor order par Q

Edwards-Beris Model for liquid crystals

Eq for hydrodynamic velocity v (aka Stokes Eq) Bacteria -> active stress

Coupling

Conservation law for bacteria conc c

Genkin Sokolov, Lavrentovich, IA, PRX 2017

Edwards-Beris Model (LC)

$$(\partial_t + \mathbf{v}\nabla)\mathbf{Q} - \mathbf{S} - \Gamma\mathbf{H} + \mathbf{F}_{\text{exter}} = 0$$

2D order parameter (OP)
Traceless anti-symmetric tensor

$$\mathbf{Q} = \begin{pmatrix} Q_{xx} & Q_{xy} \\ Q_{xy} & -Q_{xx} \end{pmatrix}$$

v – fluid flow
H – molecular field, **S**-tensor
$\mathbf{F}_{\text{exter}}$ – external aligning field (anchoring)
Γ – rate constant

Order parameter in 2D $\mathbf{Q} = q\left(\mathbf{nn} - \frac{1}{2}\mathbf{I}\right)$

$$\mathbf{n} = (\cos(\theta), \sin(\theta))$$

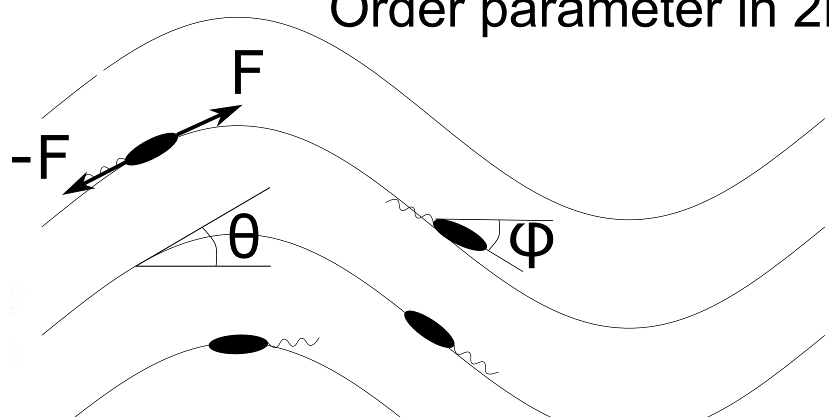

Edwards-Beris Model

S couples **Q** to the velocity gradient tensor **W**

Molecular field $$\mathbf{H} = -\frac{\delta F}{\delta \mathbf{Q}} - \frac{\mathbf{I}}{2}\mathrm{Tr}\frac{\delta F}{\delta \mathbf{Q}}$$

Ginzburg-Landau-de Gennes free energy
(single constant approximation for elastic energy)

$$F = \int d\mathbf{r}\left(\frac{a}{2}Q_{\alpha\beta}Q_{\alpha\beta} - \frac{b}{3}Q_{\alpha\beta}Q_{\beta\gamma}Q_{\gamma\alpha} + \frac{c}{4}\left(Q_{\alpha\beta}Q_{\beta\alpha}\right)^2 + \frac{L_1}{2}\left(\partial_\gamma Q_{\alpha\beta}\right)^2 + ...\right)$$

Linear momentum equation (coupled to order par equation, generalization of Stokes eq)

$$\nabla\left(\overset{\substack{\text{symmetric}\\ \downarrow}}{\sigma_{\mathrm{a}}}+\overset{\substack{\text{anti-symm}\\ \downarrow}}{\sigma_{\mathrm{s}}}+\overset{\substack{\text{active (bact)}\\ \downarrow}}{\sigma_{\mathrm{act}}}+\overset{\substack{\text{viscous}\\ \downarrow}}{\sigma_{\mathrm{visc}}}-\overset{\substack{\text{pressure}\\ \downarrow}}{p}\mathbf{I}\right)-\xi\overset{\substack{\text{wall friction}\\ \downarrow}}{\mathbf{v}}=0$$

v – hydrodynamic velocity
stress tensors σ are functions of **Q,v**
ξ - friction coefficient

Bacteria impose active stress σ_{act},
drive the system out of equilibrium

Active stress due to bacteria swimming

$$\sigma_{\mathrm{act}} = \lambda c \left(\mathbf{pp} - \frac{\mathbf{I}}{2} \right)$$

$$\mathbf{p} = (\cos(\phi), \sin(\phi))$$

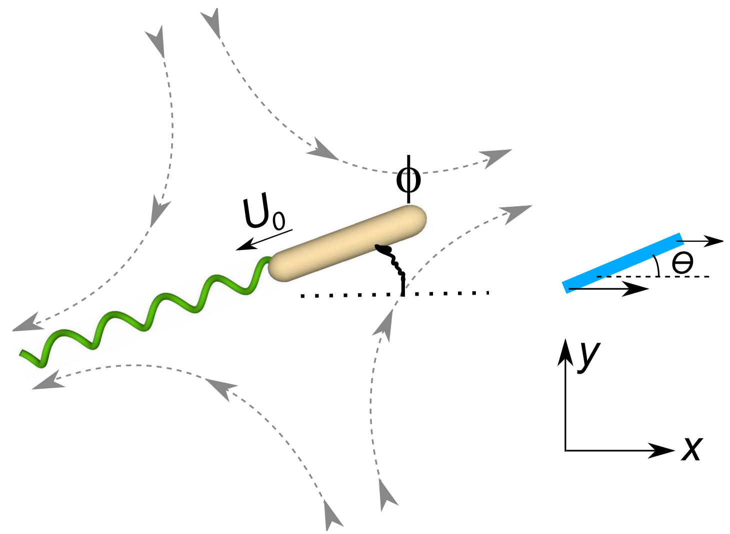

p –orientation of bacteria

$\lambda<0$ – stresslet strength (pusher)

c – concentration of bacteria

ϕ – orientation of bacteria

θ– orientation of a nematic

$$\partial_t \phi = \frac{q}{\tau_0} \sin(2\theta - 2\phi) + \ldots$$

$\tau_0<<1$ – fast relaxation towards nematic direction

$\phi=\theta,\ \theta+\pi \rightarrow$ **p=n, p=-n**

Conservation law: transport of bacteria

- bacteria swim parallel/antiparallel to the director:
  $\phi=\theta,\ \phi=\theta+\pi$ or **p=n**, **p=-n**
- bacteria randomly reverse direction with the rate $1/\tau$
- c_+ parallel to **n**, c_- antiparallel: $-\pi/2<\theta<\pi/2$

self-propulsion advection reversals diffusion

$$\partial_t c_+ + \nabla\left(V_0 \mathbf{n} c_+ + \mathbf{v} c_+\right) = -\frac{c_+ - c_-}{\tau} + D_c \nabla^2 c_+$$

$$\partial_t c_- + \nabla\left(-V_0 \mathbf{n} c_- + \mathbf{v} c_-\right) = -\frac{c_- - c_+}{\tau} + D_c \nabla^2 c_-$$

$$c = c_+ + c_-$$

V_0- swimming speed

The mechanism of reversal: two flagella bundles

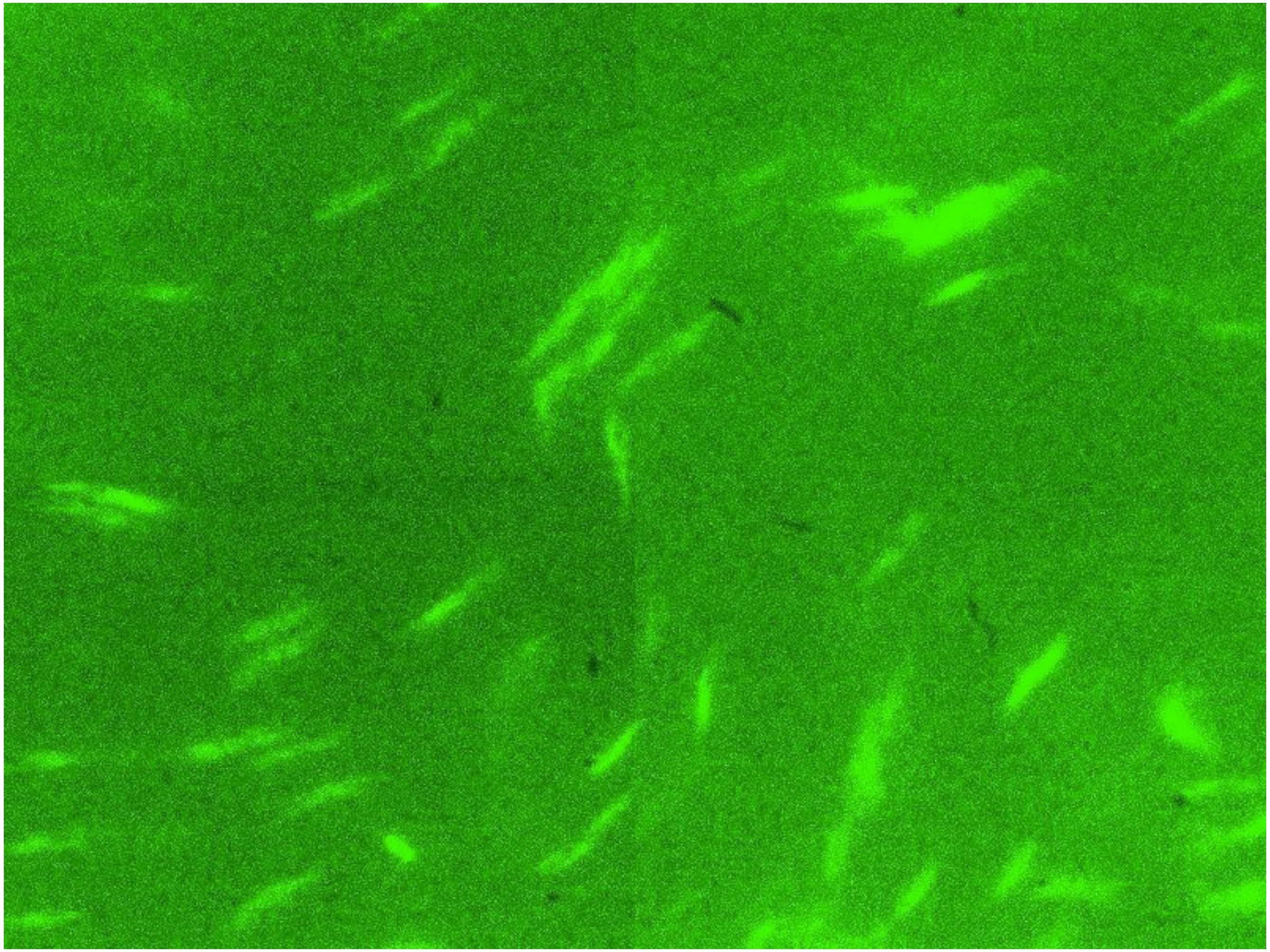

Nuris Figueroa , PSU

Relation to Active Nematic Model

- Amin Doostmohammadi, Julia Yeomans, others

- Equation for the OP

$$(\partial_t + \mathbf{v}\nabla)\mathbf{Q} - \mathbf{S} - \Gamma\mathbf{H} + \mathbf{F}_{\mathrm{exter}} = 0$$

- Linear momentum

$$\nabla\left(\sigma_{\mathrm{a}} + \sigma_{\mathrm{s}} + \sigma_{\mathrm{act}} + \sigma_{\mathrm{visc}} - p\mathbf{I}\right) - \xi\mathbf{v} = 0$$

- Constant density. These eqs can be obtained in the limit of very small reversal time (unphysical limit)

Analytical linear stability of the aligned state in bacteria-nematic system

homogenous steady state: $\mathbf{n}=(1, 0)$, $c_+=c_-=c_0/2$

perturbations ~ $\exp(\sigma(\mathbf{k})t + i\,\mathbf{kr})$

long-wave instability: zero anchoring

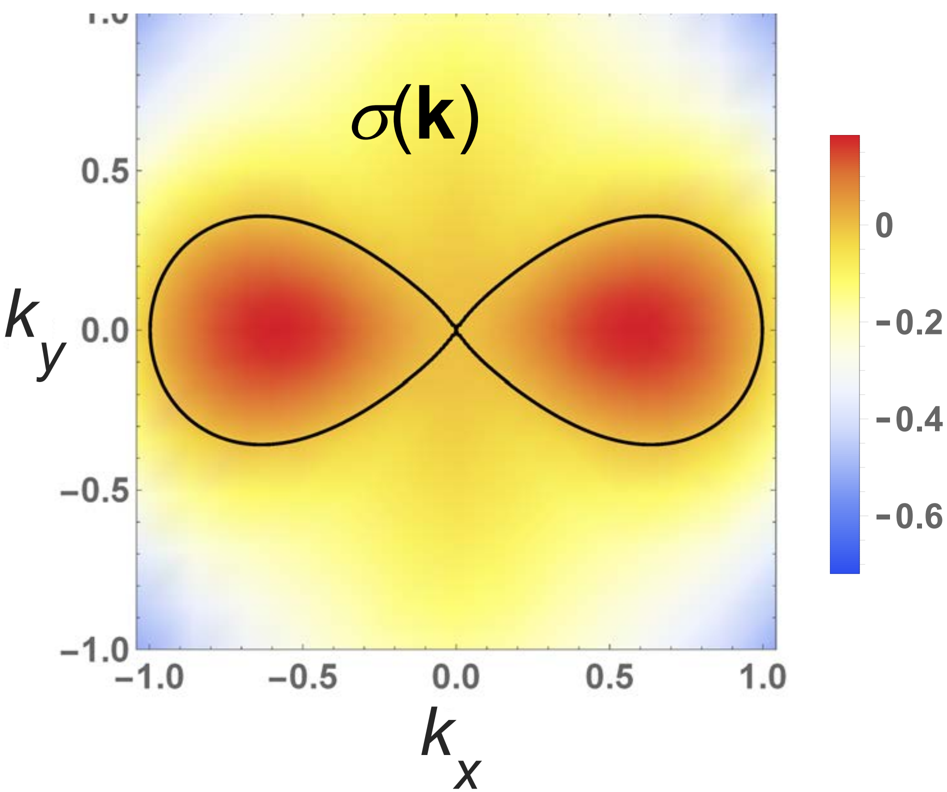

short-wave instability: nonzero anchoring

k_{cr}~(Er ξ_{an})$^{1/4}$

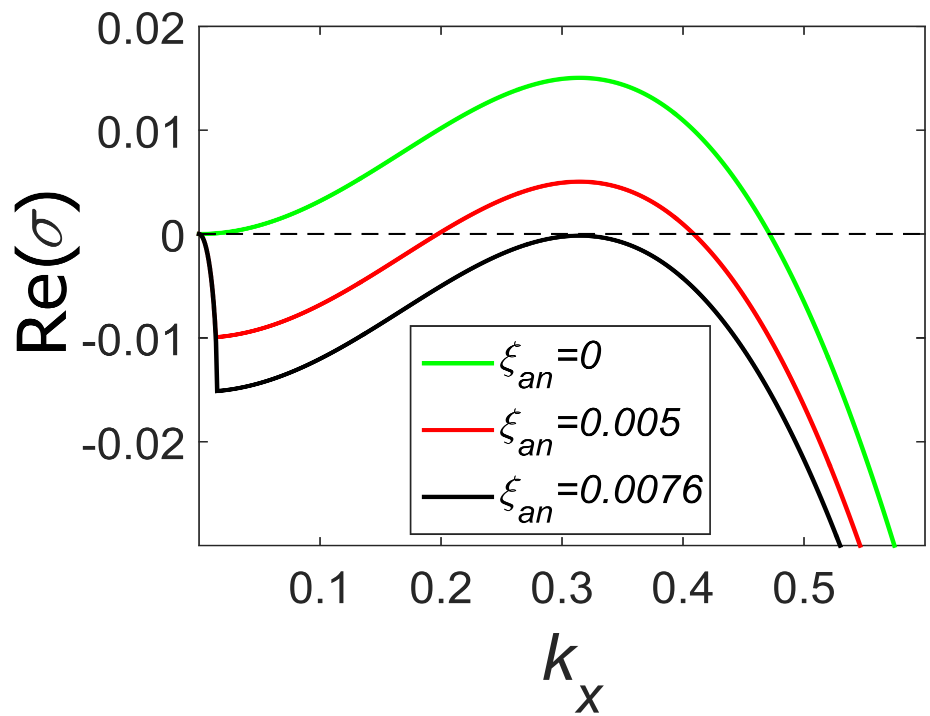

Comparison with the Experiment

$$\xi = \sqrt{\frac{Kh}{\alpha l c U_0}}$$

experiment

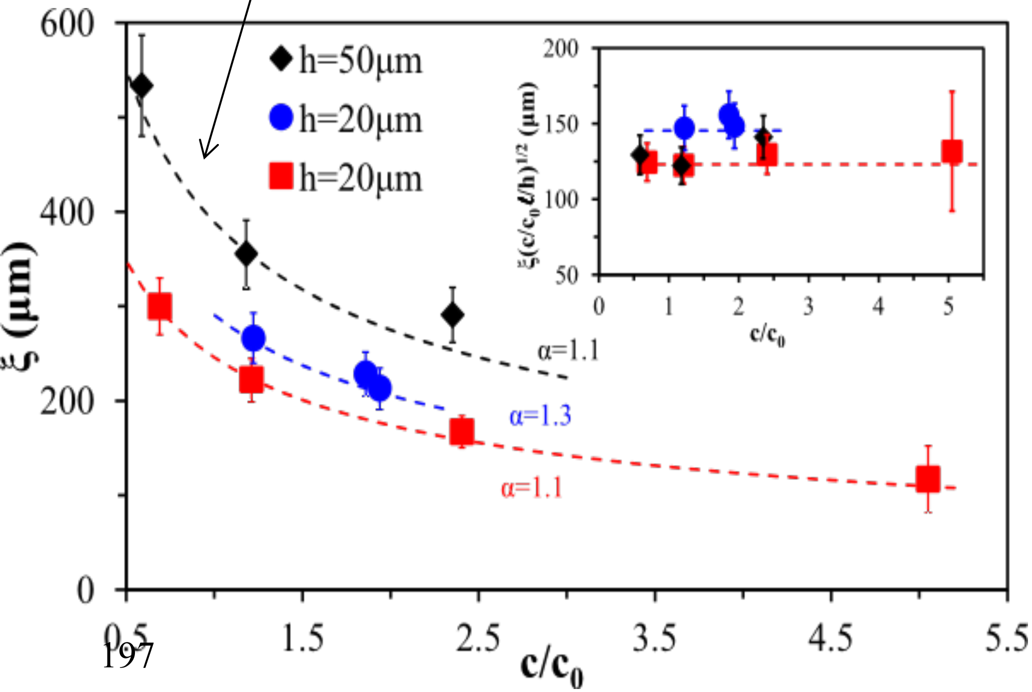

linear stability

$$L_{\rm cr} \sim \frac{1}{\sqrt{c_0}}$$

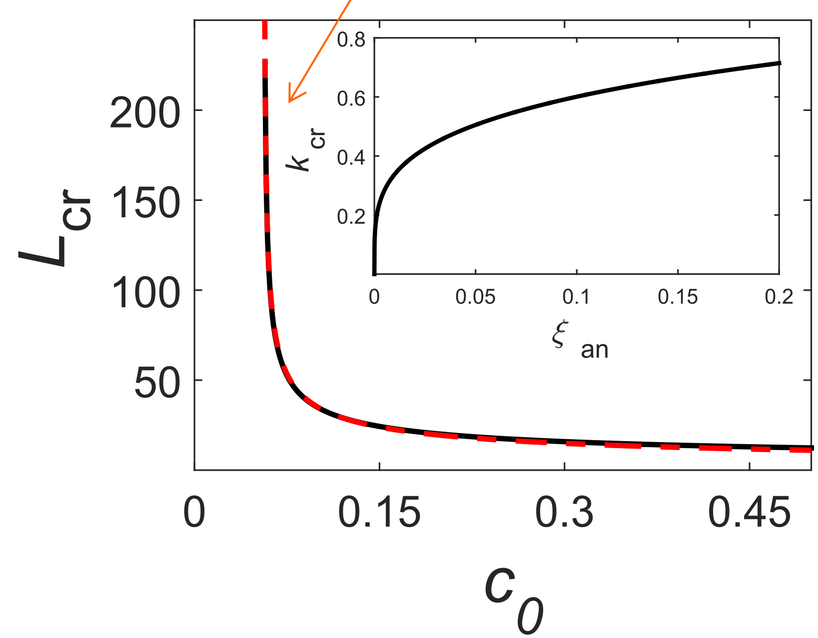

Computational Analysis: tensorial eqs coupled to conser law

- Semi-implicit quasi-spectral method (FFT)
- Massive parallel, implemented on the GPU
- # of mesh points 1024^2, results checked for 2048^2
- Nvidia CUDA programming language
- Visualization – Matlab
- Custom-made defect tracking algorithm

Fundamental problem of algorithm

- Mapping a vector field (flux of bacteria) to a nematic field is ambiguous
- Nematic director **n**=(cos(θ), sin(θ)), nematic angle $-\pi/2<\theta<\pi/2$
- Bacterial fluxes $J_\pm = \pm V_0\mathbf{n}$ are discontinuous for θ changing from $-\pi/2$ to $\pi/2$: no standard numerical approach works

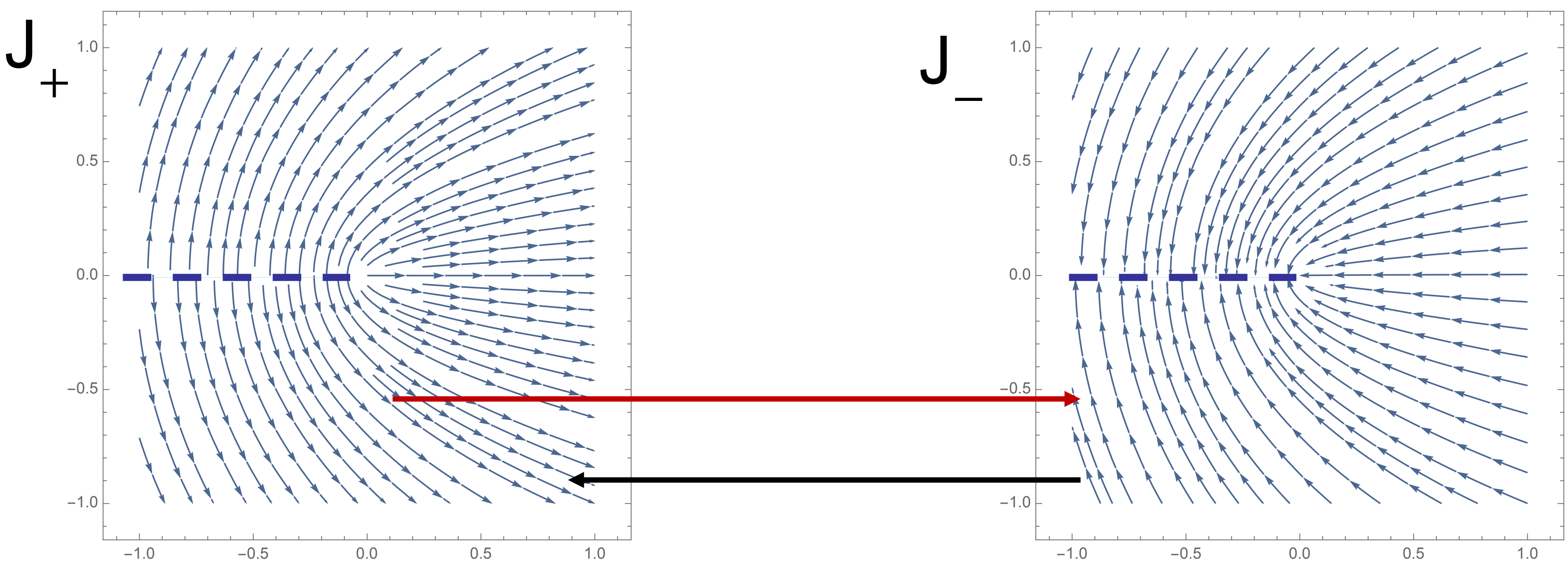

resolving angle ambiguity

- nematic angle is defined between $-\pi/2<\theta<\pi/2$
- directions $-\pi/2$ and $\pi/2$ are identical for the nematic
- but the flux $V_0\sin(\theta)$ changes sign: $\partial_t c \pm V_0 \nabla \mathbf{n} c + \ldots$
- unphysical discontinuities for $c_\pm$ along these lines

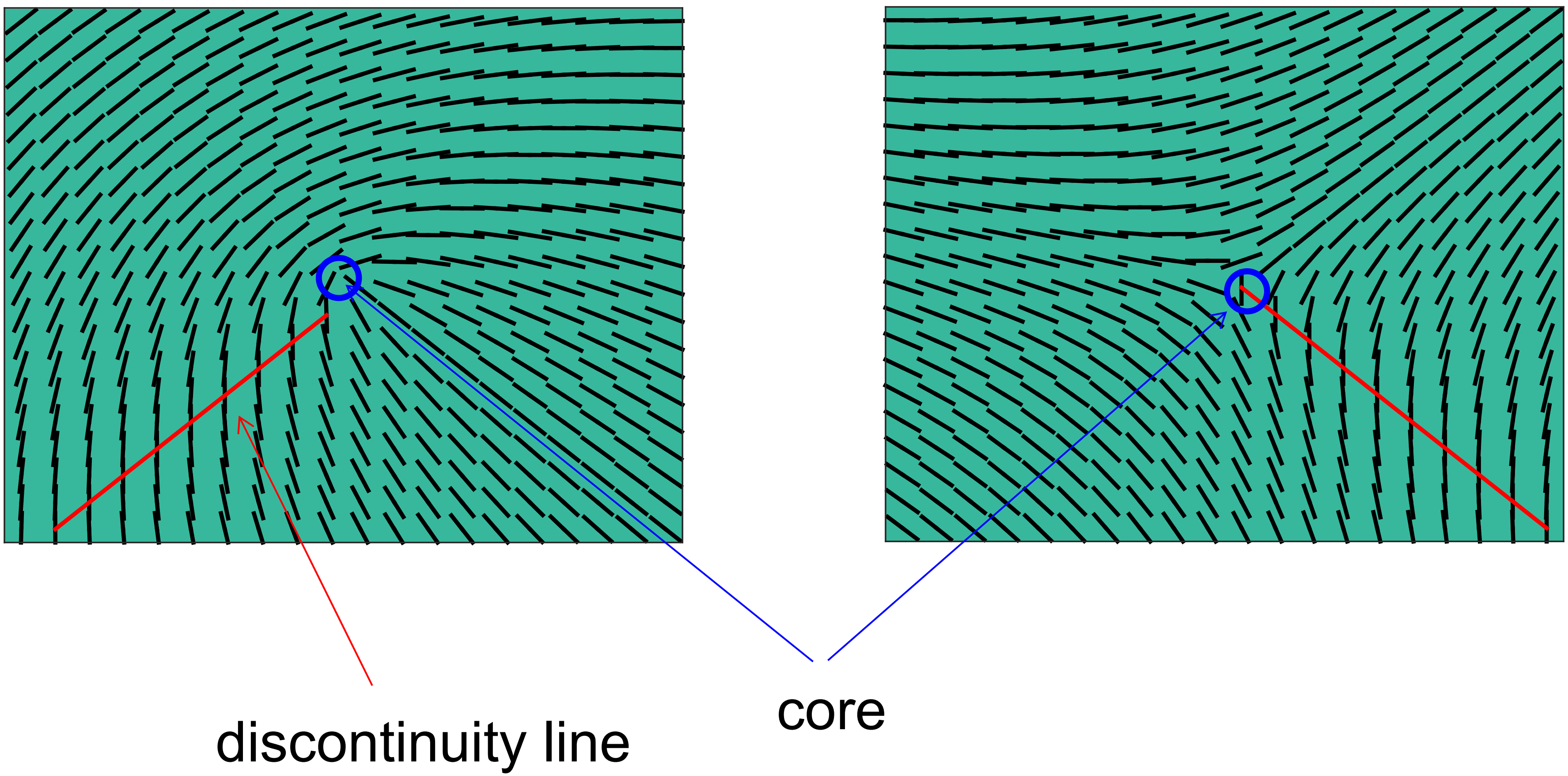

Solution of PDEs - Phase diagram

- narrow band of periodic states
- hysteretic transition

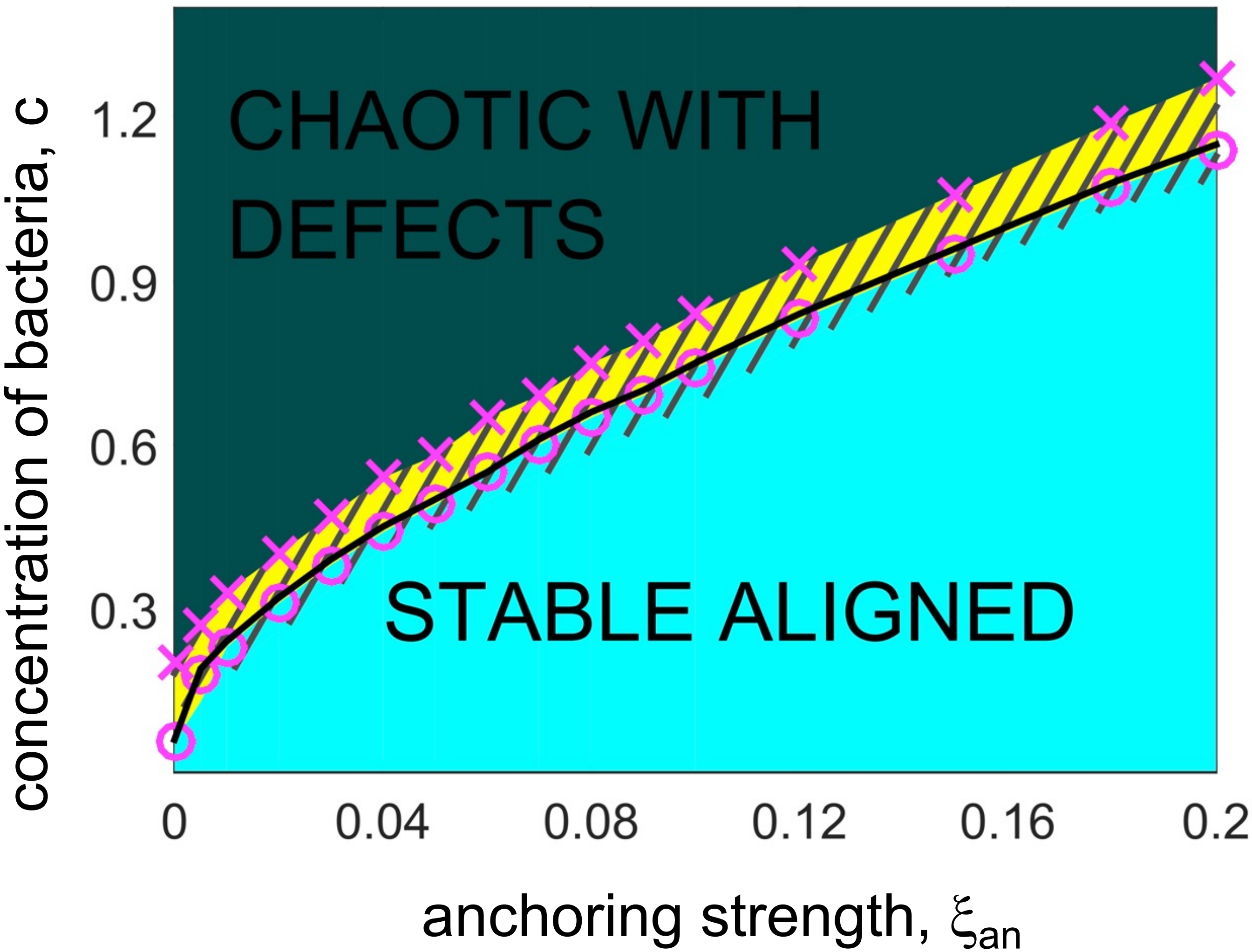

instability, near threshold

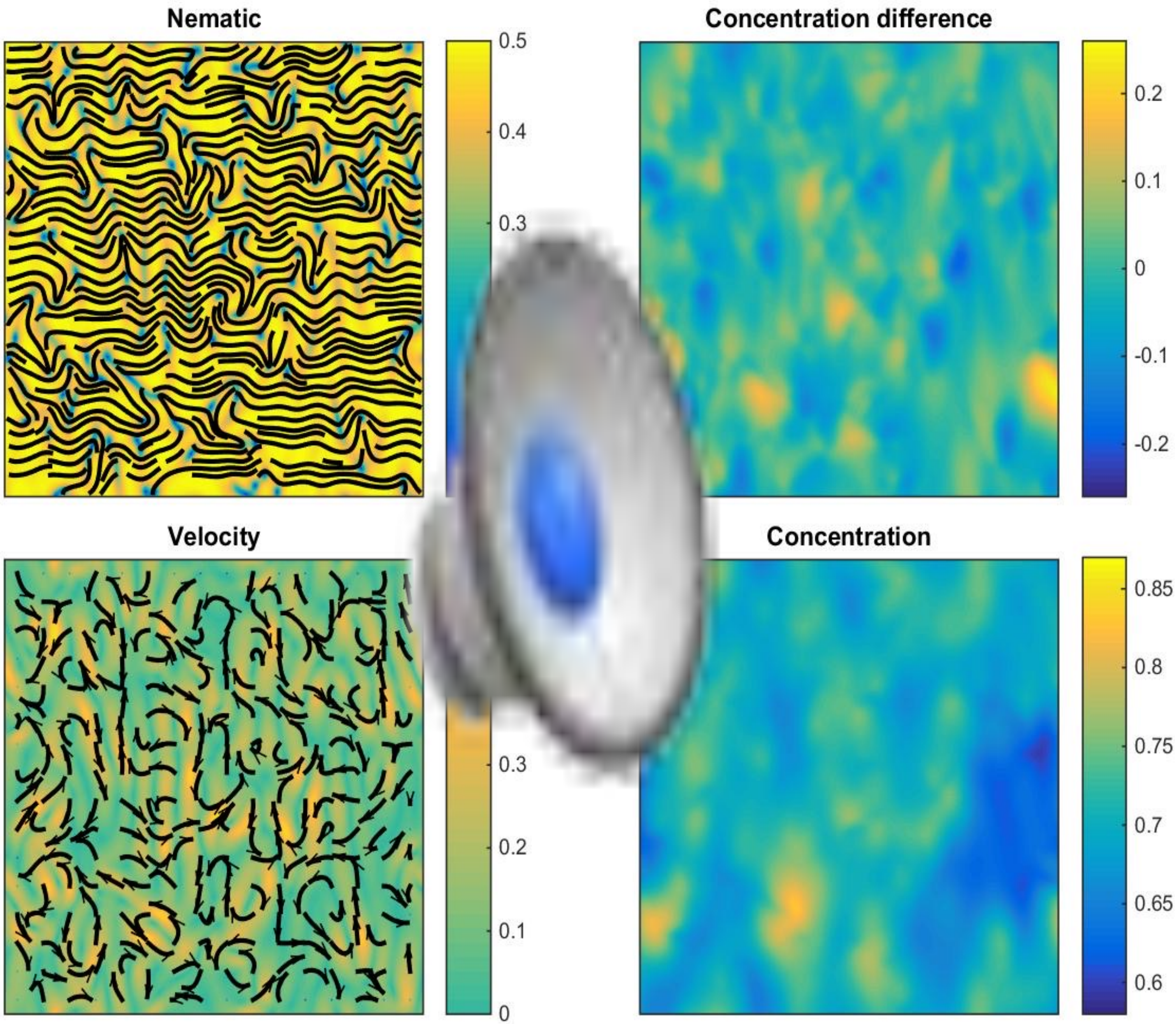

Anchoring, periodic modulations

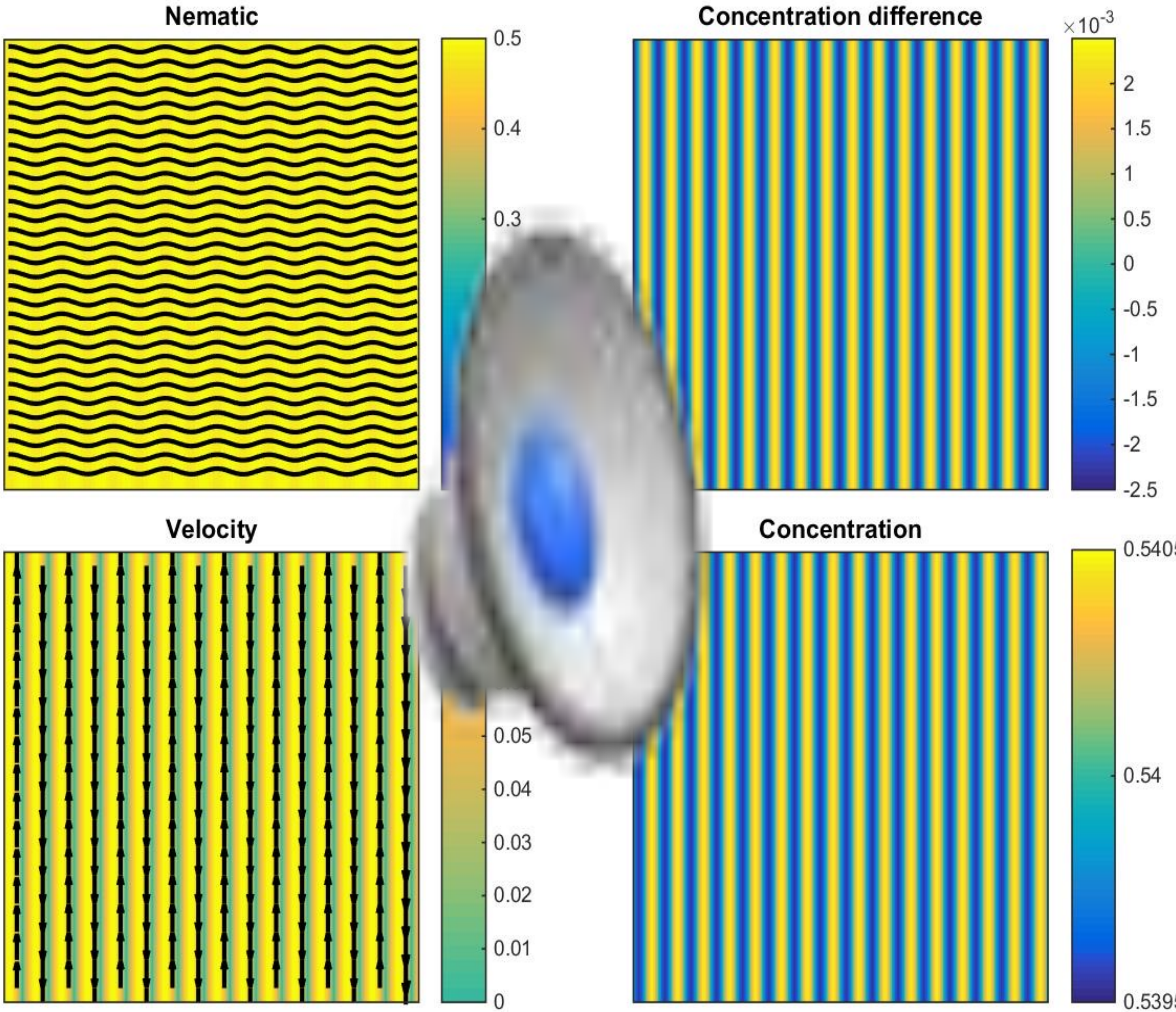

Strong anchoring, bound pairs

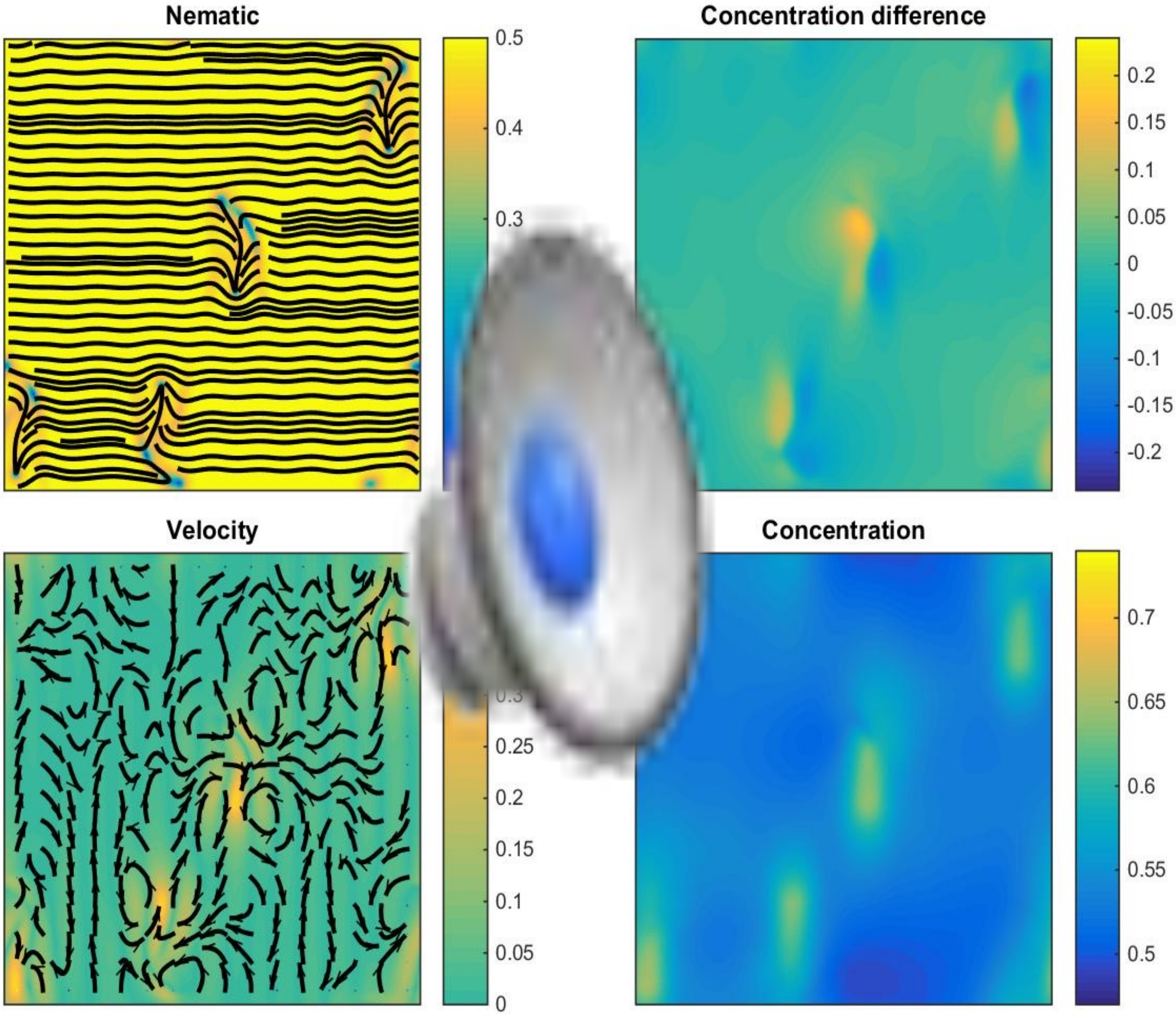

Topological defects in a nematic

Topological charge $$k = \frac{1}{2\pi} \oint_\gamma \nabla\theta \cdot d\mathbf{l}$$

θ orientation of director, γ contour

Integer defect (unstable)

Stable half-integer defects (disclinations)

k=1 k=1/2 k=-1/2

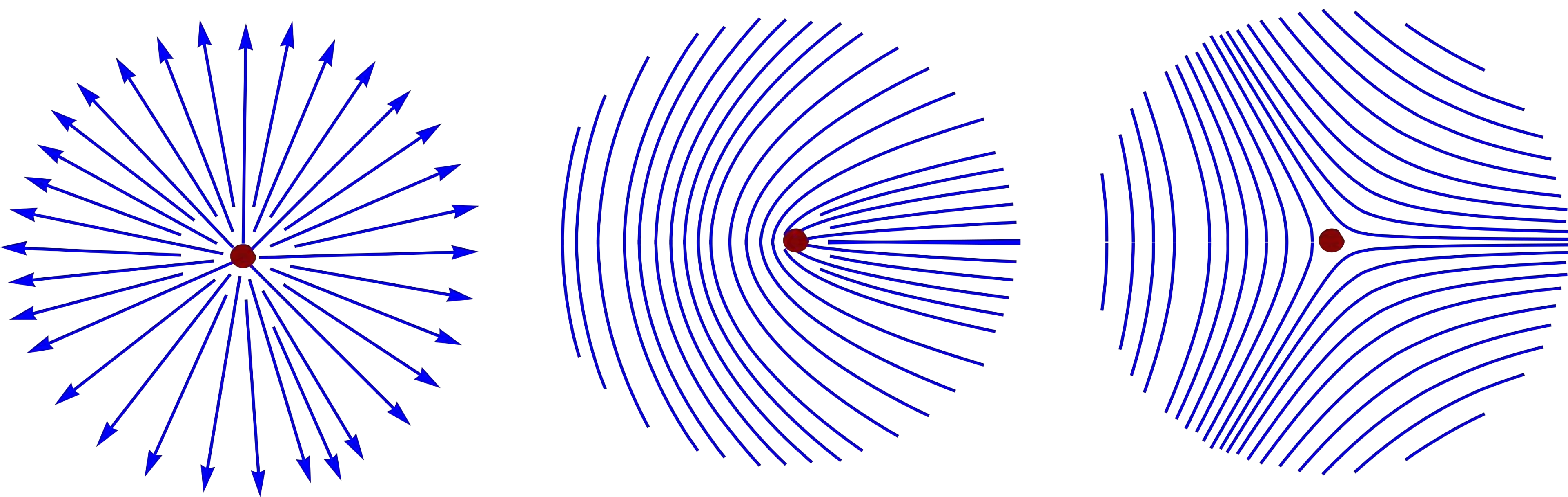

passive versus active nematic

<u>passive nematic</u>: isolated topological defects are immobile

<u>active nematic</u>: -½ defect is immobile (symmetry), but ½ defect moves spontaneously

½ defect: migration

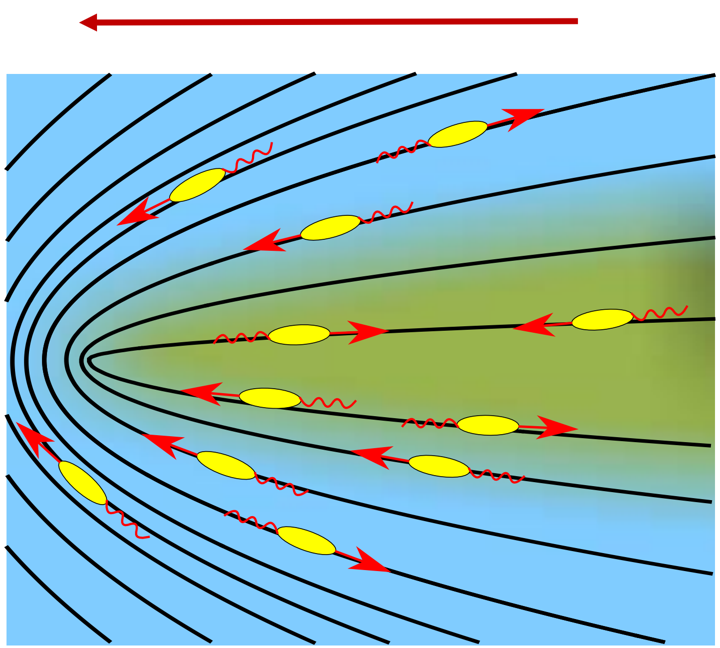

-½ defect: stationary

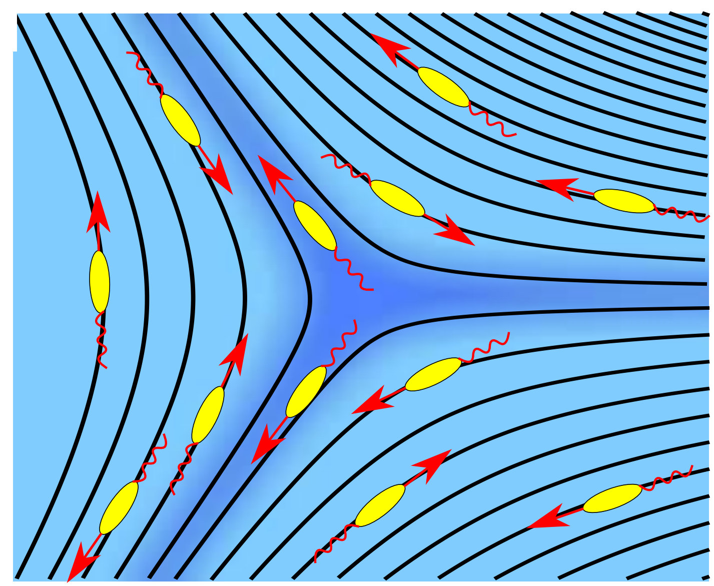

Defect’s statistics

- +1/2 defects persistently moving, -1/2 defects are immobile
- Gaussian velocity distributions for high concentrations
- Stretched exponential for low concentrations (1<ξ<2)

Defect’s speed

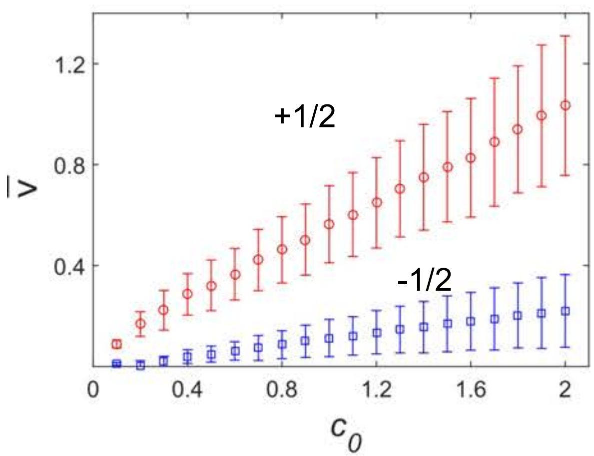

-1/2 defects

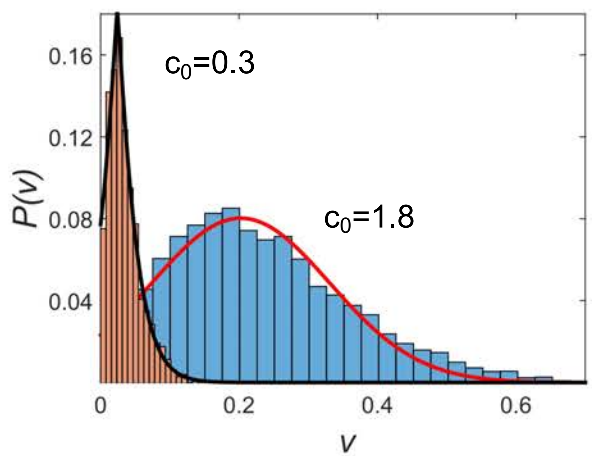

1/2 defects

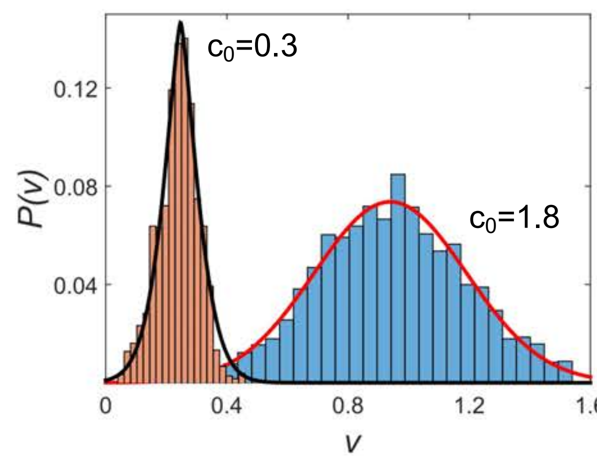

Accumulation/depletion of bacteria in the cores of defects
Relation between activity and topology

½ accumulation
-½ depletion

dependence on concentration

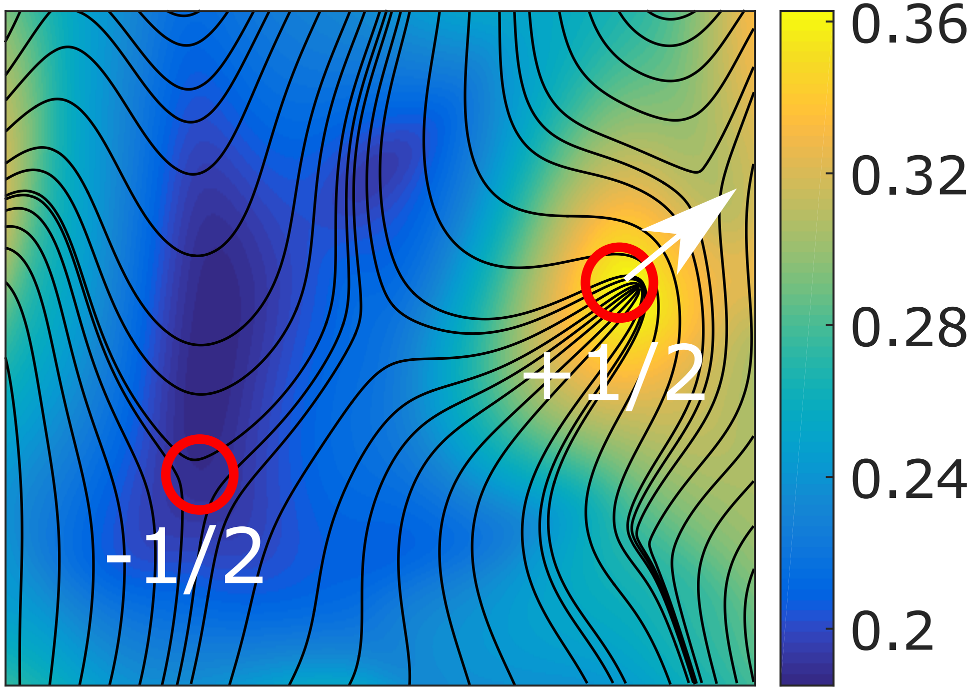

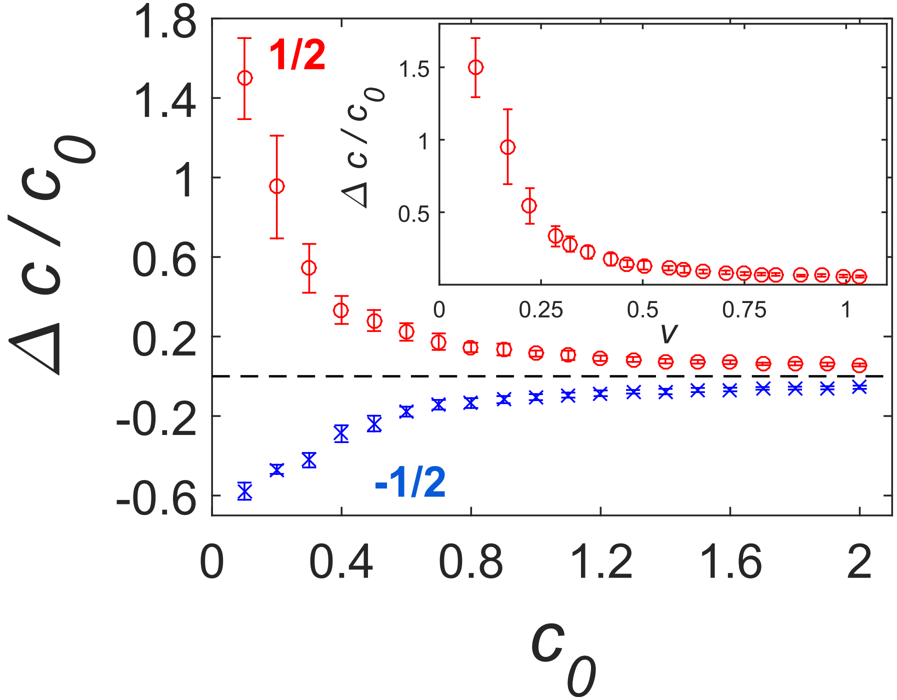

Accumulation/depletion

large reversal time

½ defect accumulation

-½ defect depletion

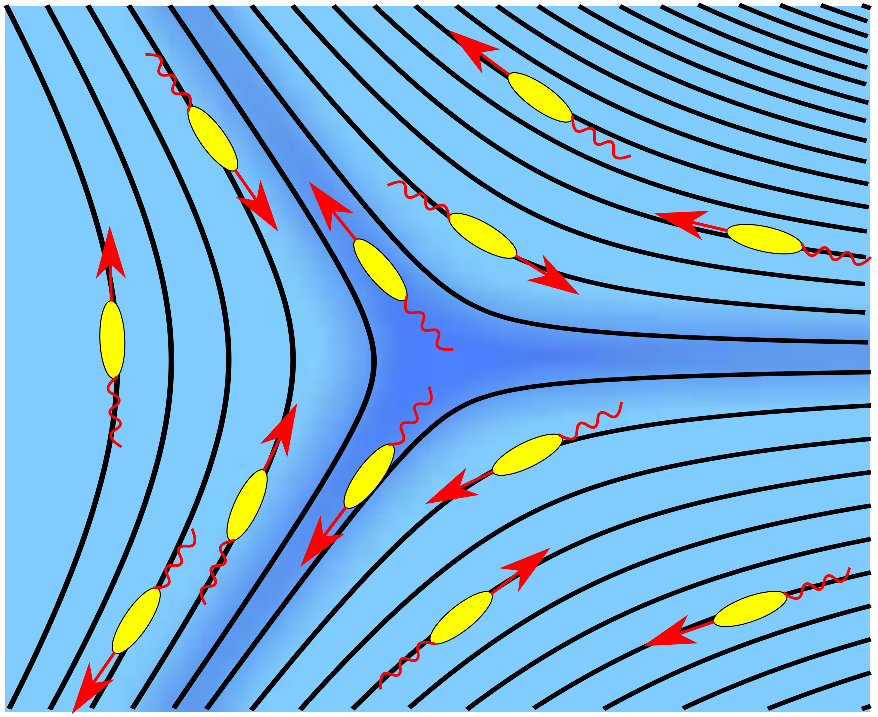

Topological defects and tissue dynamics

LETTER

doi:10.1038/nature22321

Topological defects control collective dynamics in neural progenitor cell cultures

Kyogo Kawaguchi[1,2,3], Ryoichiro Kageyama[4] & Masaki Sano[1,3]

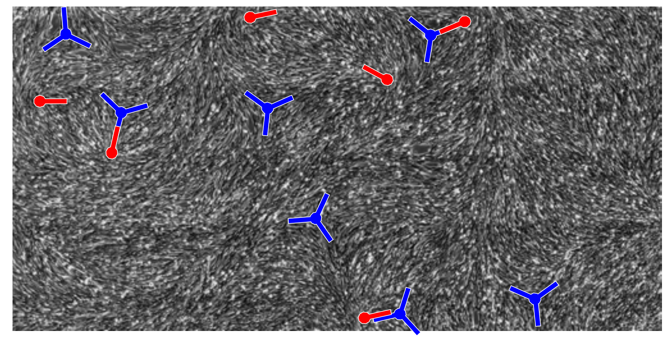

LETTER

doi:10.1038/nature21718

Topological defects in epithelia govern cell death and extrusion

Thuan Beng Saw[1,2]*, Amin Doostmohammadi[3]*, Vincent Nier[4], Leyla Kocgozlu[1], Sumesh Thampi[3,5], Yusuke Toyama[1,6,7], Philippe Marcq[4], Chwee Teck Lim[1,2], Julia M. Yeomans[3] & Benoit Ladoux[1,8]

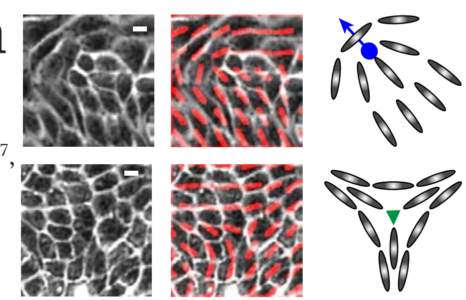

Simplified conservation law

$$c_\pm(x, y, t) \to c_\pm(x - Vt, y)$$

V - velocity of the defect
Discontinues flux of bacteria $V_0\mathbf{n}$
n= (cos(θ), sin(θ)), $\theta=\pm\varphi/2$ topological ±½ defect
φ – polar angle

$$\begin{aligned} -V\partial_x c_+ & \boxed{+ \quad V_0 \nabla \mathbf{n} c_+} = -\frac{c_+ - c_-}{\tau} + D_c \nabla^2 c_+ \\ -V\partial_x c_- & \boxed{- \quad V_0 \nabla \mathbf{n} c_-} = -\frac{c_- - c_+}{\tau} + D_c \nabla^2 c_- \end{aligned}$$

Additional boundary condition along the branch cut $\theta=\pm\pi/2$
Regularization removes discontinuity

Analytical solution for τ->0 (small reversal time)

$$c_{1/2} \approx c_0 + \frac{\tau V_0^2 c_0}{8 D_\mathrm{c}} \cos\varphi$$

$$c_{-1/2} \approx c_0 - \frac{\tau V_0^2 c_0}{24 D_\mathrm{c}} \cos 3\varphi$$

no accumulation /depletion

Numerical solution (large reversal time)

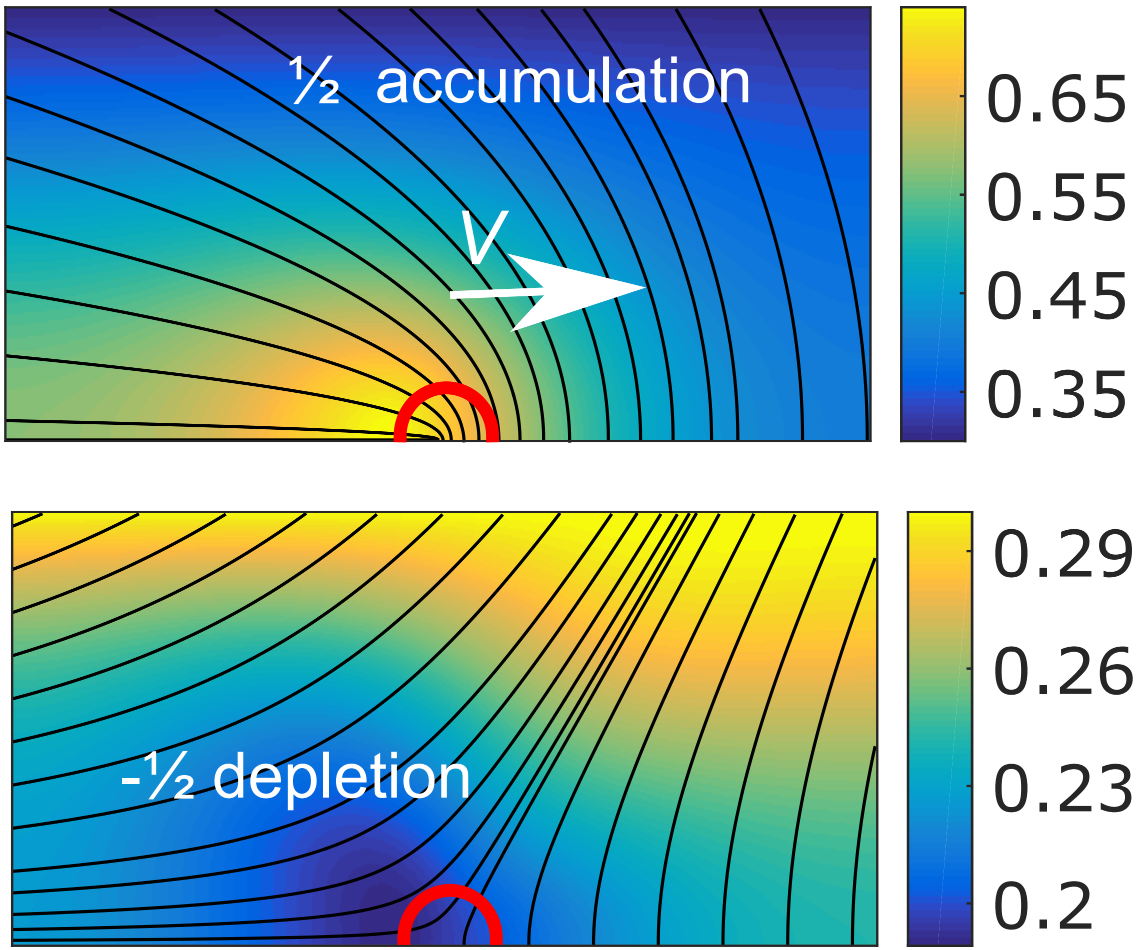

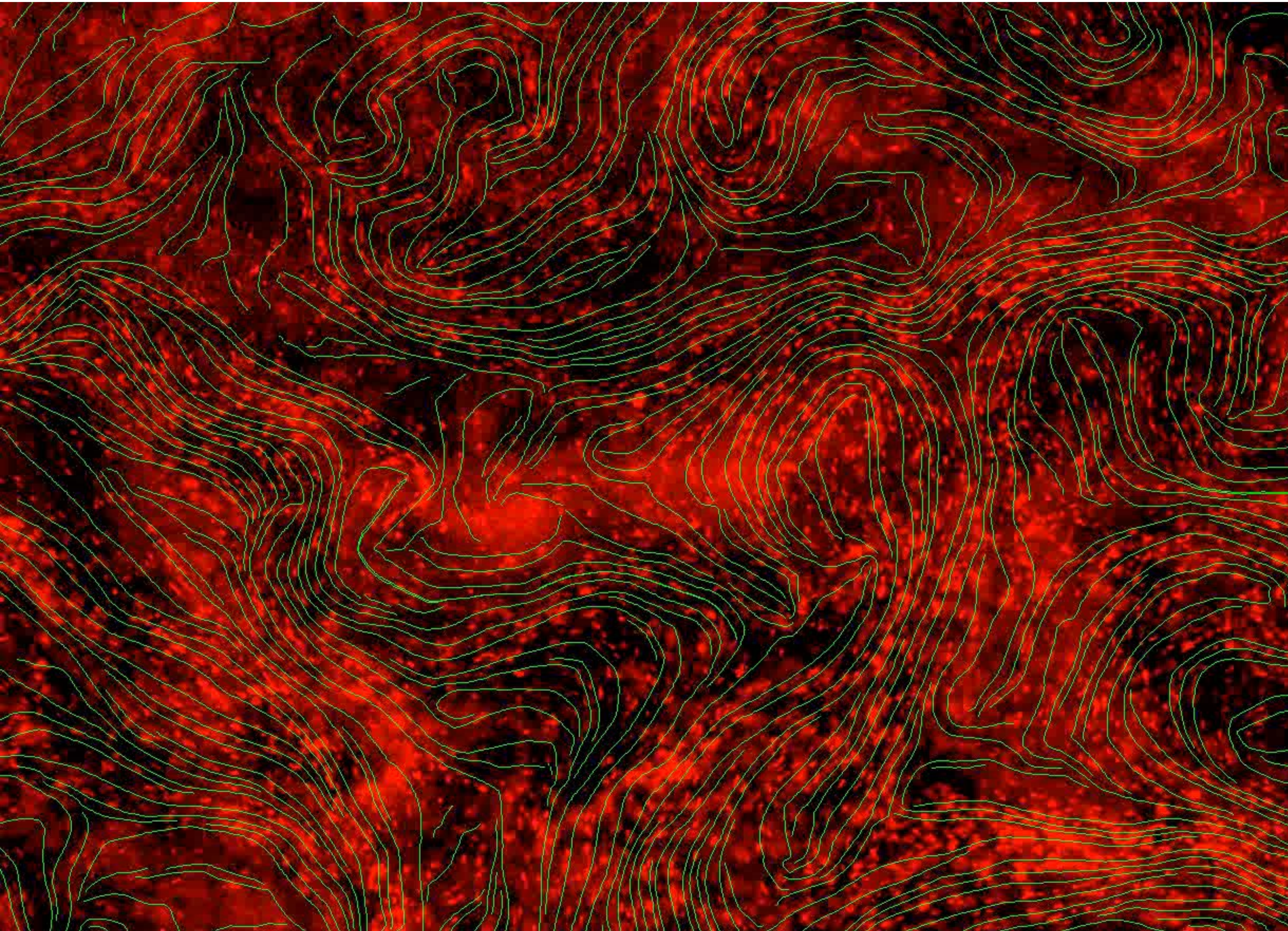

Comparison of theory and experiment

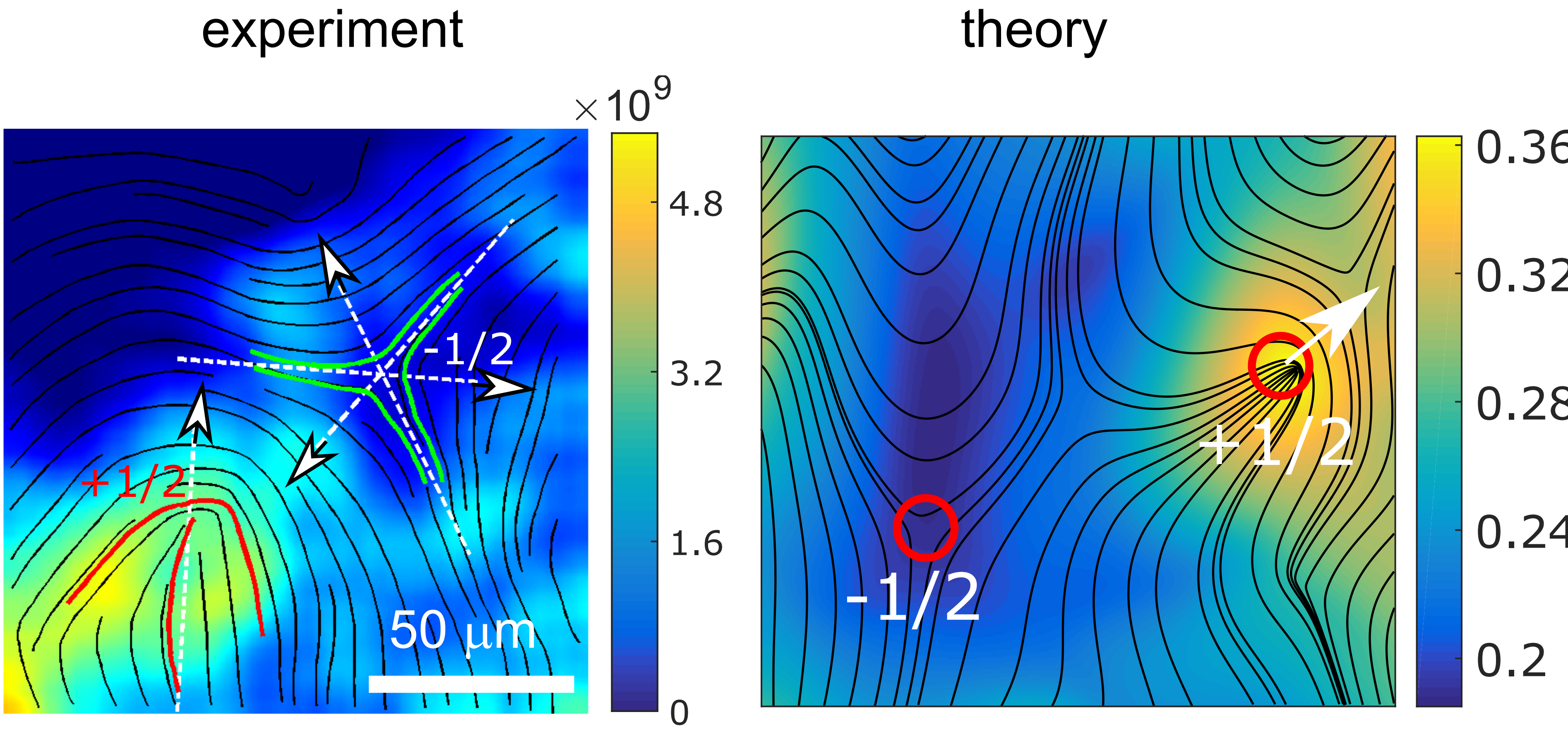

Tactoids and Turbulence

- Isotropic inclusions in nematic phase
- Shape, size, etc. is determined by interplay of tension on the I-N interface and elasticity of the nematic phase

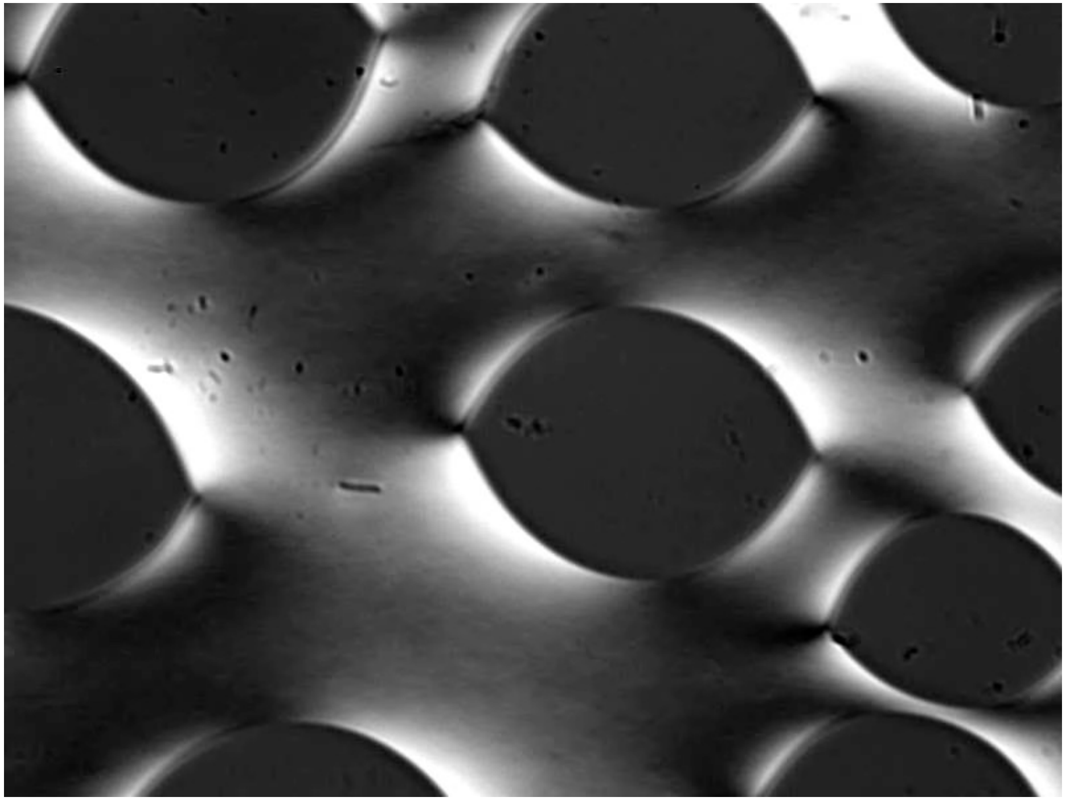

Numerical implementation of tactoids

- Landau-de Gennes free energy:

$$\mathcal{F} = \int dr^3 \left(-\frac{a}{2}\boldsymbol{Q}{:}\boldsymbol{Q} + \frac{c}{4}(\boldsymbol{Q}{:}\boldsymbol{Q})^2 + \frac{K}{2}\,(\nabla\boldsymbol{Q}{:}\nabla\boldsymbol{Q}) \right)$$

- Equilibrium amplitude of the OP:

$$q = \begin{cases} \sqrt{\dfrac{a}{2c}}, & a > 0, c > 0 \\ q = 0, & a < 0, c > 0 \end{cases}$$

- Set $q = 0$ in I phase, $q \neq 0$ in N phase
- Set normal to the surface parallel to the gradient of the OP

- Tactoids shape is dynamically adjusted
- Planar and homeotropic anchoring

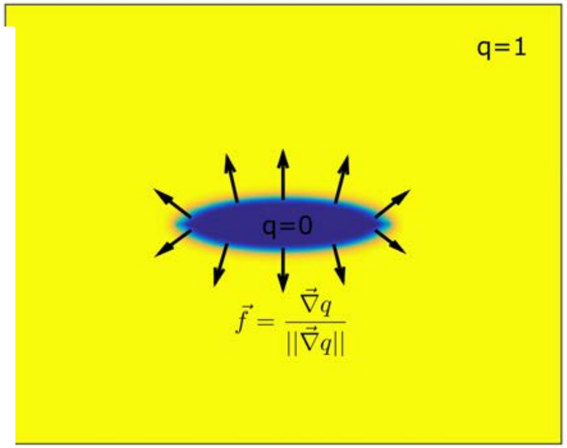

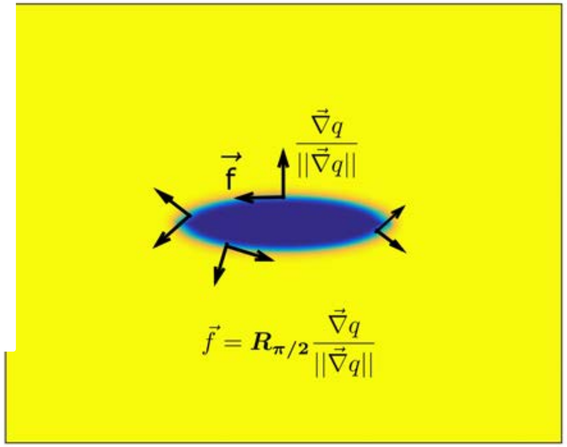

Genkin, Sokolov, IA, NJP , 2018

Enforcing the alignment

- Typically, a planar alignment on the tactoid's surface
- Alignment enforced by the Rapini-Papoluar condition

(equivalent to Robin b.c.)

$$\sigma = w(\theta_0 - \theta)^2$$

- θ_0 – easy direction
- w – strength of anchoring
- σ – surface energy
- Here we introduce surface anchoring on the diffused interface via an external force F_{exter}

Numerical integration

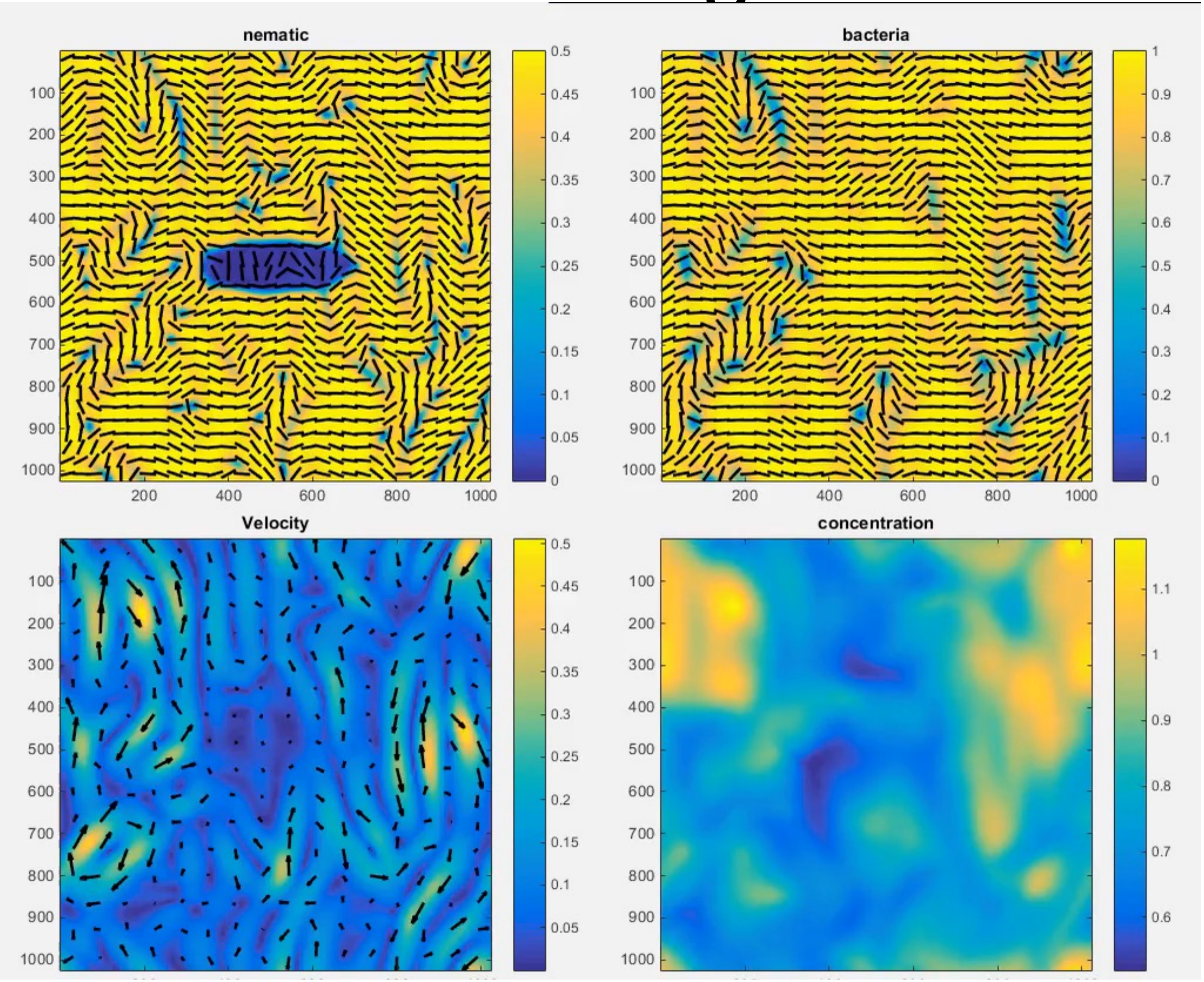

Results

- Tactoids carry non-zero average topological charge
- Strong fluctuations
- Topological charge first increases, then decreases with the bacteria concentration
- Topological charge increases with tactoid's size

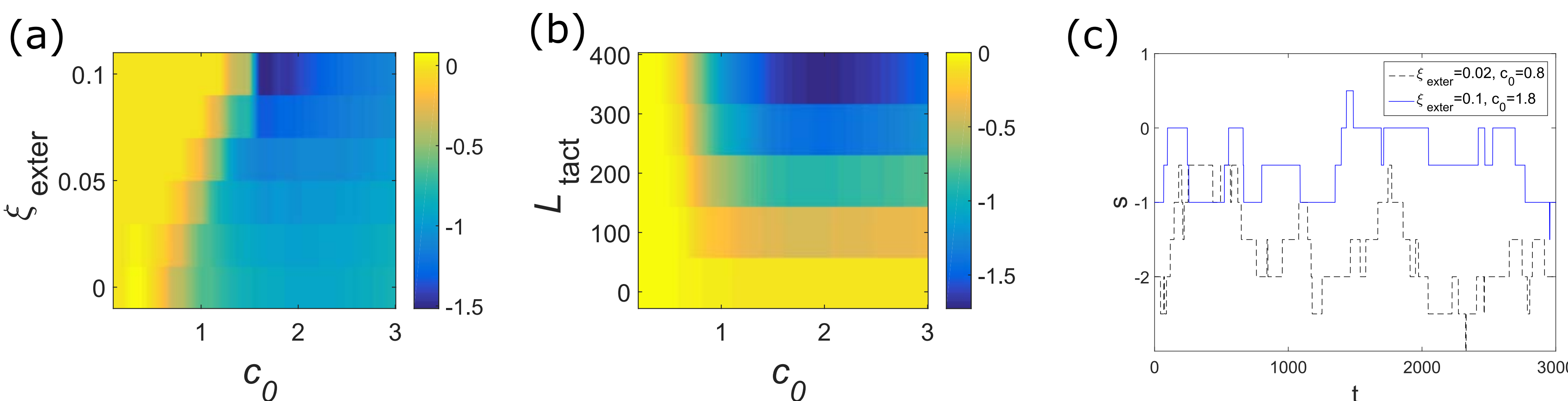

Different defect mobility→ charging

- Charging of tactoids due to different mobility of $\pm 1/2$ defects
- Topological defects with the same sign attract and with different repel
- $+1/2$ defects have higher mobility
- Potential barrier at the I-N interface
- P^{+}, P^{-} concentrations of + and – defects
- P^{+}, P^{-} proportional to bact concertation c_0

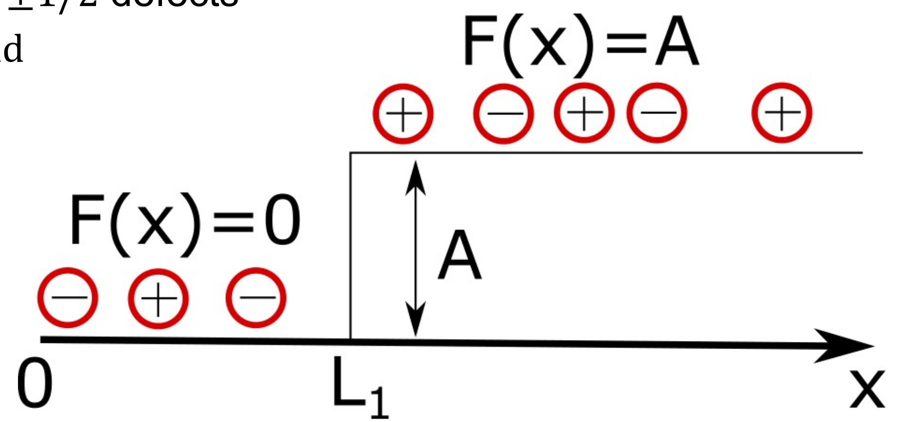

$$\partial_t P^{+} = D^{+}\partial_{xx}P^{+} - \partial_x\left(\left(-F'(x) + \mu\int_0^{\infty}\frac{P^{+}(x',t) - P^{-}(x',t)}{x - x'}dx'\right)P^{+}\right)$$
$$\partial_t P^{-} = D^{-}\partial_{xx}P^{-} - \partial_x\left(\left(-F'(x) + \mu\int_0^{\infty}\frac{P^{-}(x',t) - P^{+}(x',t)}{x - x'}dx'\right)P^{-}\right)$$

Asymptotic solution

- Steady-state equation for P^-:

$$D^-\partial_{xx}P^- - \partial_x\left(\left(-F'(x) + \mu\int_0^\infty \frac{P^-(x') - P_0}{x - x'}dx'\right)P^-\right) = 0$$

- Solution for weak interaction: $\mu = \varepsilon\mu_1,\ \ P^- = P_0^- + \varepsilon P_1^- + \cdots$

$$s = P_0\left(1 - e^{A/D^-}\right)\left(1 - \frac{\mu}{D^-}P_0\log(L/L_1)e^{A/D^-}\right)$$

- Describes both isotropic and nematic tactoids

Experimental Verification

- LC is quenched in the biphasic domain by rapid heating
- Bacteria orientation is extracted from the microscopy images
- 17 tactoids are processed

Comparison with the theory

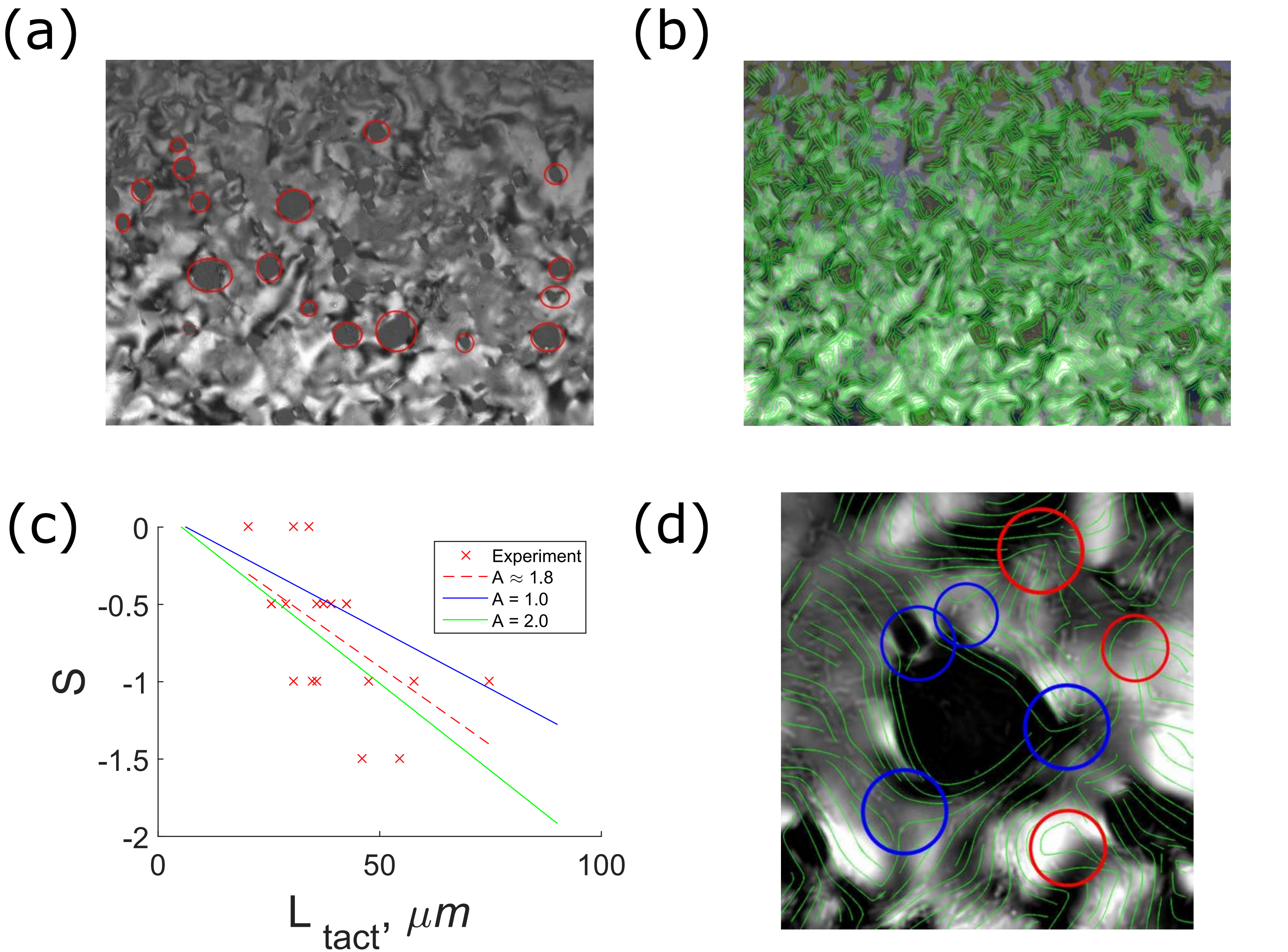

Pinning of active topological defects

- Periodic array of artificial obstacles
- Only negative defects are pinned
- Positive defects freely move

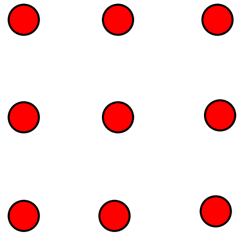

Combing bacterial turbulence

- 3D printed pillar arrays with different spacing
- Two photon laser lithography system Nanoscribe, resolution 200 nm

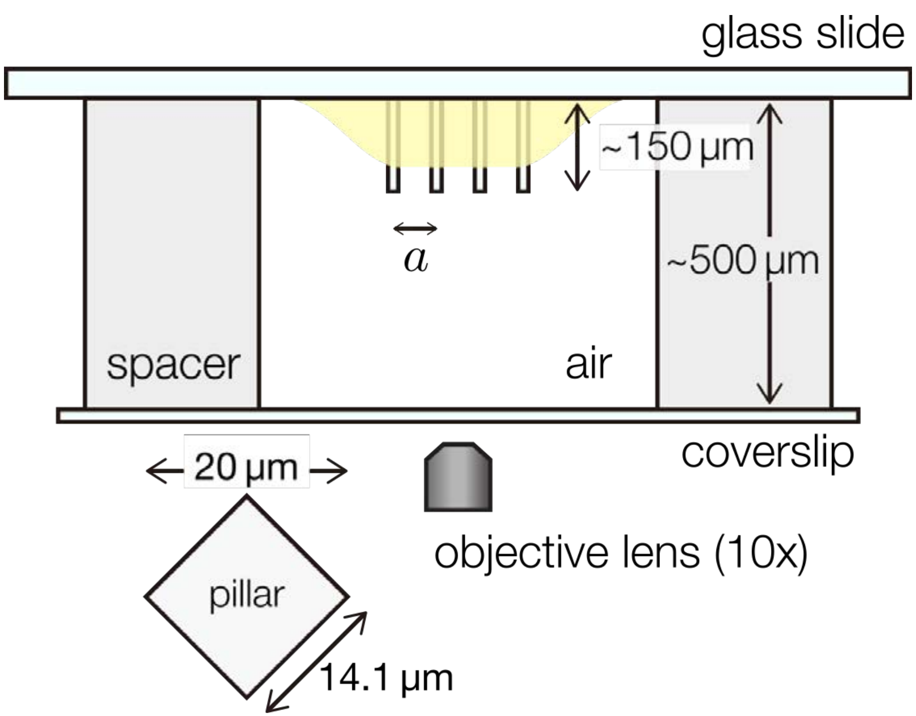

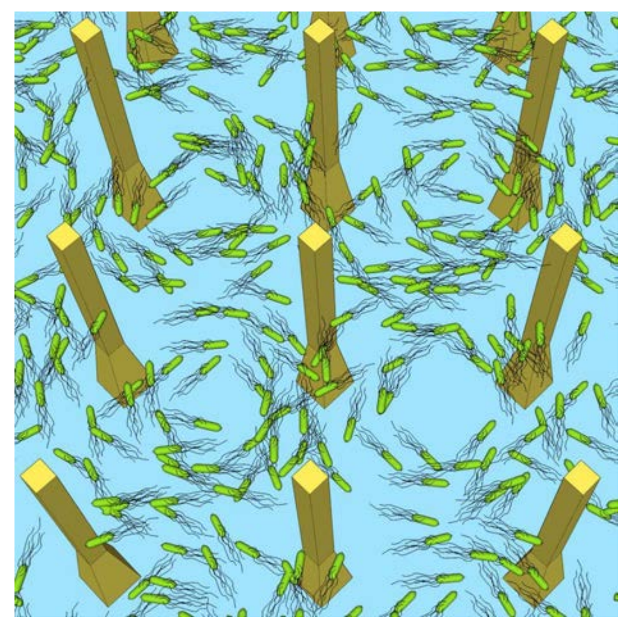

Nishiguchi et al IA, Nature Comm 2018

Pillars in Liquid Crystals

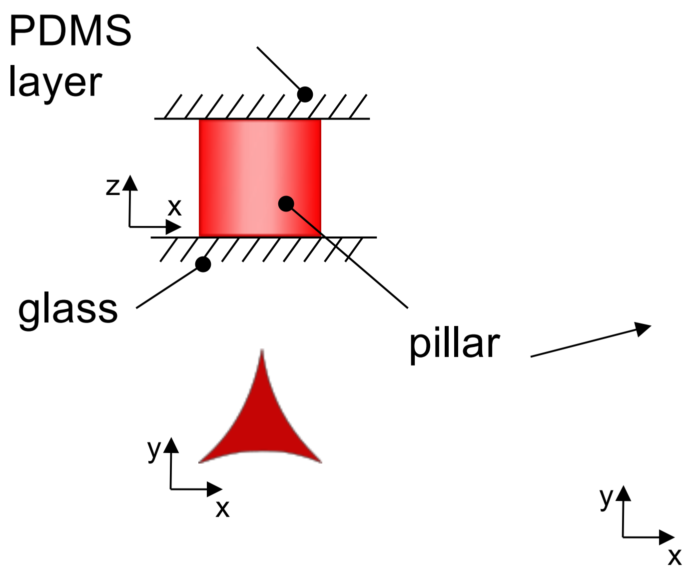

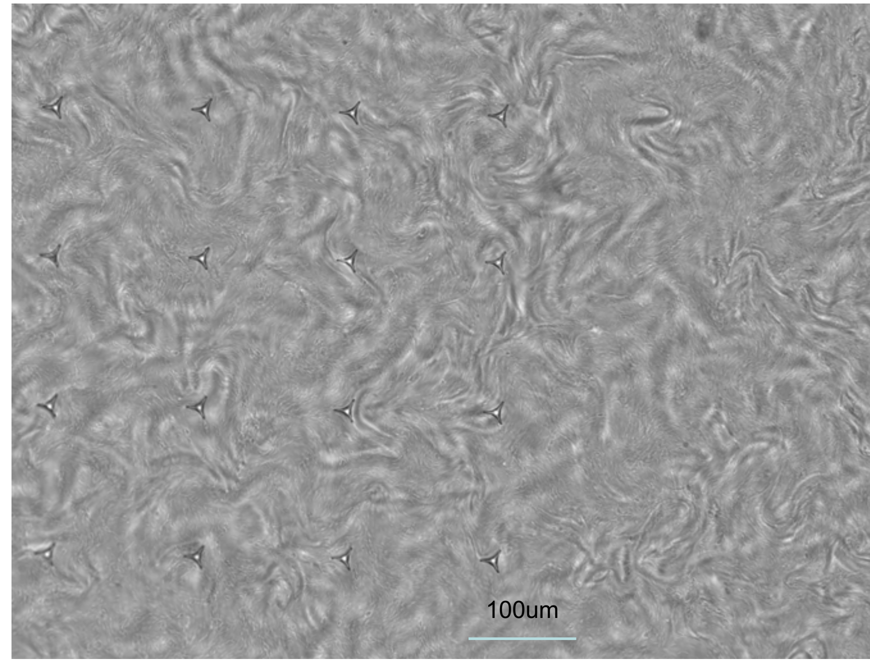

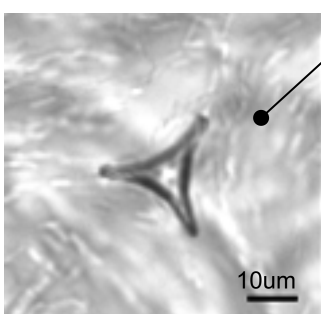

Bacillus
subtilis
+
DSCG

Pillar

Nematic
field lines

Nematic defects
+1/2
-1/2

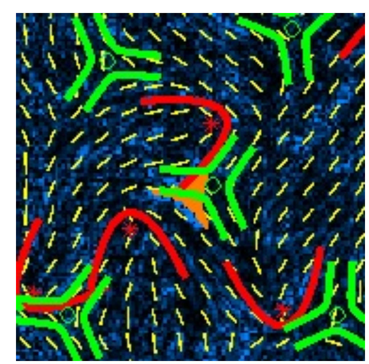

With vs Without Pillars

Average along Y

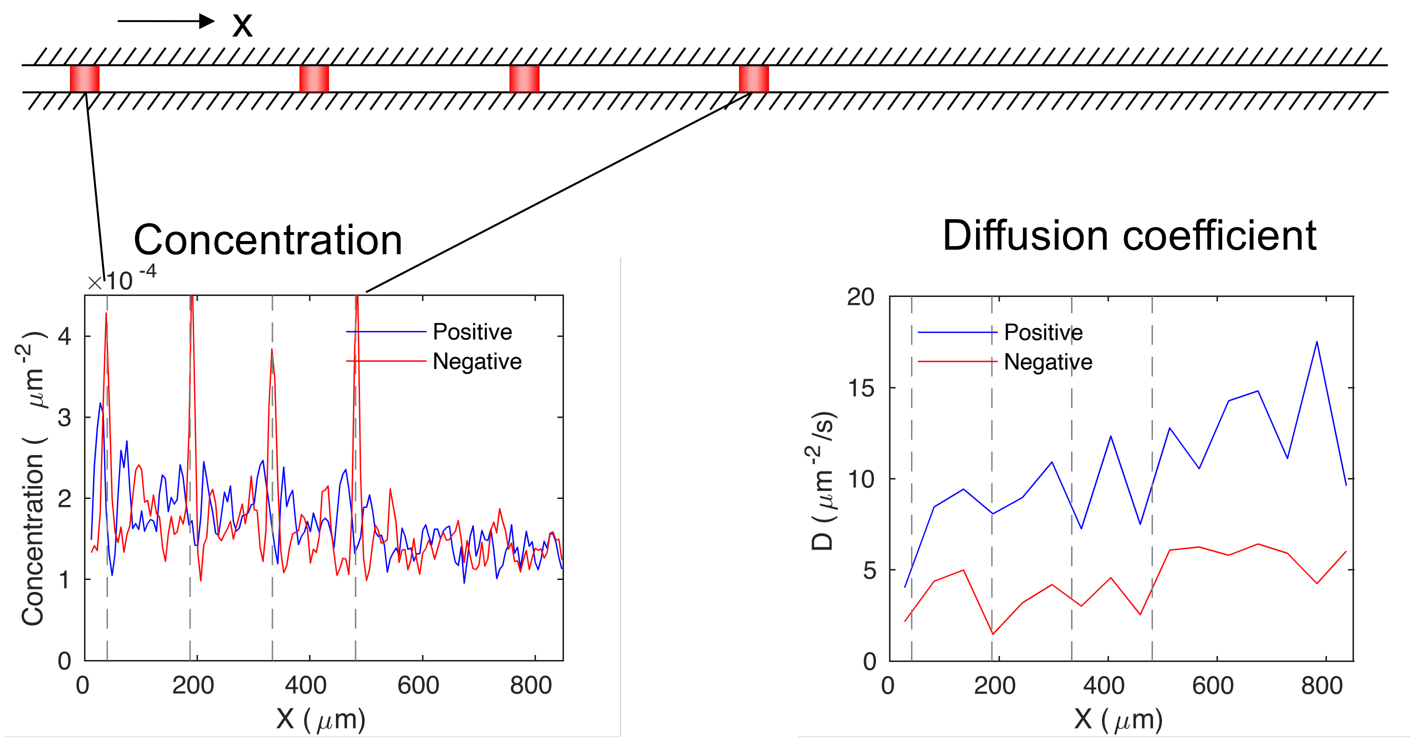

Concentration around pillars

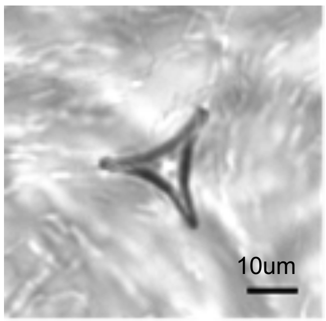

-1/2

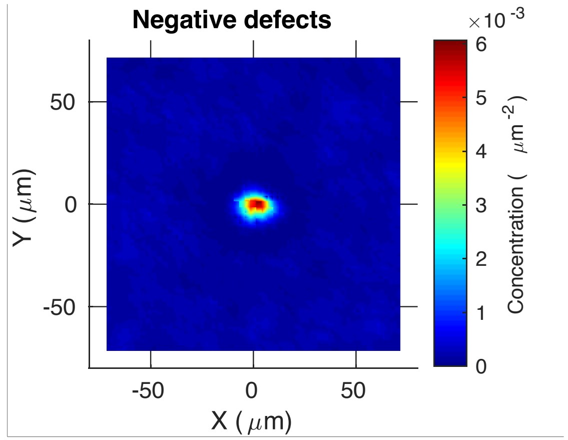

+1/2

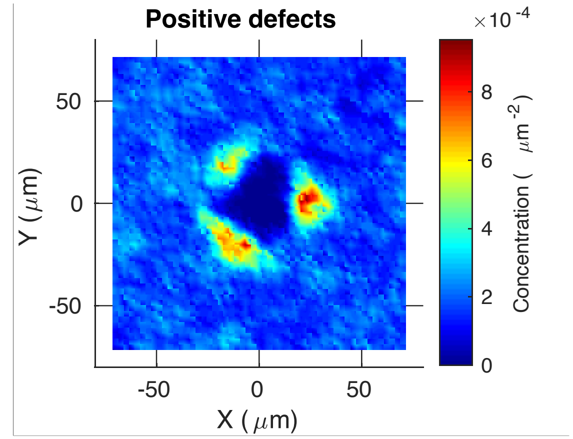

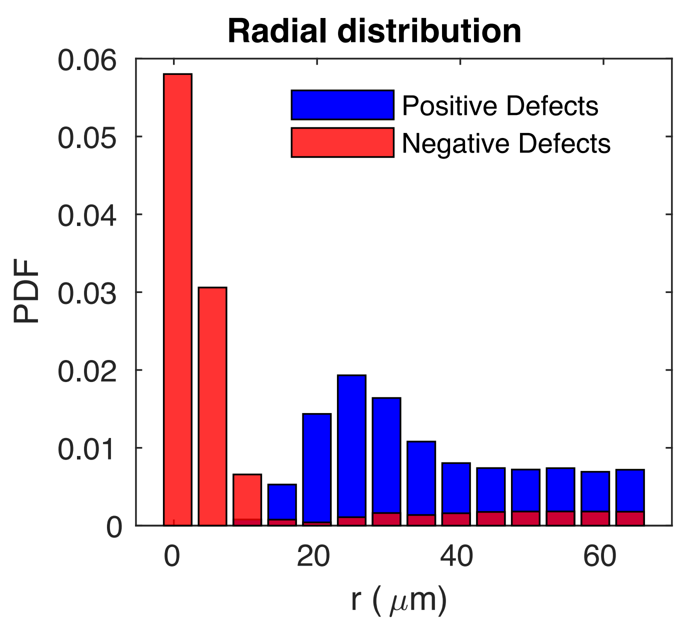

Simulation results

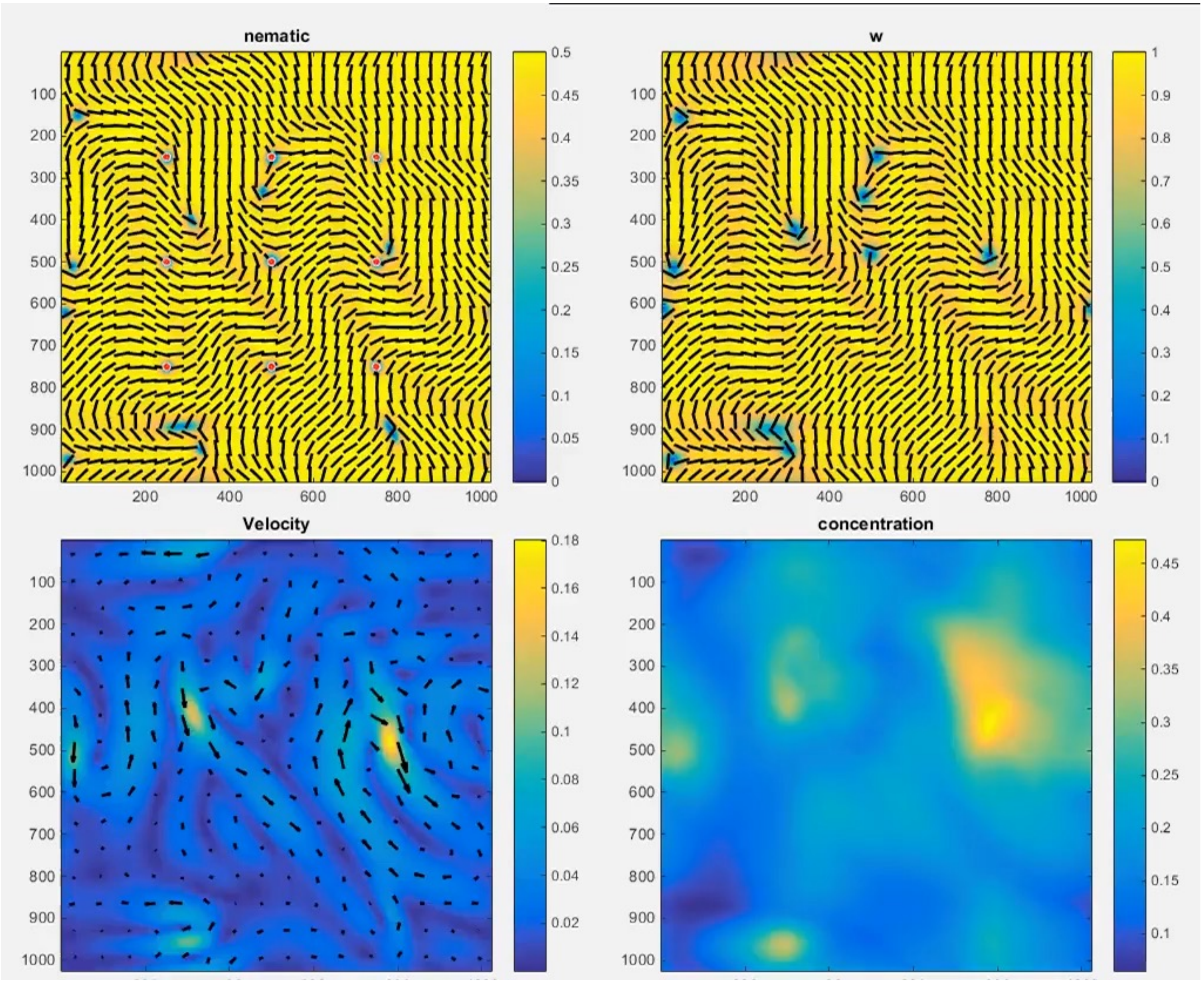

Simulation results

-1/2

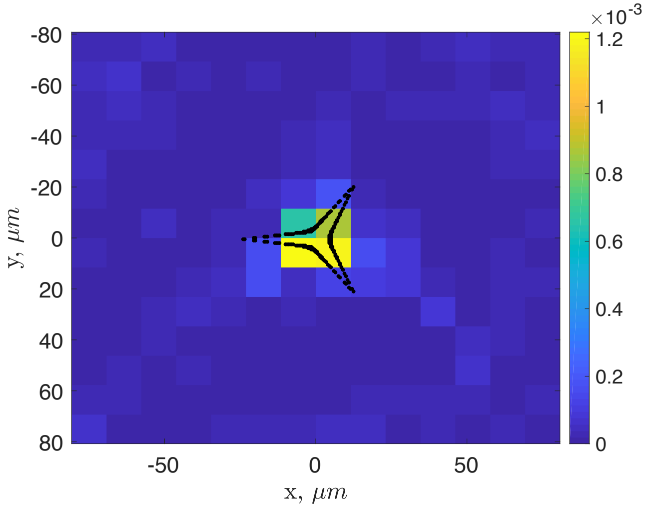

1/2

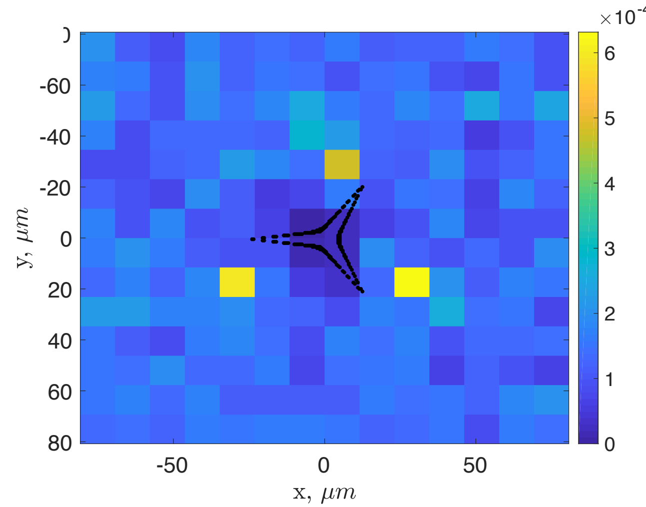

Radial PDF

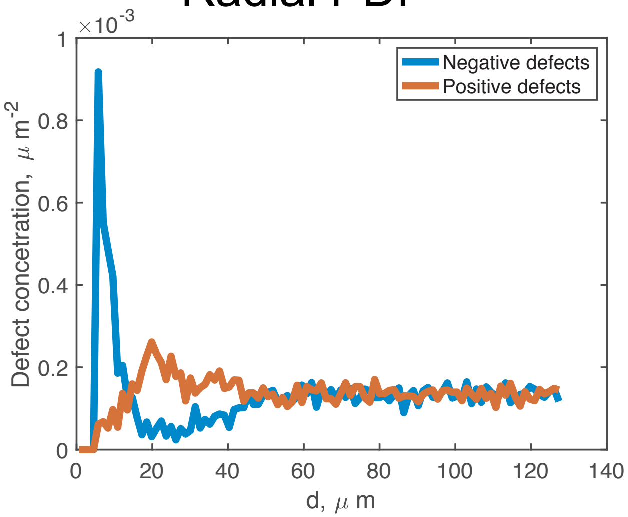

Diffusivity

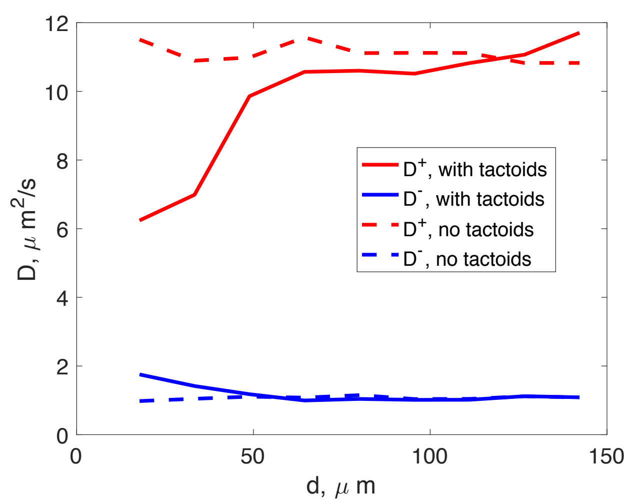

Formation of Polar Bacterial Jets

Photo-patterned nematic: Arrays of C-stripes

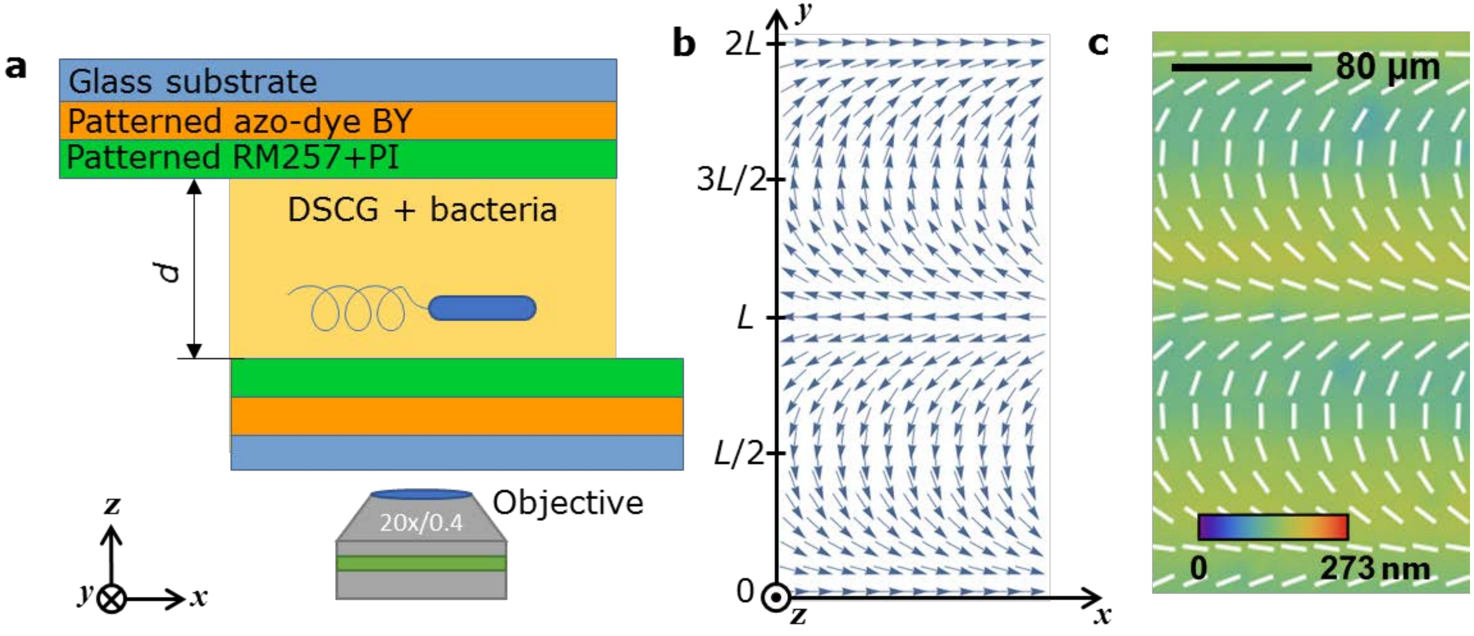

Taras Turiv, Runa Koizumi, Kristian Thijssen, Mikhail M. Genkin, Hao Yu, Chenhui Peng,
Qi-Huo Wei, Julia M. Yeomans, Igor S. Aranson, Amin Doostmohammadi, Oleg D. Lavrentovich, Nature Physics 2020

Director pattern

$$\hat{\mathbf{n}}_0 = \left[\cos\left(\pi y / L\right), -\sin\left(\pi y / L\right), 0\right]$$

Pure splay deformations are located at

$$y = 0, \pm L, \pm 2L, \ldots$$

Bend Deformations

$$y = \pm L / 2, \pm 3L / 2, \ldots$$

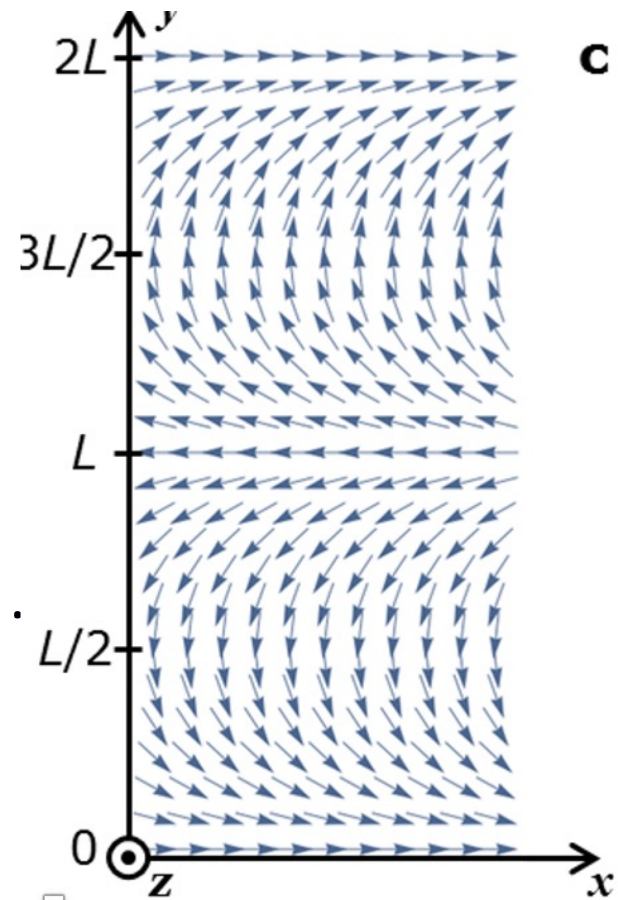

Raw images of bacteria

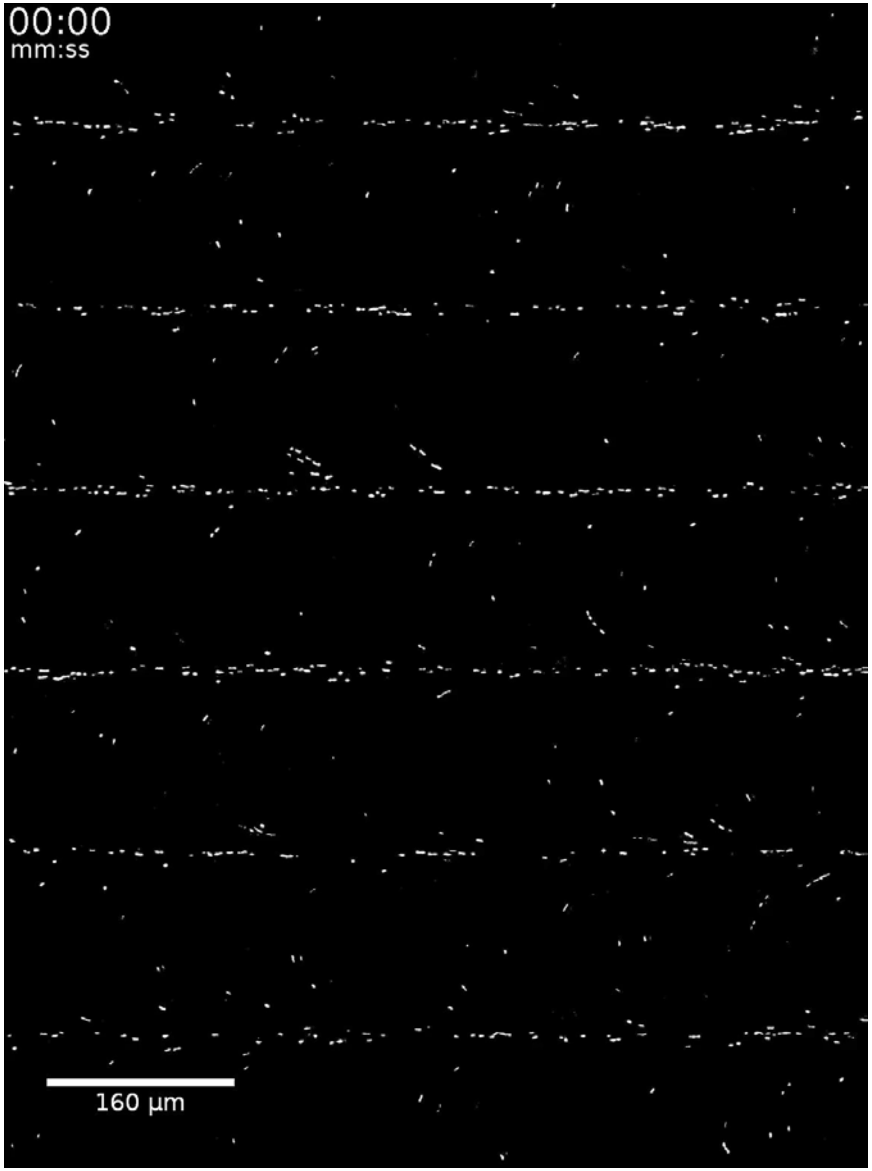

Undulations for higher concentration

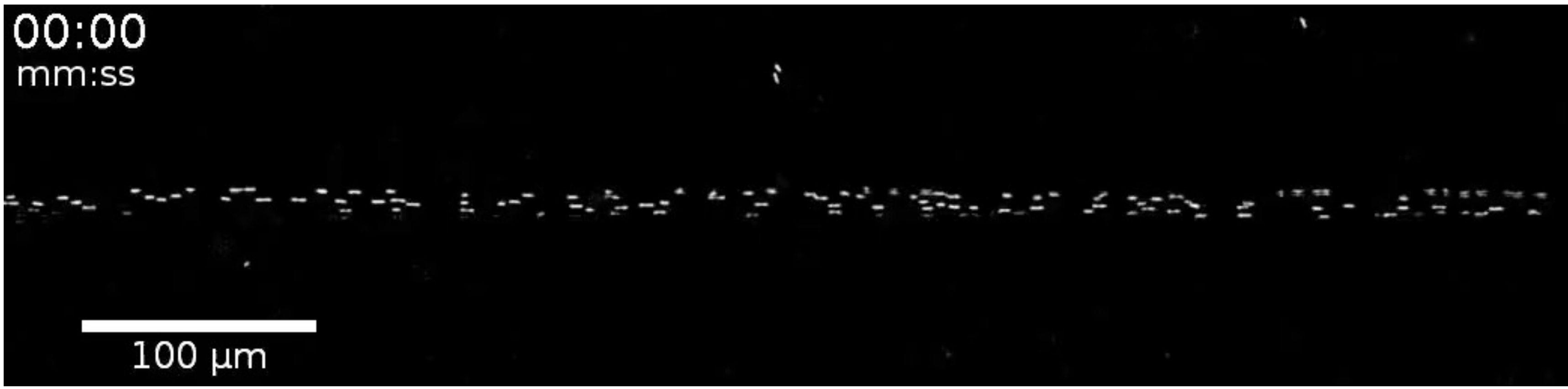

Bacteria Condense in Polar Jets

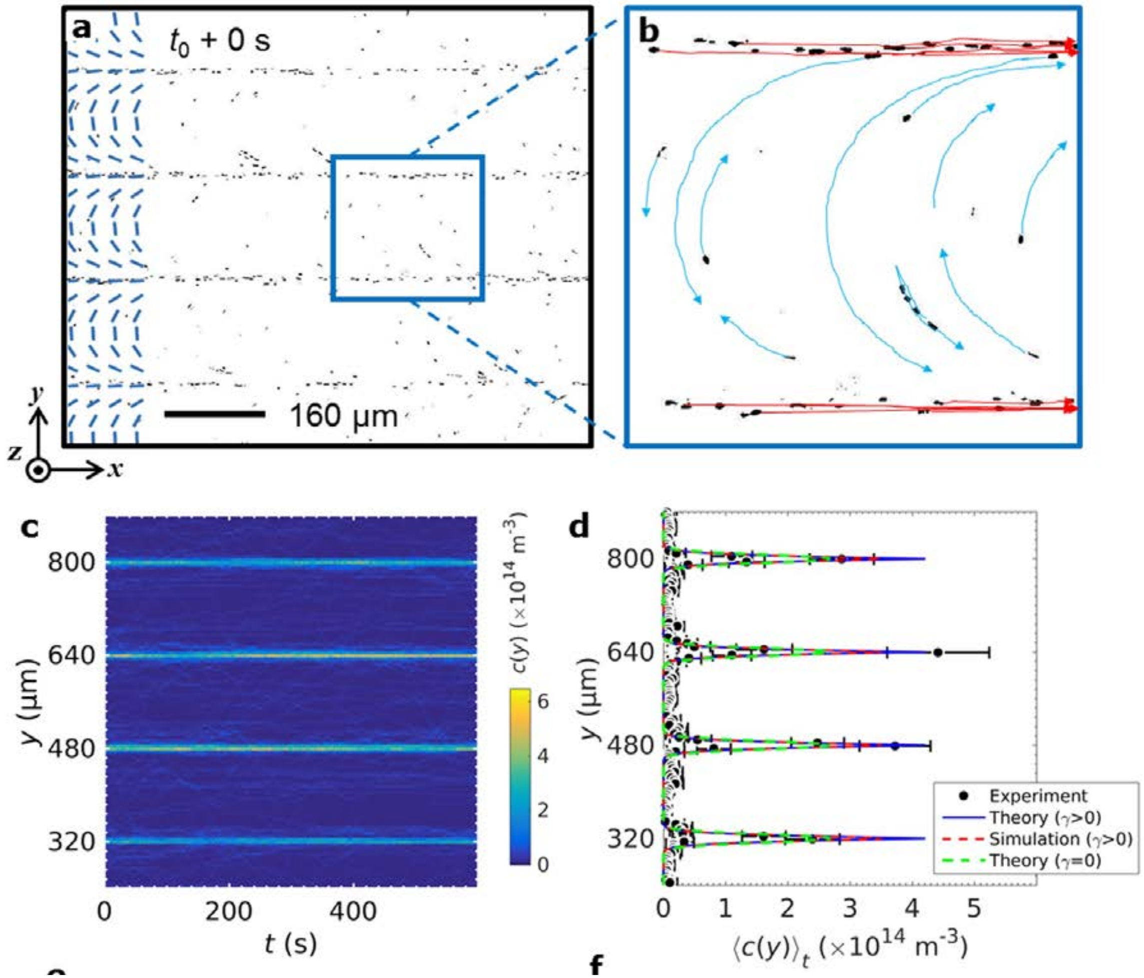

Theoretical understanding: two bacterial populations

$$\partial_t c^{\pm} + \nabla \cdot \left(\pm v_0 \hat{\mathbf{n}} c^{\pm} + \mathbf{v}_f c^{\pm} \right) = \mp \frac{c^{+} - c^{-}}{\tau} + D_c \nabla^2 c^{\pm}$$

- Infinite reversal time τ
- Neglect fluid flow
- Stationary solution
- Very dilute suspension – no realigning effect

Suppression one of the population

- Analytical result

$$c^{\pm} = C^{\pm}\exp\left(\pm\frac{v_0 L}{\pi D_c}\cos\frac{\pi y}{L}\right)$$

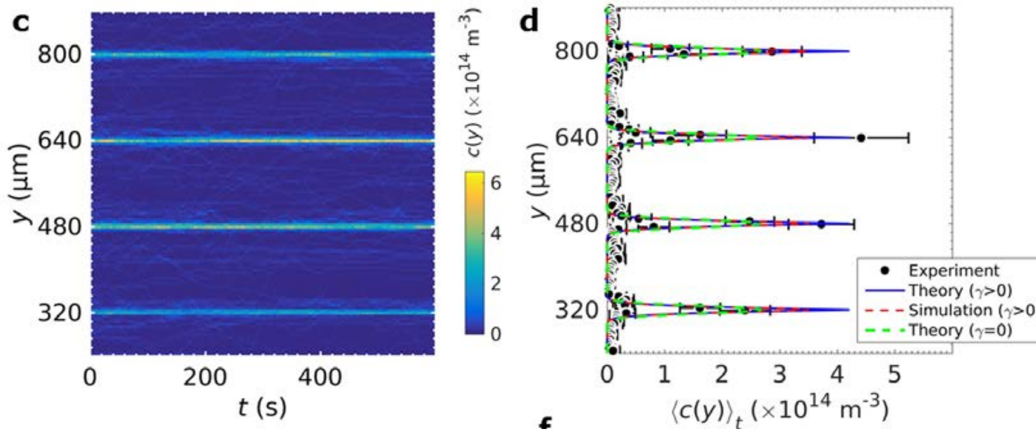

- c^+ population is exponentially amplified
- c^- population is exponentially suppressed
- However, the peaks are not sharp

Less dilute suspension: realignment of director by bacteria

$$\partial_t \hat{\mathbf{n}} = -\hat{\mathbf{n}} \times \hat{\mathbf{n}} \times \left(\alpha \hat{\mathbf{n}}_0 + \gamma \mathbf{F} \right)$$

Landau-Lifshitz equation ensures $\hat{\mathbf{n}}^2 = 1$

$\hat{\mathbf{n}}_0$ prescribed director

$\mathbf{F} = \nabla \cdot \boldsymbol{\sigma}$ active force created by bacteria

$\boldsymbol{\sigma} \sim c\mathbf{Q}$ – active stress, $\mathbf{Q}$ – nematic OP

Solution with sharp peaks

$$c^{+}=-\frac{W\left\{-\dfrac{\gamma v_0 U_0}{aD_c}C^{+}\exp\left[\dfrac{v_0 L}{\pi D_c}\cos(ky)\right]\cos(2ky)\right\}}{\dfrac{\gamma v_0 U_0}{aD_c}\cos(2ky)}$$

W – Lambert W function

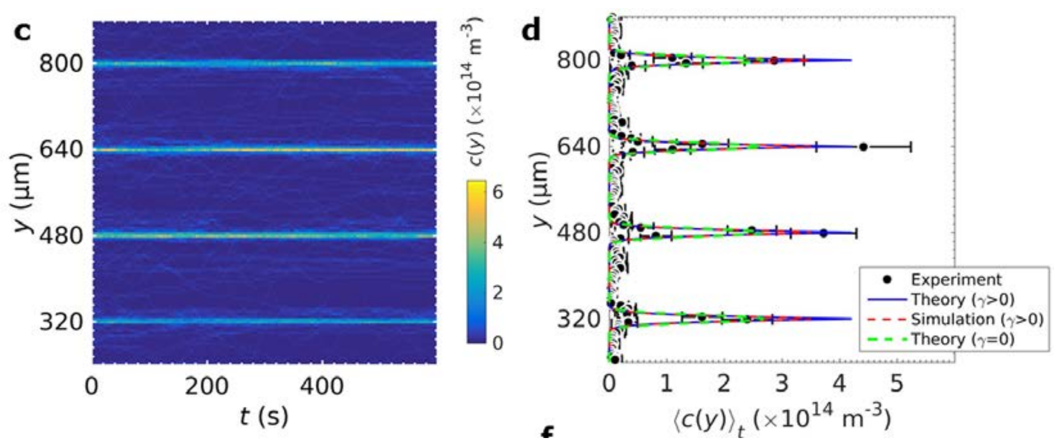

Results of comp modeling

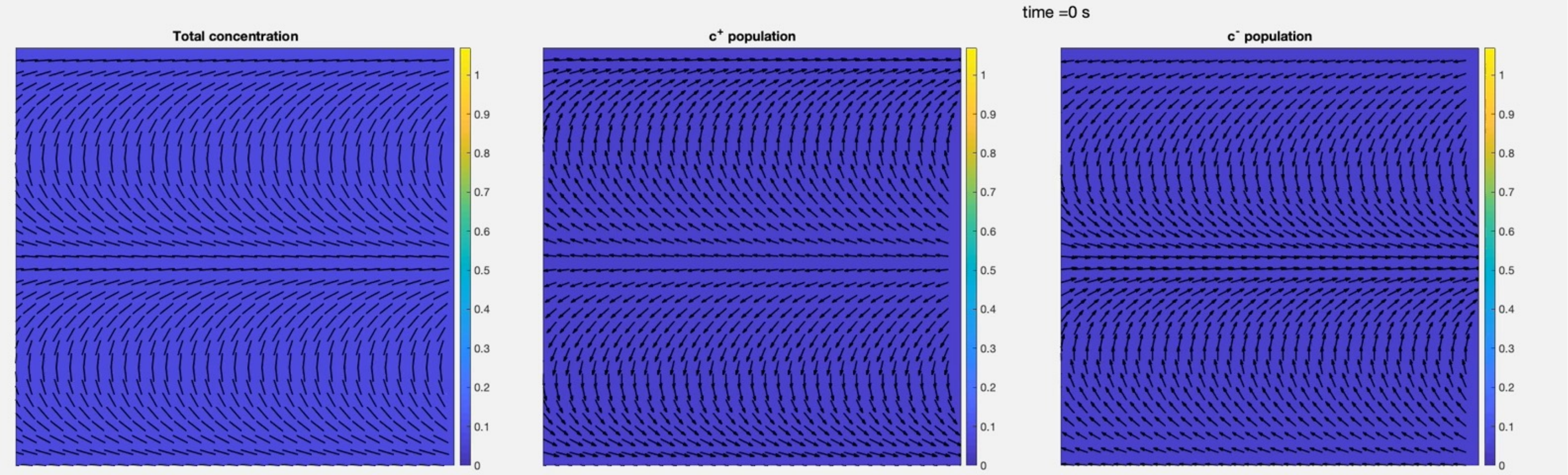

Control of bacteria by spiral nematic vortices

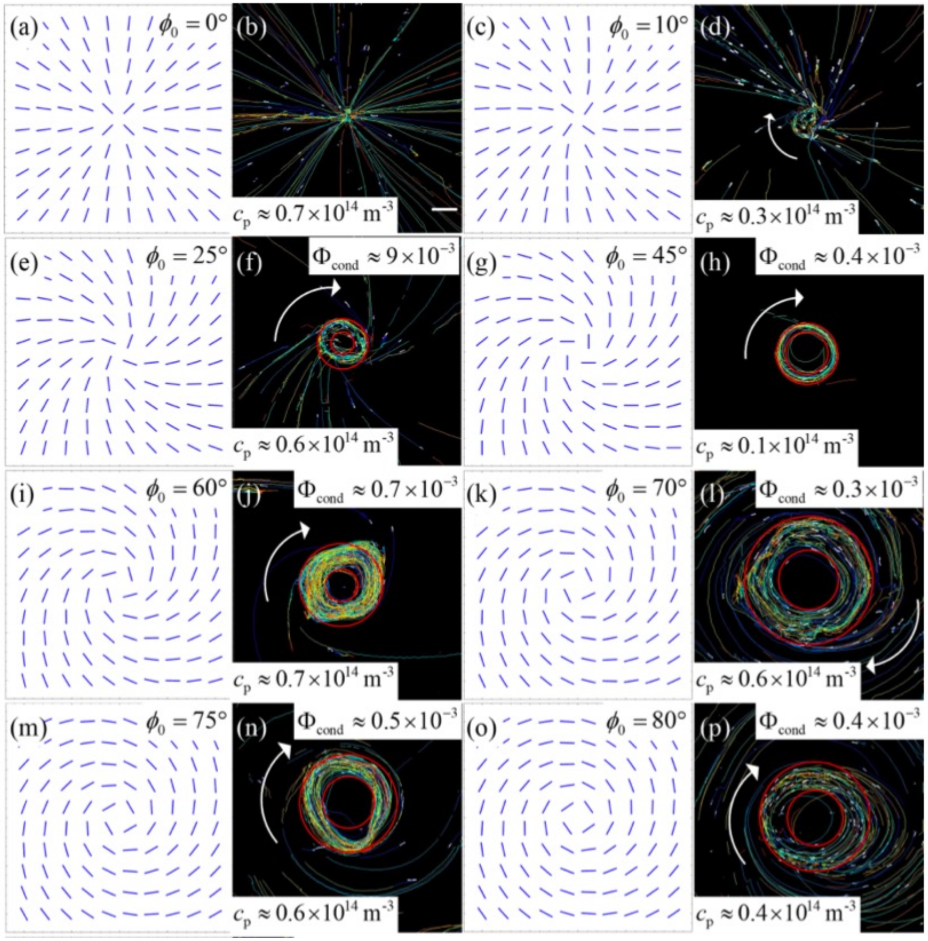

Runa Koizumi, Taras Turiv, Mikhail M. Genkin, Robert J. Lastowski, Hao Yu, Irakli Chaganava, Qi-Huo Wei, Igor S. Aranson, Oleg D. Lavrentovich, PR Research 2020

Vortices and limit cycles

- Prepatterned director: spiral with different pitch
- Low concentration of bacteria – scattering from the center of the spiral
- Higher concentration: limit cycles
- Most stable cycles for the tilt angle 45^o

Stable cycles

Low concentration

ϕ=25^o

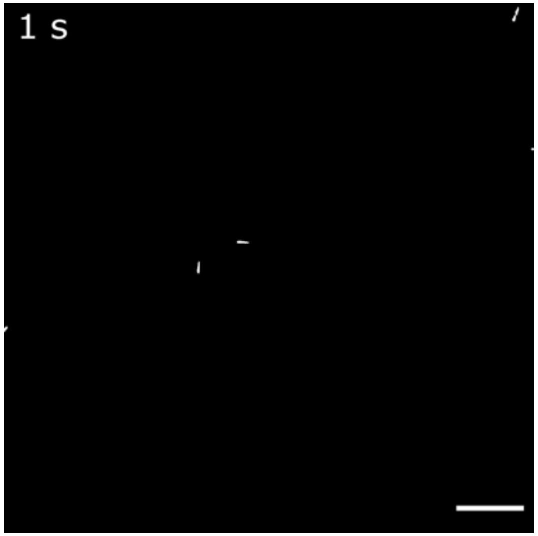

High concentration

ϕ=25^o

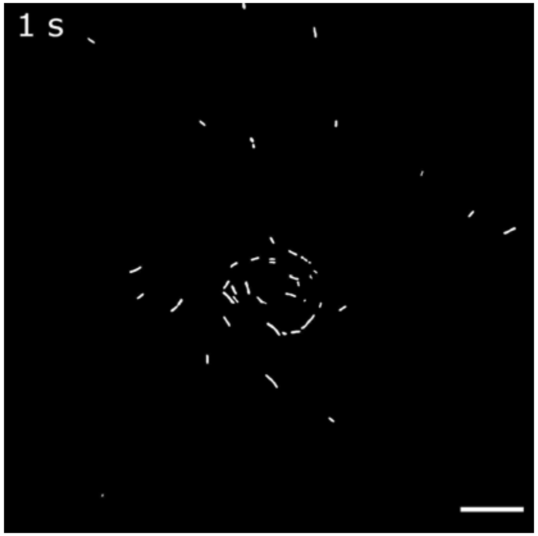

ϕ=75^o

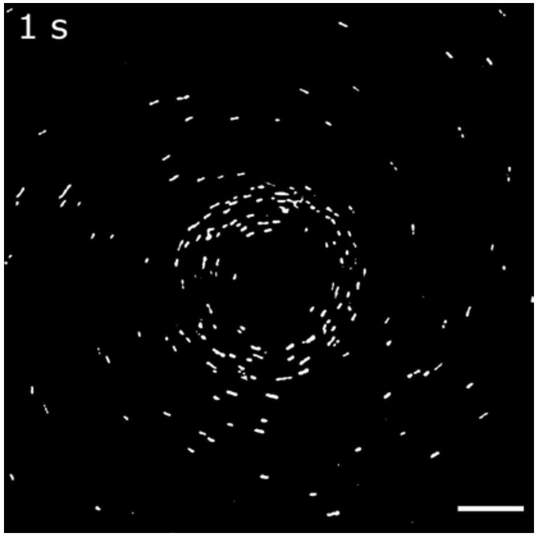

Agent-based simulations

- Bacteria swim with the speed V along the director

$$\partial_t \theta = \gamma_{\mathrm{B}} \sin\left[2\left(\phi_0 - \theta\right)\right]$$

- Bacteria realign the director

$$\partial_t \hat{\mathbf{n}} = -\hat{\mathbf{n}} \times \hat{\mathbf{n}} \times \left(\gamma_{\mathrm{s}} \hat{\mathbf{n}}_0 - 2a\mathbf{F}_{\mathrm{act}} + K\Delta\hat{\mathbf{n}}\right)$$

- Active Force $\mathbf{F}_{\mathrm{act}} = \nabla \cdot \sum \boldsymbol{\sigma}_{\mathrm{act}}$
- Active stress $\boldsymbol{\sigma}_{\mathrm{act}} = -\lambda \mathbf{Q}_{\mathrm{B}} f\left(\mathbf{r}\right)$
- Nematic tensor $\mathbf{Q}_{\mathrm{B}} = \hat{\mathbf{p}}\hat{\mathbf{p}} - \mathbf{I}/2$
- K- elastic constant
- f- shape of the bacterium

Function of the Number of Bacteria

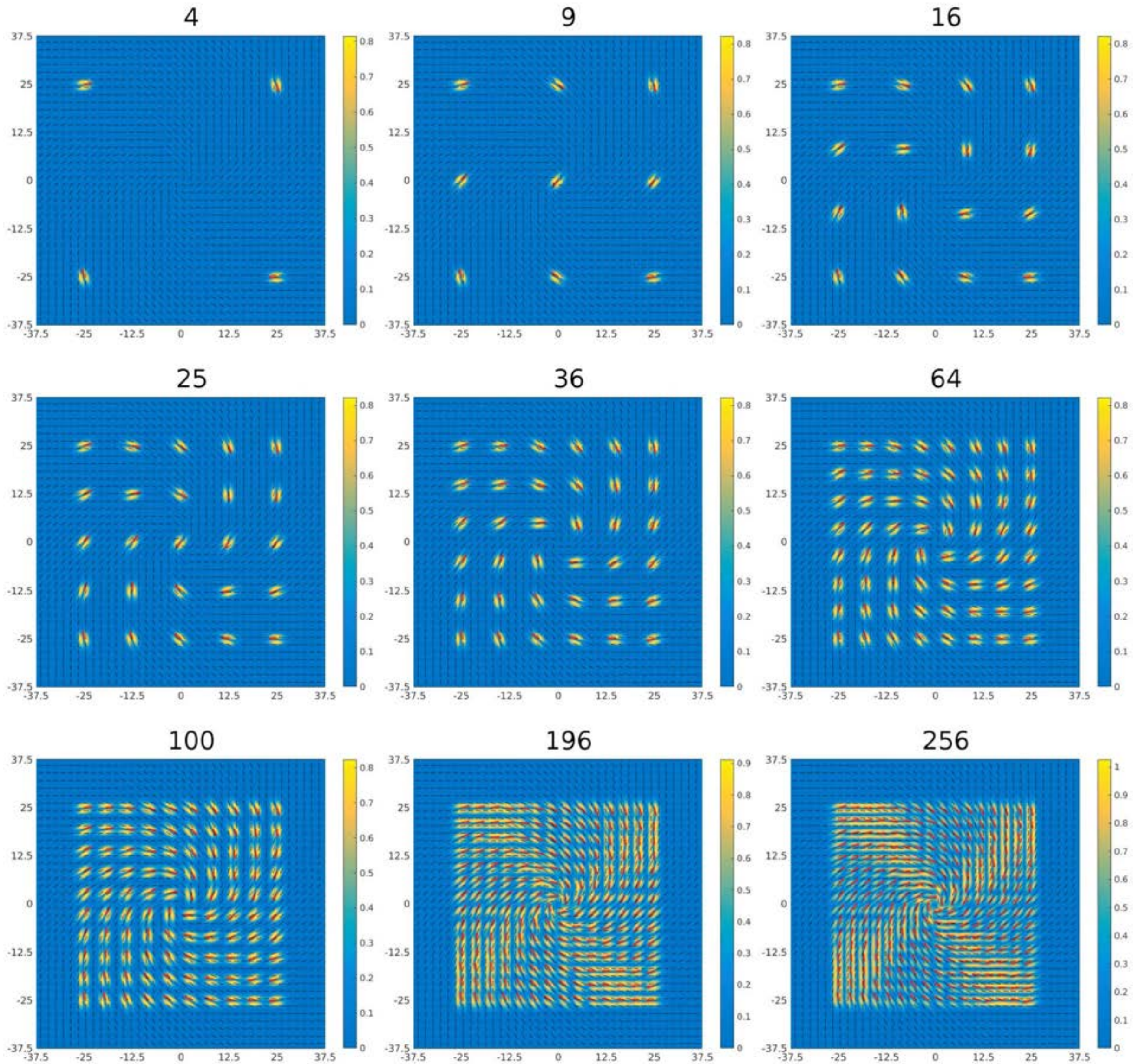

Function of the Tilt Angle

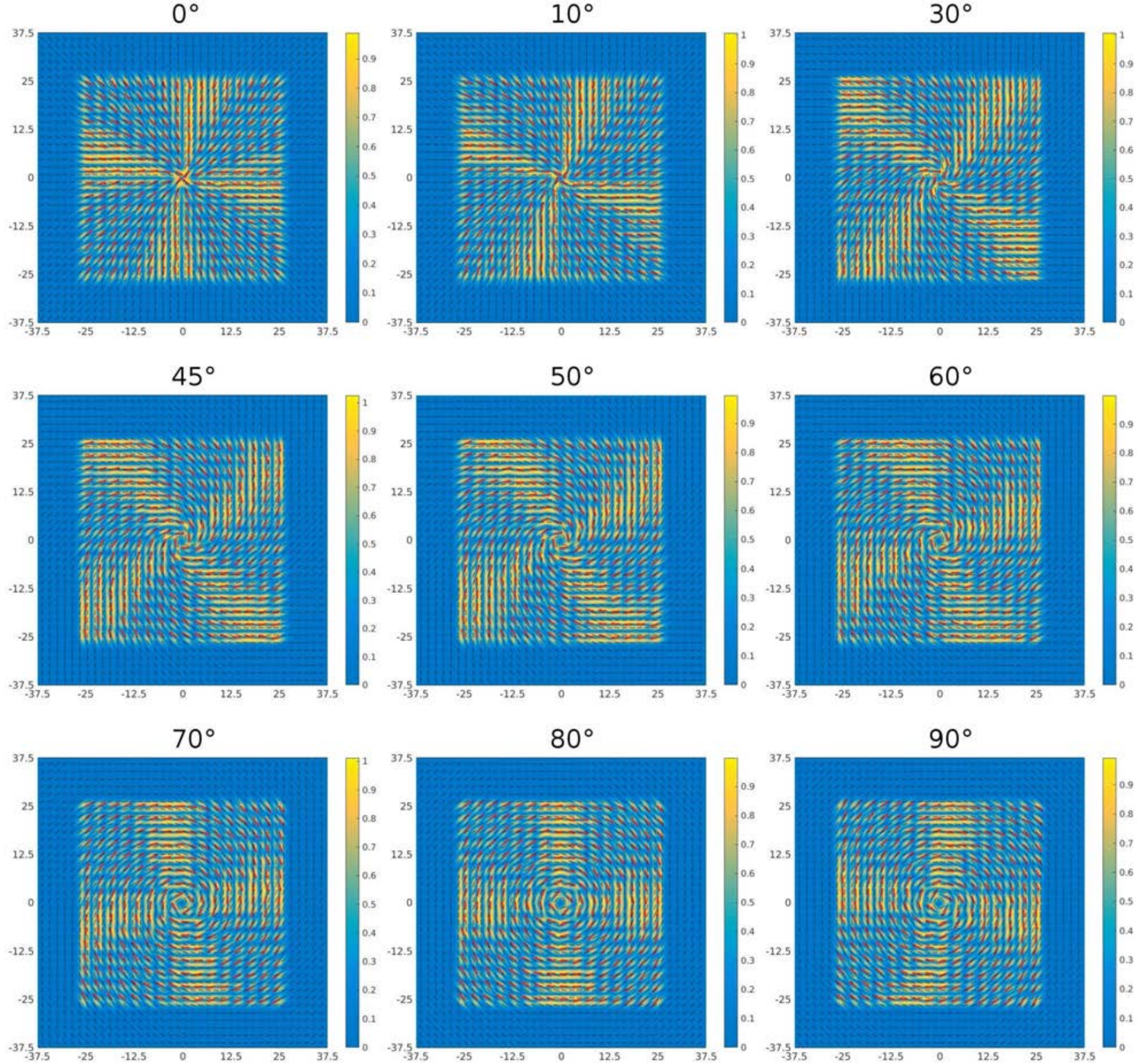

References

- Zhou, Sokolov, Lavrentovich, IA Living Liquid Crystals PNAS 2014
- Genkin, Sokolov, Lavrentovich, IA PRX 2017
- Genkin, Sokolov, IA, NJP , 2018
- Taras Turiv, Runa Koizumi, Kristian Thijssen, Mikhail M. Genkin, Hao Yu, Chenhui Peng, Qi-Huo Wei, Julia M. Yeomans, IA, Amin Doostmohammadi, Oleg D. Lavrentovich, Nature Physics 2020
- Runa Koizumi, Taras Turiv, Mikhail M. Genkin, Robert J. Lastowski, Hao Yu, Irakli Chaganava, Qi-Huo Wei, IA, Oleg D. Lavrentovich, PR Research 2020

Review paper to appear: Bacterial Active Matter, Reports on Progress in Physics, 2022

Summary:

- LLC exhibit coupling between activity and topology
- Computational model is in faithful agreement with experiment
- Experiments fully support our theoretical predictions
- Bacteria accumulate in the cores of ½ defects and expelled from the cores of -½ defects
- Asymmetric pinning
- Control of bacterial motion by surface patterning